N65 19775

(ACCESSION NUMBER)

(PAGES)

(NASA CR OR TMX OR AD NUMBER)

(THRU)

(CODE)

3C

(CATEGORY)

FACILITY FORM 602

iiTRi

IIT Research Institute

GPO PRICE $ _____

OTS PRICE(S) $ _____

Hard copy (HC) ___4.00___

Microfiche (MF) ___1.00___

OFFICIAL FILE – TECHNICAL REPORT
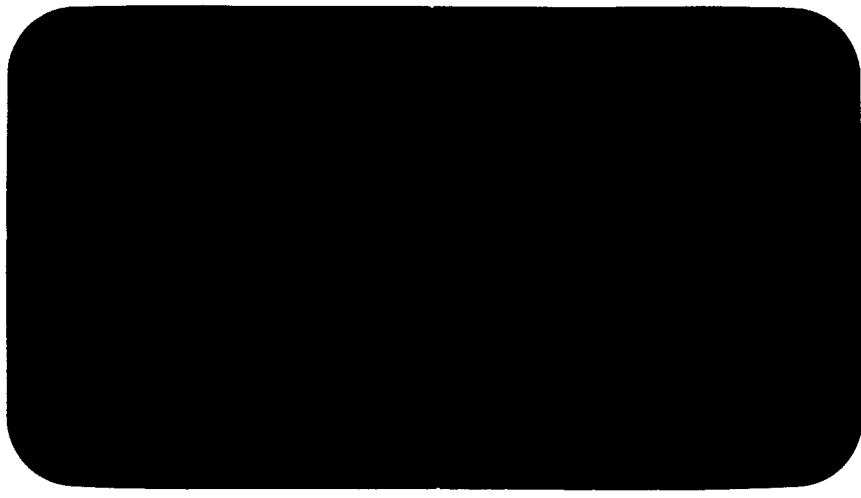
IITRI Project No. M272 (Phase II)
(Final Report)

STUDIES OF LUNAR SOIL MECHANICS

Contract No. NASr-65(02)

February, 1965

IIT RESEARCH INSTITUTE
Technology Center
Chicago, Illinois 60616

IITRI Project No. M272 (Phase II)
(Final Report)

STUDIES OF LUNAR SOIL MECHANICS

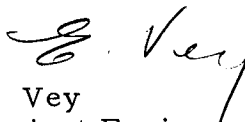Contract No. NASr-65(02)

by

E. Vey and J. D. Nelson

February, 1965

PREFACE

This report represents the final report on Phase II of IIT Research Institute Project No. M272, sponsored by the National Aeronautics and Space Administration under Contract No. NASr-65(02). The research reported herein was performed during the period June 15, 1963 to December 15, 1964. Persons who contributed materially to this work are: W. J. Courtney, W. E. Jamison, A. Kirch, J. D. Nelson, R. D. Rowe, R. W. Rusin, E. Vey and R. A. Wetzel. C. Solbrig at the Institute of Gas Technology prepared Appendix B of this report with assistance from D. Gidaspow.

Respectfully submitted,
IIT RESEARCH INSTITUTE

E. Vey
Project Engineer

APPROVED:

E. Sevin, Director
Solid Mechanics Division

IIT RESEARCH INSTITUTE

ii

ABSTRACT

19775 over

An experimental research program was conducted to investigate the properties of simulated lunar soils in the lunar environment. Experiments were performed on samples of quartz and olivine powders and fine and coarse grained quartz sand having various grain size distributions. Vacuum levels ranged from atmospheric pressure to the low 10^{-11} torr range with temperatures from approximately 250 deg F to 0 deg F.

It was observed that the vacuum in the pores of a soil sample could be 2 to 3 orders of magnitude less than the chamber vacuum. However, the dominant factor effecting the soil properties was not the actual vacuum level in the chamber of soil pores but rather the amount of adsorbed gas removed from the soil grains.

The removal of adsorbed gas resulted in the development of attractive interparticle forces in both materials. These forces caused an increase primarily in the apparent cohesion at room temperature with further removal of gas under elevated temperatures causing an increase primarily in the angle of internal friction. Low temperatures also caused an increase in apparent cohesion under vacuum. In the olivine powder, the vacuum had little if any effect at room temperature but caused an increase in apparent cohesion at elevated temperatures. In sand, ultra-high vacuum and elevated temperatures had little effect on the apparent cohesion but increased the angle of internal friction.

A decrease in consolidation under vacuum was also observed which, together with the increase in shear strength, resulted in a higher static bearing capacity. Under dynamic loading, pore air pressures decreased the penetration resistance in atmosphere. Under rough vacuum the dynamic penetration resistance was approximately the same as for static loading except for inertial effects while ultra-high vacuum increased both the inertial resistance of the soil and the resistance due to soil shear strength.

A substantial amount of adhesion occurred between soil and other materials and on some surfaces resulted in "cold welding". The amount

IIT RESEARCH INSTITUTE

iii

of "cold welding" appeared to depend somewhat on the free electrons in the material.

Craters formed in fine grained soil under low velocity impact were radically different under rough vacuum than in atmosphere with little difference occurring for the coarse grained materials. This was attributed to the absence of pore air pressures and/or vacuum effects on the propagation of stress waves.

CONTENTS

CONTENTS (Cont'd)

LIST OF ILLUSTRATIONS

LIST OF ILLUSTRATIONS (cont.)

LIST OF TABLES

STUDIES OF LUNAR SOIL MECHANICS

I. INTRODUCTION

With the present emphasis on exploration of the other celestial bodies in our solar system and in particular the use of the moon as a space station, it is necessary to learn more about the properties of the materials which are expected to be encountered on these bodies. The success of the lunar mission is particularly dependent upon the correct interpretation of observations and in-situ measurements on the lunar surface as well as the proper design of vehicles and structures to be placed on the moon. There-fore, it is essential to have a basic knowledge of the engineering properties of the materials composing the lunar surface.

Because of the extreme differences between the lunar and terrestrial environments, the most important of which is the virtual absence of an atmosphere on the moon, one would not expect that the lunar soil would have the same properties as a similar material on earth. An experimental program was performed, therefore, in order to investigate the effects of lunar environmental conditions on the behavior of soils having a high probability of being representative of the actual lunar surface material and to provide basic engineering data on the properties of these materials to aid in the design and construction of vehicles and shelters on the moon.

The investigation reported herein is a continuation of previous research.[1] It consists primarily of the determination of the effect of ultra-high vacuum and extreme temperatures on the shear strength and static and dynamic bearing capacity of simulated lunar soils.

Although the research program has been largely an experimental investigation of specific properties of selected soils under prescribed

---

[1] Vey, E. and J. D. Nelson, "Studies of Lunar Soil Mechanics", IITRI Project M272, Phase I, Contract No. NASr-65(02), June 1963.

environmental conditions, an important underlying concept throughout the conduct of the program has been to allow sufficient latitude so that at least some of the results would indicate true lunar soil behavior according to almost any reasonable estimate of the lunar surface.

II. DESCRIPTION OF REPRESENTATIVE SOILS

The two materials selected for use in this investigation consisted of quartz and olivine. A complete discussion providing the basis for selection of these materials is given in the final report on Phase I.[2] In summary, the quartz is a commonly found nonmetallic mineral of low specific gravity while the olivine represents a material of meteoritic origin.

The quartz and olivine were both used in a powder form having the grain size distributions shown in Fig. 1 and 2. Some experiments were also performed on quartz samples having coarser grain sizes (Fig. 3). On the basis of grain size the olivine and quartz powders would be classified as silts whereas the coarser quartz samples would be classified as sands.

The quartz samples are commercially available in the gradations used. The powder form is commonly referred to as silica flour while the sand samples are referred to as Ottawa sand since they are obtained from sandstone deposits near Ottawa, Illinois. This sand is almost pure silicon dioxide and has an absolute specific gravity of 2.64.

The olivine was mined in Jackson County, North Carolina and was obtained in rock form. The rock material was ground in a ball mill and the portion of the material thus produced which passed a No. 200 mesh sieve was separated and used for experimentation (Fig. 2, curve c). The material retained on the No. 200 mesh sieve was further ground in an 8 inch rubber-lined fluid energy mill, to provide the gradations shown by curves a and b in Fig. 2.

The olivine is a ferromagnesium silicate having a specific gravity of 3.27. This relatively low value indicates that its composition is predominantly magnesium silicate, the ratio of magnesium to iron being roughly from 12:1 to 16:1.

---

[2] Vey, E. and J. D. Nelson, "Studies of Lunar Soil Mechanics", IITRI Project M272, Final Report Phase I, July 1963 and Quarterly Reports Phase II, September, December 1963, March, June, September 1964.

IIT RESEARCH INSTITUTE
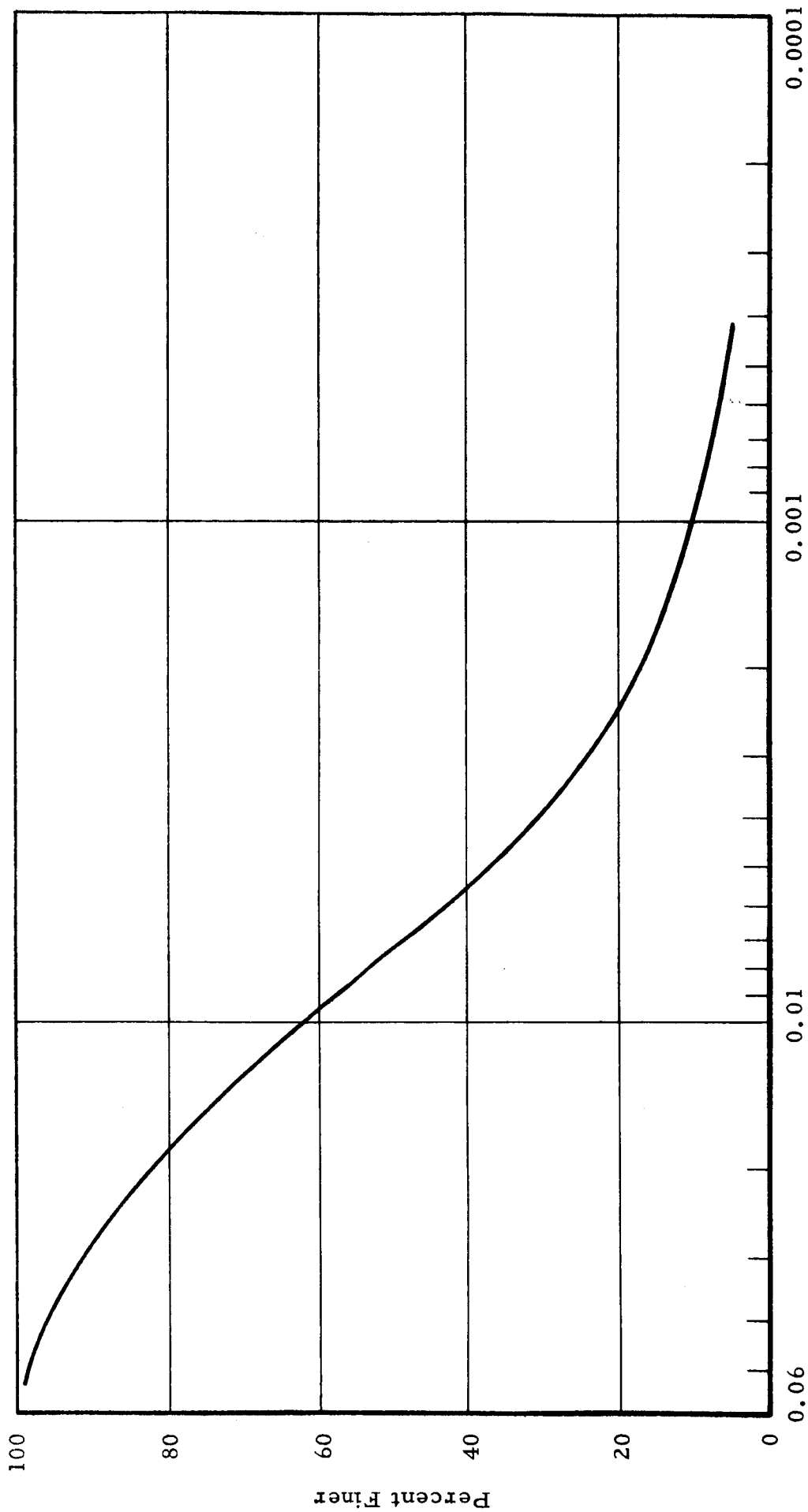
Fig. 1   GRAIN SIZE DISTRIBUTION OF QUARTZ POWDER
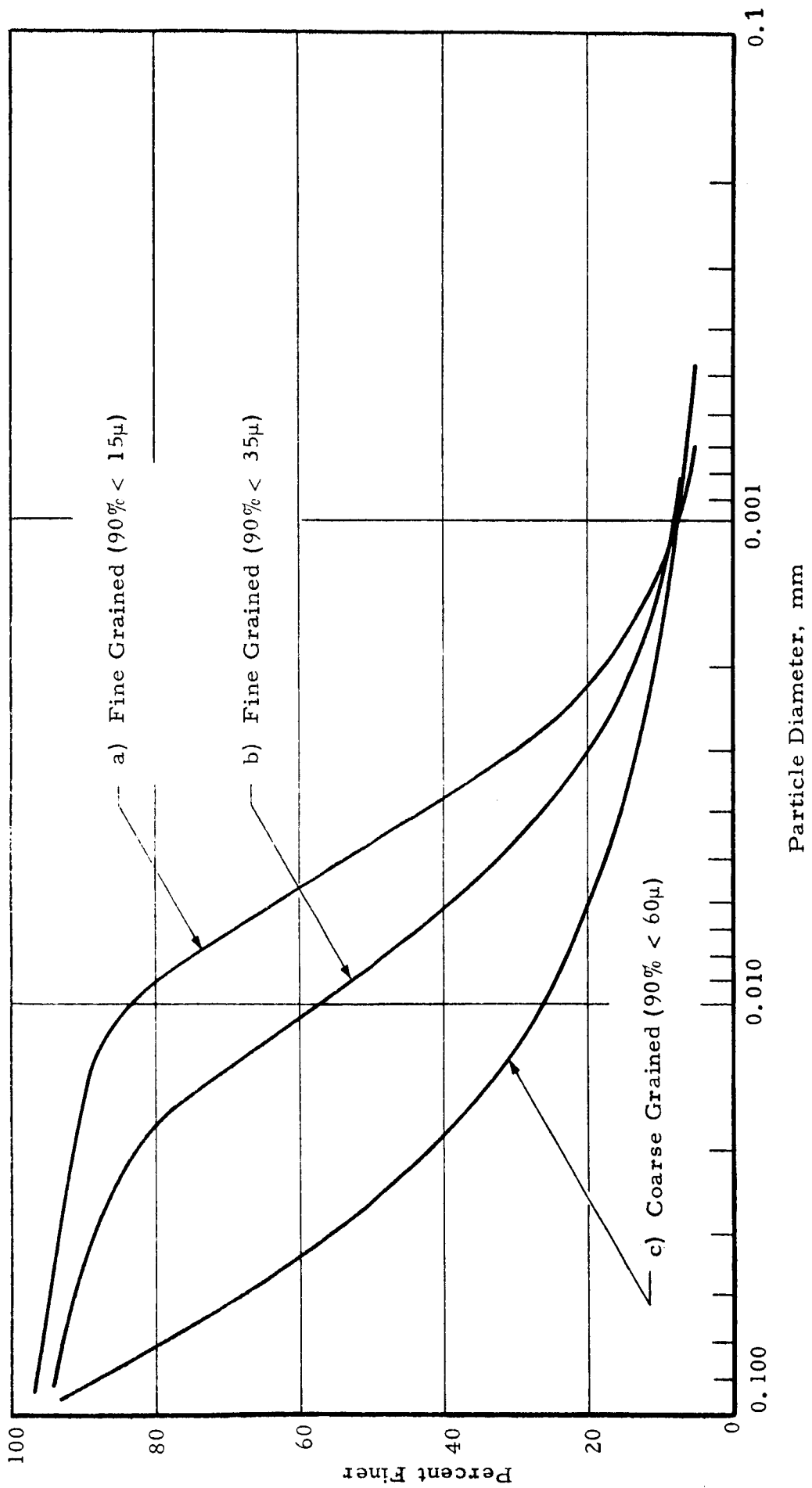
Fig. 2 GRAIN SIZE DISTRIBUTION OF OLIVINE POWDER
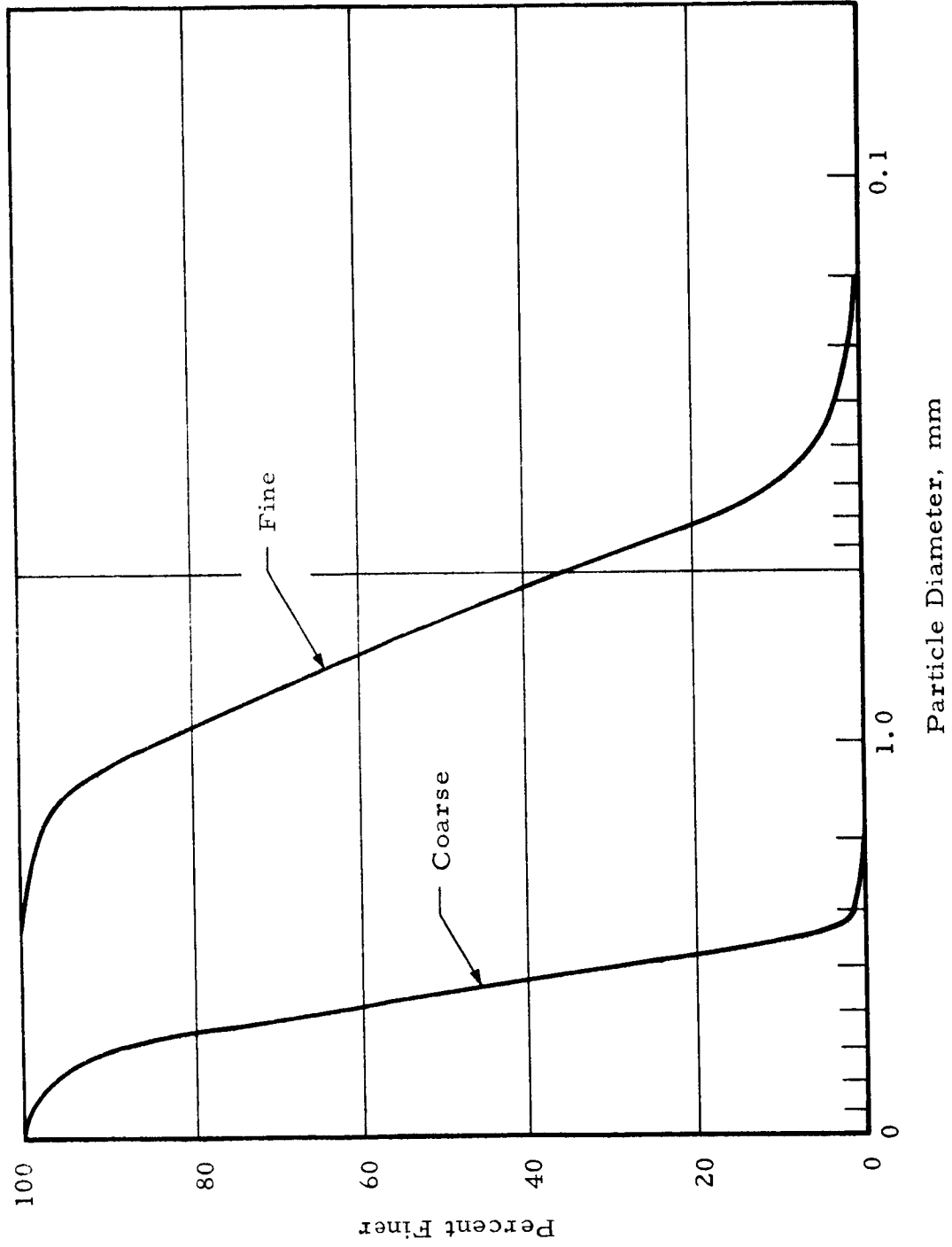
Fig. 3   GRAIN SIZE DISTRIBUTION OF FINE AND COARSE SAND

In selecting these two minerals there is a reasonable degree of certainty that their major constituents would be found in the lunar surface material, and there is a high probability that the major constituents of at least one of the materials would also be the major constituent of some sections of the lunar surface. Within the confines of what is known categorically of the lunar surface it was deemed unwise to try to base the study outlined in this report on a more precise definition of the true lunar soil.

III. VACUUM IN SOIL PORES IN RELATION TO CHAMBER VACUUM

It is known that the vacuum which is measured in the vacuum chamber is generally higher than that which actually exists in the soil pores.[2] Consequently, experiments were performed in which the vacuum at various points in soil samples was measured and compared with that measured outside the soil in the chamber.

The apparatus used in these experiments is shown schematically in Fig. 4. The thermocouple gages were used to measure pressures above 10μ. Below this level the ionization gages were used. Because of the long tabulation on the ionization gages the apparatus was placed in the vacuum chamber without soil and the gages calibrated against one mounted on the wall of the chamber. All readings were found to agree within approximately 0.1 to 0.2 orders of magnitude.

Readings of low vacuum levels (10^{-3} torr range) could be taken using the ionization gages by reducing the emission current. Although the calibration may not be linear in this region it is believed that the accuracy of these readings was within one half of an order of magnitude. The experiments were performed using only loose quartz powder, because of the length of time required to complete an experiment.

Figure 5 shows the vacuum measured (1) near the chamber wall, (2) near the soil surface, and (3) at a depth of 6-1/2 inches in a sample of size 12 x 12 x 12 inches. The curve for the vacuum below the surface is very nearly parallel to that for the chamber vacuum and consequently, even after pumping had continued for more than 350 hours a difference of almost three orders of magnitude remained. Thus, although the vacuum in the chamber was 1×10^{-8} torr, the actual vacuum in the soil pores was barely in the 10^{-6} torr range.

This experiment was repeated in a vacuum system in which the chamber could be separated from the pump by a valve. A smaller container (approximately 6 inches deep) was necessary in this experiment because of a smaller vacuum chamber and, therefore, the vacuum in the soil was measured at a depth of 3-1/2 inches below the surface. After the vacuum

①	Ionization Gages
②	Thermocouple Gages
③	Shields
▦	Soil
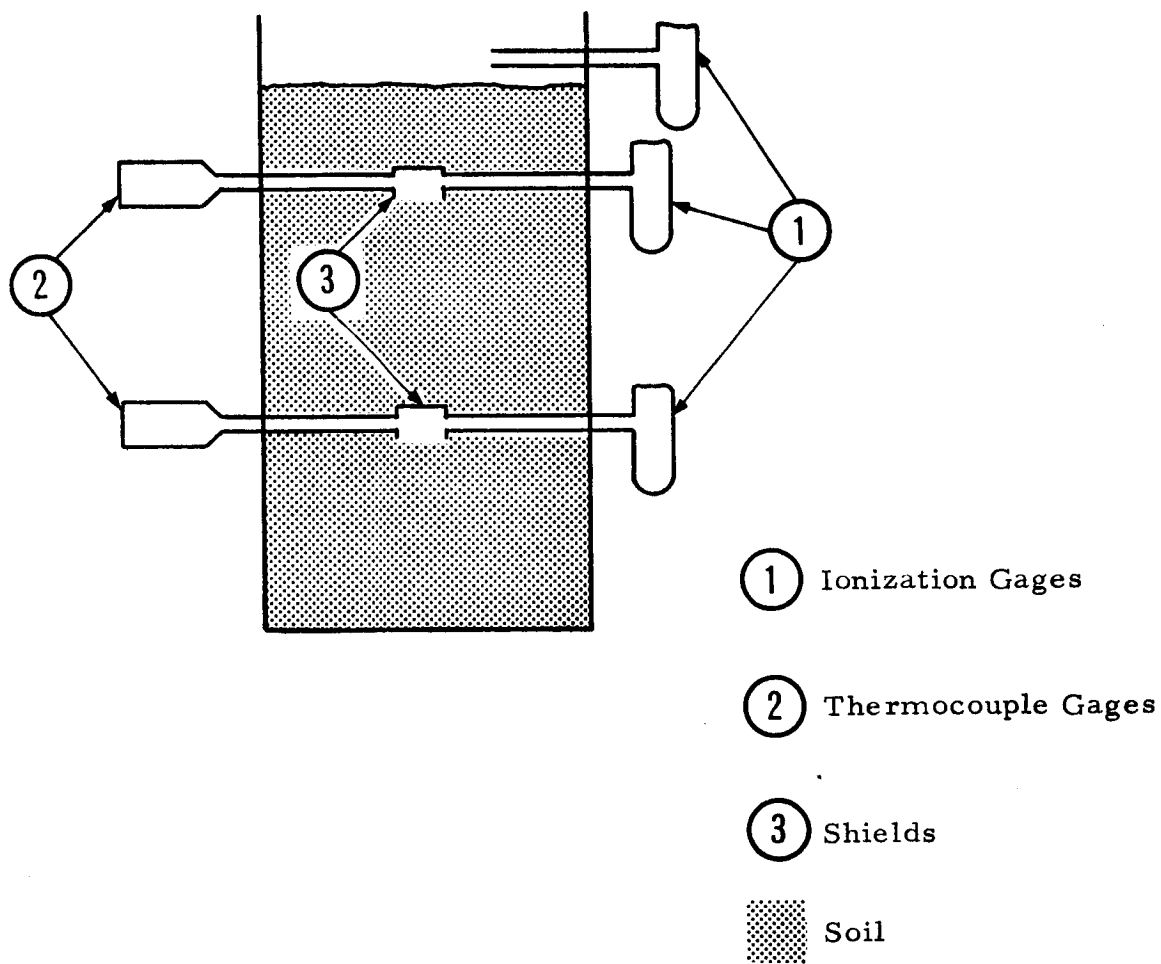
Fig. 4   APPARATUS FOR MEASURING VACUUM IN SOIL
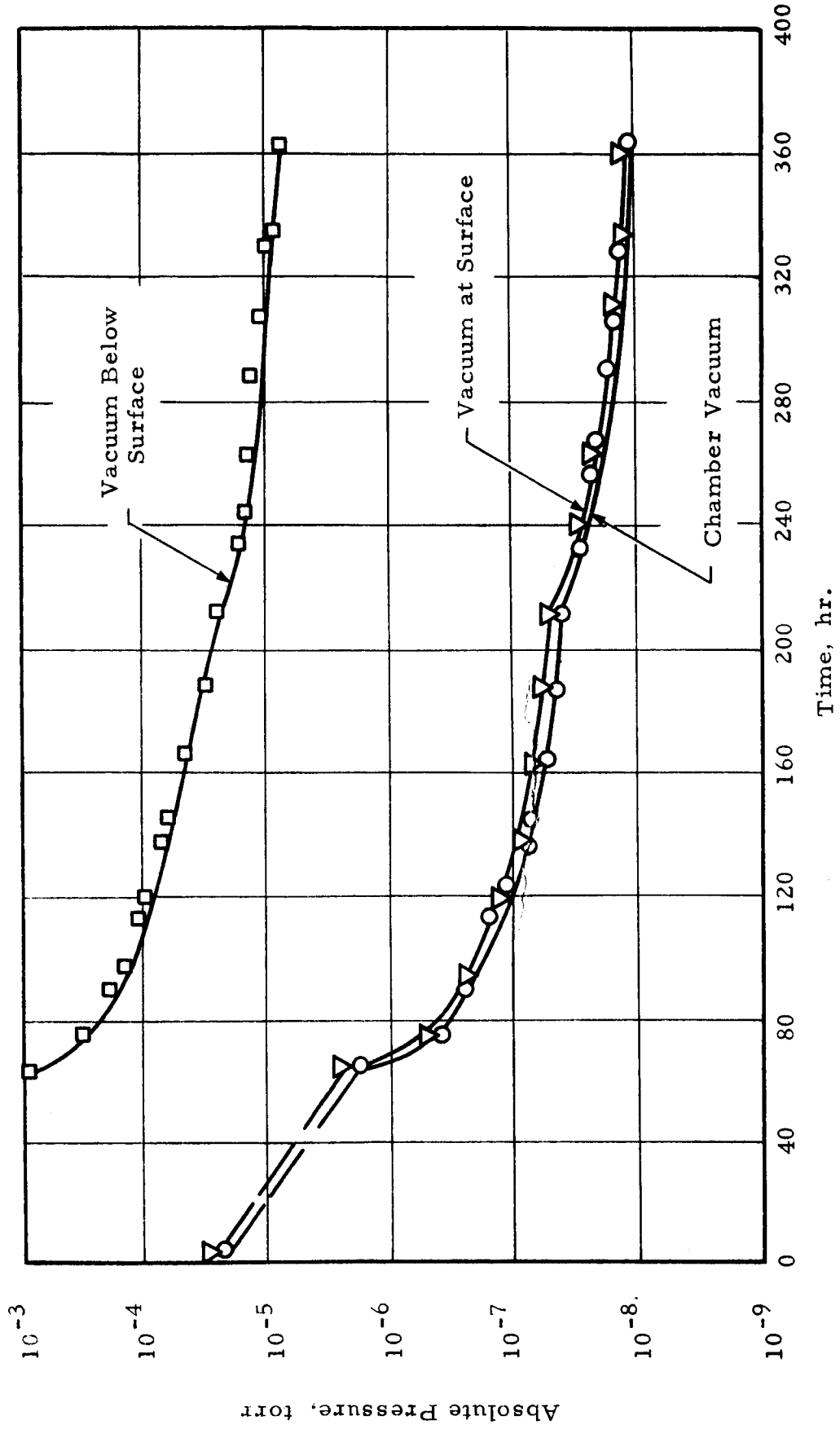
Fig. 5 VACUUM IN SOIL AND CHAMBER AS A FUNCTION OF TIME

in the chamber had leveled off at 4×10^{-7} torr the valve was closed, and the vacuum level at both points was monitored for a period of 140 minutes after which the valve was reopened. The vacuum as a function of time for this experiment is shown in Fig. 6, and as seen, the vacuum at both points responded to closing the valve at the same instant of time. Very soon thereafter the pressure in the chamber rose to a point slightly higher than that in the soil and remained so until the valve was again opened. The fact that the pressure at both points responded simultaneously would indicate that the permeability of the soil is very high and offers little resistance to the flow of gas. Also the fact that the chamber pressure rises to a point slightly higher than the soil pressure suggests that the source of gas which raised the pressure was due to a leak in the chamber.

After approximately 140 minutes the valve was opened and as shown in Fig. 6 the pressure at both points responded almost immediately. However, while the vacuum in the chamber leveled off quite rapidly at a point very nearly the same as that which existed prior to closing the valve, the vacuum in the soil pores leveled off at a point more than three times its original level. It may be reasoned that some of the gas which was supplied to the system when the valve was closed was readsorbed on the soil and was not removed quickly upon opening the valve.

Thus, the indication of a high permeability and the fact that the vacuum in the soil did not return to its original level suggests that the problem of outgassing a soil mass is primarily one of removing the adsorbed gas and not so much resistance to flow.

If one considers a soil sample which is open only at the top (Fig. 7) pumping may take place only in the upward direction. For any elemental volume of soil in the container the change in vacuum level or pressure in any period of time will then depend on the net amount of gas which enters or leaves the element. Neglecting effects due to the walls of the container and since pumping can occur only in the z-direction, it may be assumed that the pressure is uniform across any cross section, and is independent of r and θ. Thus, considering an element as shown in Fig. 7, and assuming that the pressure in the sample increases with depth, then the net flow of gas, q, across the faces of the element will be in the upward direction.
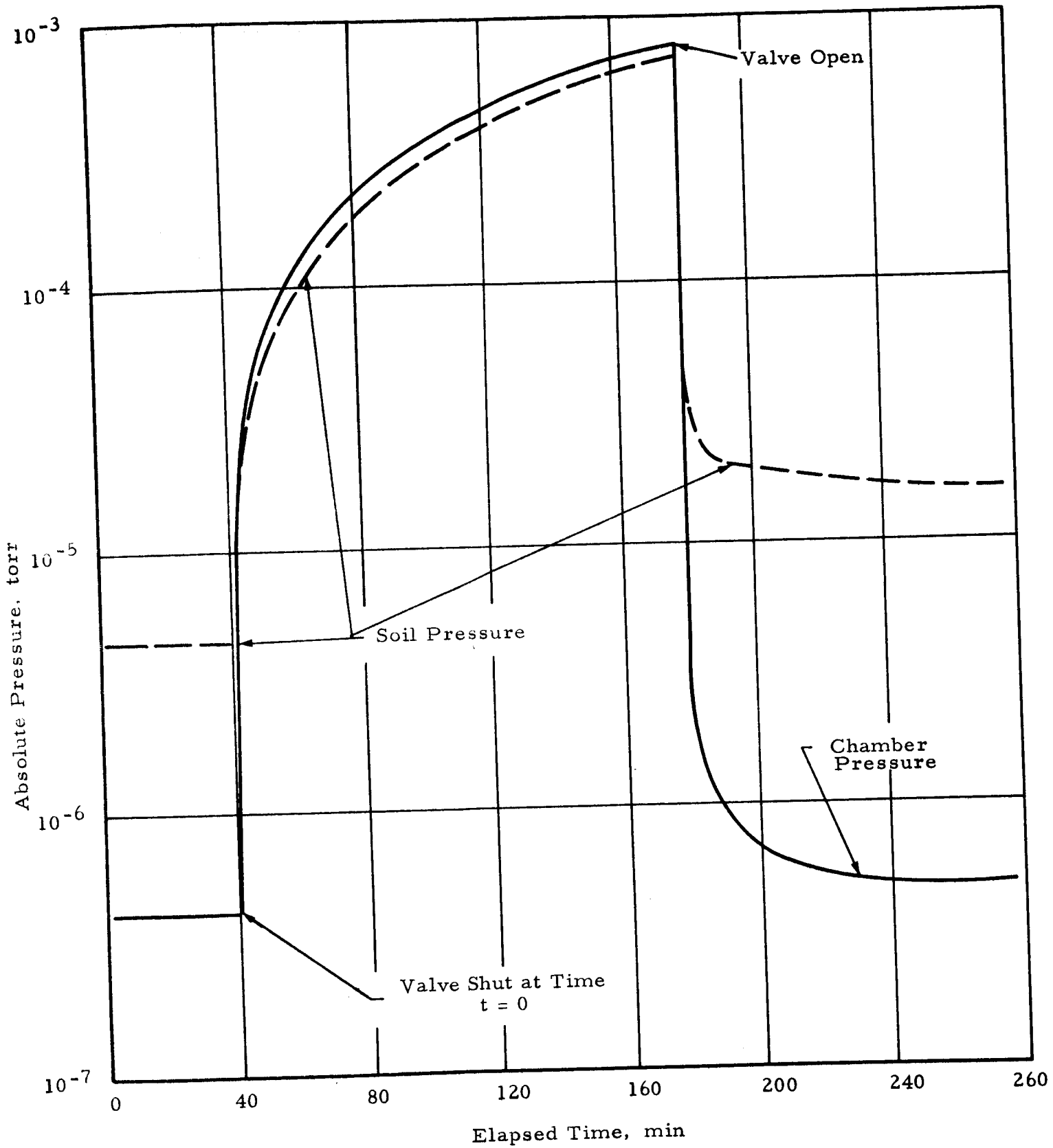
Fig. 6 VACUUM IN SOIL PORES AND CHAMBER AS A FUNCTION OF TIME
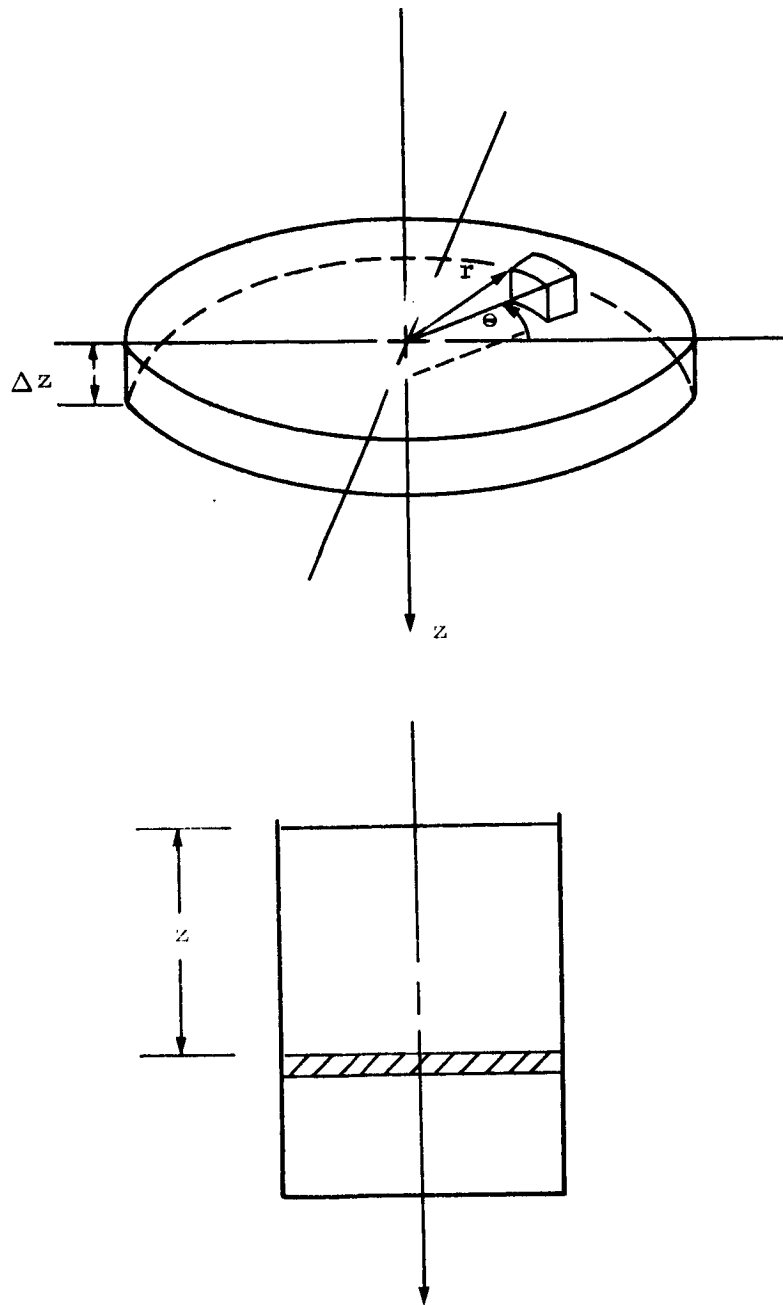
Fig. 7   ELEMENTAL VOLUME OF SOIL

Some of the net amount of gas which enters the element will be readsorbed on the surfaces of the soil grains while the remainder may be thought of as leaving through the upper face. In addition, some gas which had been present in the element at the beginning of pump down will also be removed. The outgassing of the soil may be considered as being a net flow of gas across an element with some internal source of gas. Since the flow has been assumed to be independent of r and θ, it reduces to the case of one-dimensional flow. By consideration of the continuity equation, the equation of the pressure in soil can be written in the form

$$\frac{\partial p}{\partial t} = K \frac{\partial^2 p}{\partial z^2} \tag{1}$$

where p is the pressure, K is a constant and t and z are the time and depth below the surface respectively. A more complete derivation of this equation is given in Appendix C.

It is assumed that after the system has been evacuated to a rough vacuum prior to starting the diffusion pump the pressure is the same throughout the chamber and the soil mass. It is further assumed that starting the diffusion pump results in an instantaneous drop in the chamber pressure.

The soil sample in Fig. 7 may then be considered as a sample of length 2L which is open at both ends with the boundary conditions,

$$p(o, t) = p(2L, t) = P_o(t)$$

$$p(z, o) = P_o(o) + P_s \tag{2}$$

in which $P_o(t)$ is a function of time only and P_s is a constant. A solution to Eq. (1) which satisfies the boundary conditions (Eq. (2)) is

$$p = P_o(t) + \sum_{n=1}^{\infty} e^{-k \frac{n^2 \pi^2 t}{4u^2}} b_n \sin \frac{n\pi z}{2L} . \tag{3}$$

At the time $t = 0$,

$$P_o(o) + P_s = P_o(o) + \sum_{n=1}^{\infty} b_n \sin \frac{n\pi z}{2L} \qquad (4)$$

from which

$$P_s = \sum_{n=1}^{\infty} b_n \sin \frac{n\pi z}{2L} \quad . \qquad (5)$$

Since Eq. (5) is the Fourier sine series for the function P_s, the coefficients, b_n, are given by the equation

$$b_n = \frac{1}{L} \int_o^{2L} P_s \sin \frac{n\pi z}{2L} \quad . \qquad (6)$$

Thus, the pressure may be represented by the equation,

$$p = P_o + \sum_{n=1}^{\infty} e^{-k \frac{n^2 \pi^2 t}{4L^2}} b_n \sin \frac{n\pi z}{2L} \qquad (7)$$

in which P_o is a function of time only and b_n is given by Eq. (6).

The function P_o is the variation of pressure with time at a point on the surface of the sample (i.e., $z = 0$). From Fig. 5 it can be seen that just above the surface, the pressure is very close to that recorded in the chamber. If it is then assumed that the pressure on the surface is the same as the chamber pressure, P_o will be the same as the drawdown curve for the system. The value of P_s may be determined from the difference between the rough vacuum at which the diffusion pump is turned on and P_o.

Experiments were performed in which the pressure was measured at three points below the surface in a cylindrical sample 10 inches in diameter and 18 inches deep using apparatus as shown in Fig. 4. The pressures were measured along the axis of the cylinder in order to insure that the results were independent of the r and θ directions and, hence, would conform with the assumptions made in the analysis.

The pressure as a function of time is shown in Fig. 8 for one experiment in which the soil and chamber were not baked. Even after a considerable amount of time the pressure in the soil is approximately the same at all depths and appears to have leveled off at a value approximately three orders of magnitude greater than the chamber pressure.

Figure 9 shows the pressure as a function of time for a similar experiment in which the chamber and sample were baked out. As would be expected, the pressure in the soil and chamber increased when the bakeout was turned on. However, when the bakeout was discontinued the pressure in the chamber changed only slightly whereas that in the soil decreased by almost three orders of magnitude.

This rapid increase in vacuum level may be attributed to the fact that at the higher temperature the gas was released from the surfaces of the particles more easily and was pumped out. As the soil cooled, however, gas was readsorbed on the soil grains resulting in an effective increase in "pumping" speed. After the soil had reached an equilibrium temperature (room temperature) the curves leveled off and as can be seen from Fig. 9 were approximately parallel.

In Eq. (7) the second term of the series is generally quite small relative to the first and in most cases need not be considered. Thus if the logarithm of pressure is plotted as a function of time as in Fig. 9 the curve should be approximately a straight line. However, when the soil is being heated or cooled this is not the case and, hence, k must be a function of temperature.

The pressure versus time for another similar experiment in which the sample and chamber were baked from the beginning of drawdown is shown in Figure 10. Using the data from the middle gage the value of k was determined and the pressure plotted as a function of depth in Fig. 11 along with the actual measured values for 140 and 260 hours. It can be seen that the predicted and measured values agree quite well. Note that at 140 hours the sample was still cooling whereas at 260 hours it had essentially reached room temperature. Consequently, the value of k was different for the two curves in Fig. 11.

IIT RESEARCH INSTITUTE

- 16 -
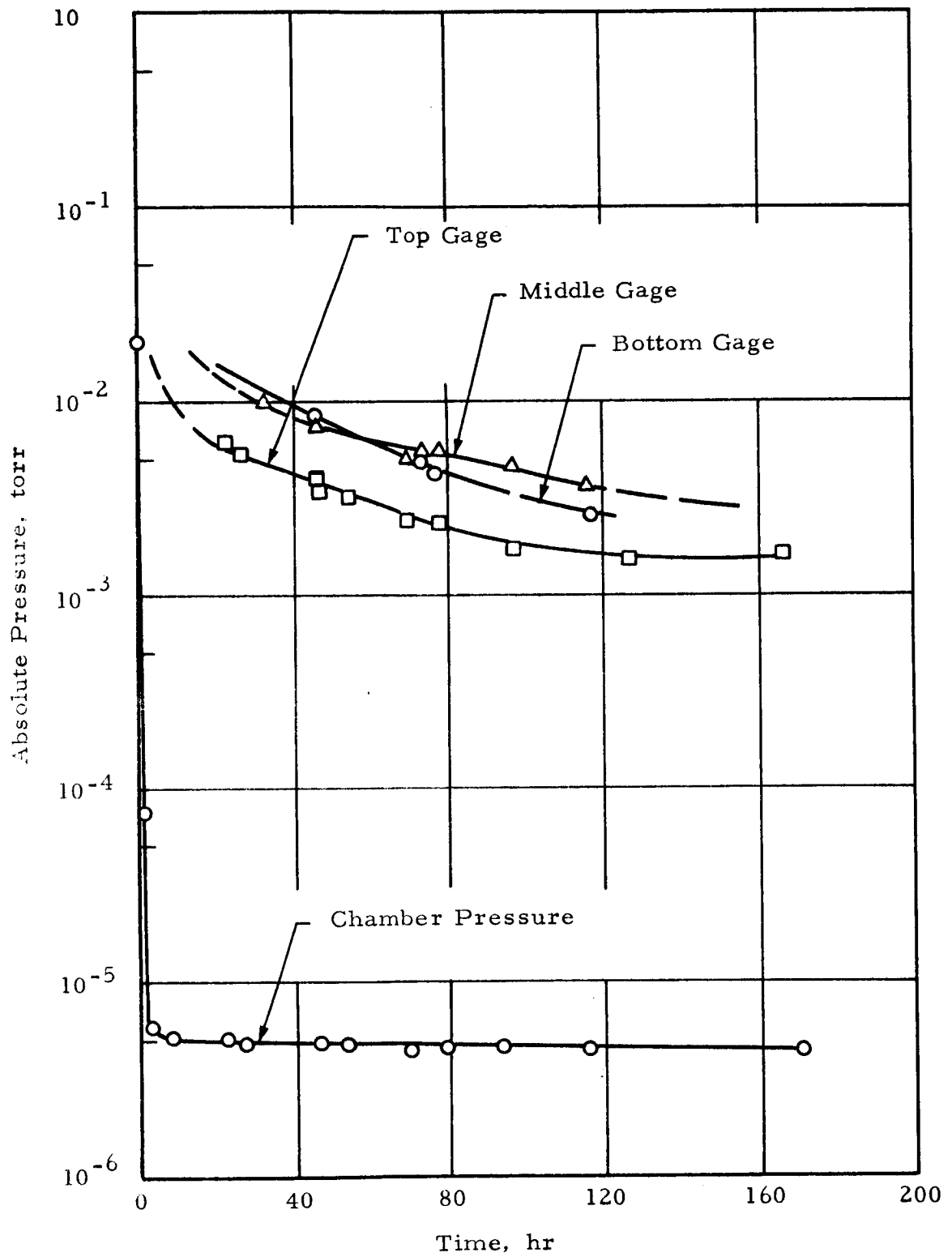
Fig. 8 VACUUM IN SOIL AND CHAMBER AS A FUNCTION
OF TIME, NO BAKEOUT
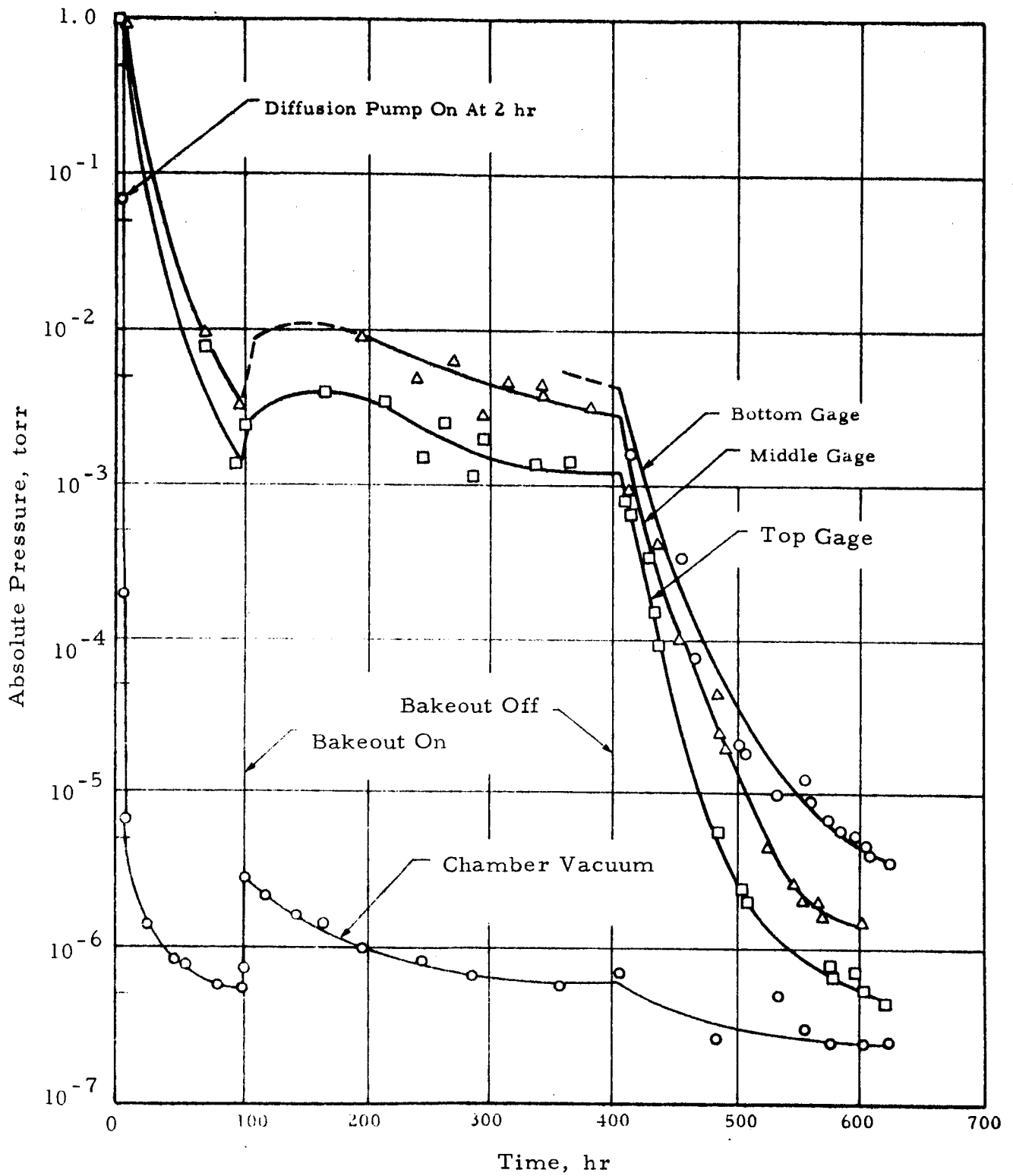
Fig. 9   VACUUM IN SOIL AND CHAMBER AS A FUNCTION OF TIME
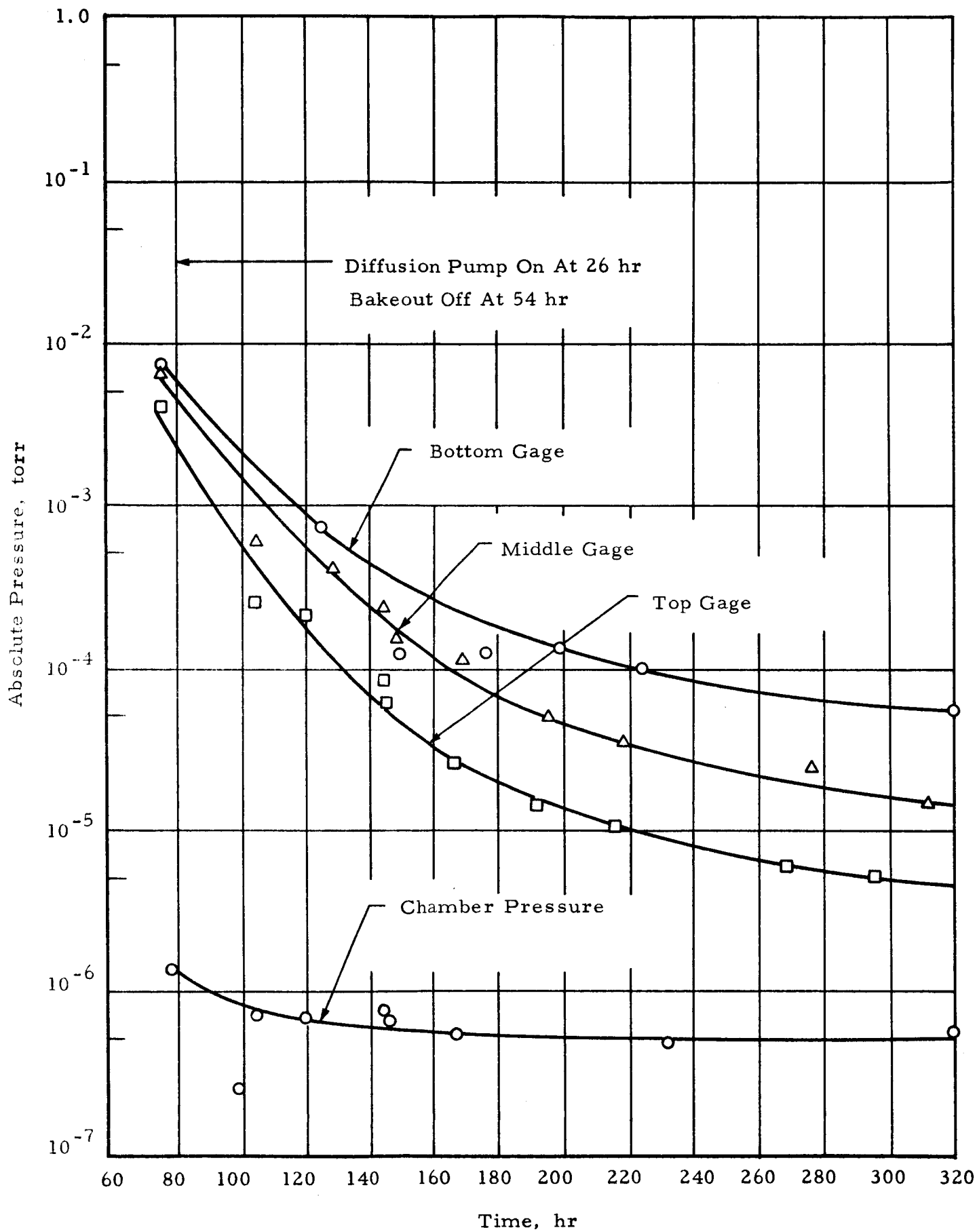
Fig. 10   VACUUM IN SOIL AND CHAMBER AS A FUNCTION OF TIME
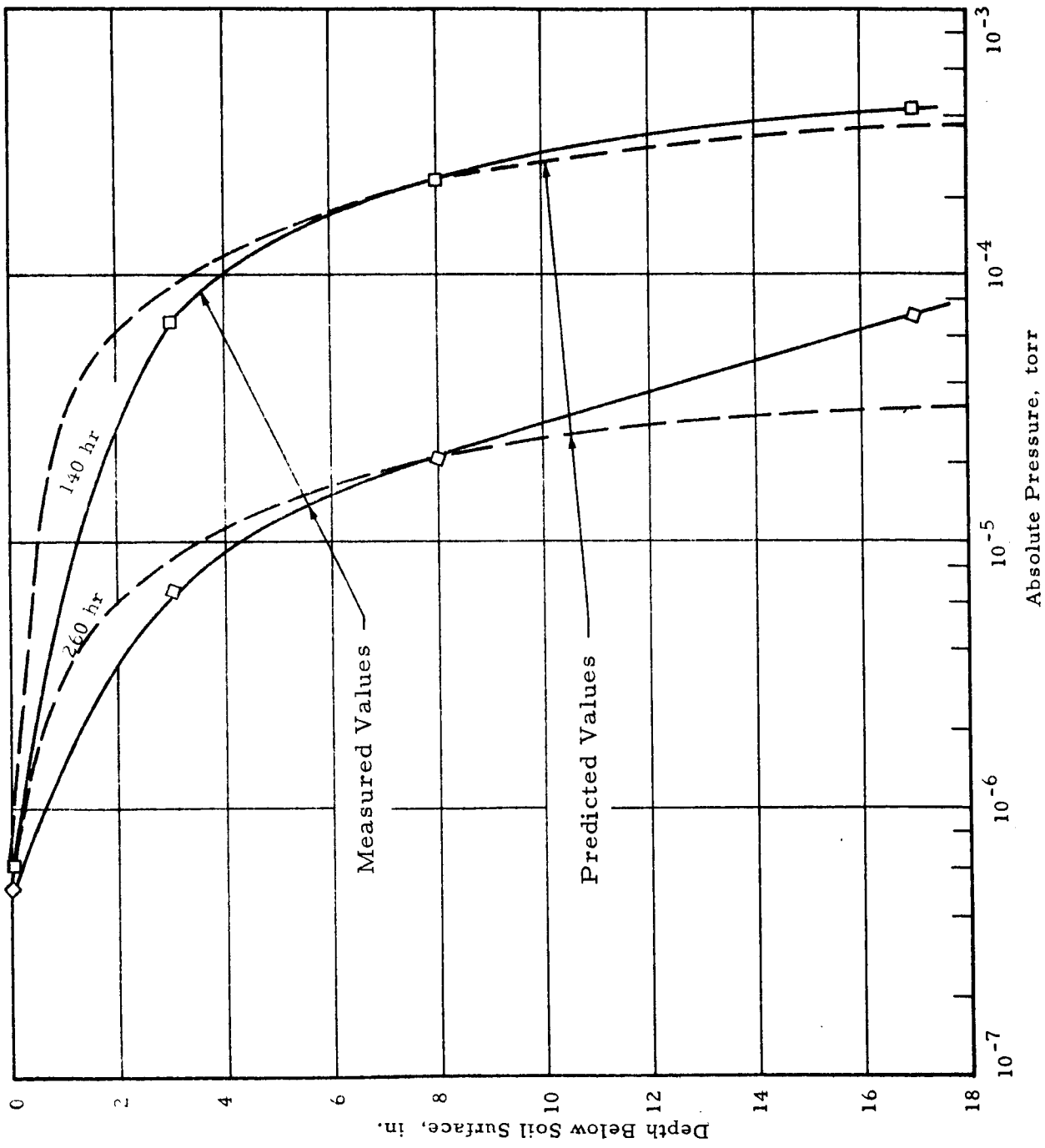
Fig. 11 VACUUM IN SOIL AS A FUNCTION OF DEPTH

While the amount of data is limited it serves to show that although high vacuum levels may be reached in the chamber, the actual environmental vacuum level in the soil may be considerably less. In order to achieve high vacuum levels in a soil mass of any appreciable size, it is almost a necessity to bake out the sample as well as the chamber and although this bakeout may not affect the chamber vacuum appreciably, it may increase the vacuum in the soil by as much as three orders of magnitude. Also, it would be expected that the length and intensity of the bakeout period would have a large effect on the pore pressures.

As was mentioned previously, a major portion of the gas remaining in the soil is that which is adsorbed on the surfaces of the soil grains. Consequently, since the amount of adsorbed gas and its removal may vary from one particular mineral to another, two different soils may exhibit different properties under the same chamber vacuum due to differences in the actual vacuum levels in the soil pores themselves.

IV. CHARACTERISTICS OF SOIL DEPOSITED UNDER VACUUM

Experiments were performed to investigate the porosity attained by soil when deposited in a vacuum environment. Experiments of this type were performed previously but as the data for the 15μ olivine at ultra-high vacuum levels was somewhat limited, further data was obtained at vacuum levels up to 8.9×10^{-10} torr to supplement the previous data.

The porosity of the deposited soil as a function of the initial chamber vacuum is shown in Fig. 12 along with the results obtained in Phase I. The effects of grain size on porosity are clearly evident from this figure and are discussed in some detail in the final report on Phase I.[2/] The effect of drop height is also evident in that an increase in the drop height from 1.44 to 2.25 inches for the 15μ olivine resulted in a decrease in the porosity. However, an increase in the drop height from 2.25 to 4.5 inches for the silica flour resulted in no apparent change.

As seen from Fig. 12 the curves for the 15μ olivine are of the same general shape as those obtained for the other two olivine samples, i.e., an increase in vacuum produces a decrease in the porosity of the soil up to a certain vacuum level. At this vacuum level the trend is reversed. However, the point at which the minimum porosity is attained for the 15μ olivine occurs at a vacuum level of approximately the same magnitude as for the coarser grained olivine (90 percent smaller than 60μ). Also, the amount by which the porosity increases at these vacuum levels is of approximately the same magnitude as for the 60μ olivine. The decrease in porosity at low vacuum levels from that under atmospheric conditions was attributed in part to the removal of interparticle bonds created by surface tensions in hygroscopic moisture. In order to study the degree to which hygroscopic moisture may aid in supporting a flocculent grain structure experiments were performed in which the soil was deposited in a oven dry atmosphere. The apparatus which had been used previously was set up in a large oven, and the sample baked from 2 to 18 hours. Experiments were performed using air dry soil at room temperature, oven dry soil at room temperature and oven dry soil at 100 deg C and 150 deg C.

IIT RESEARCH INSTITUTE
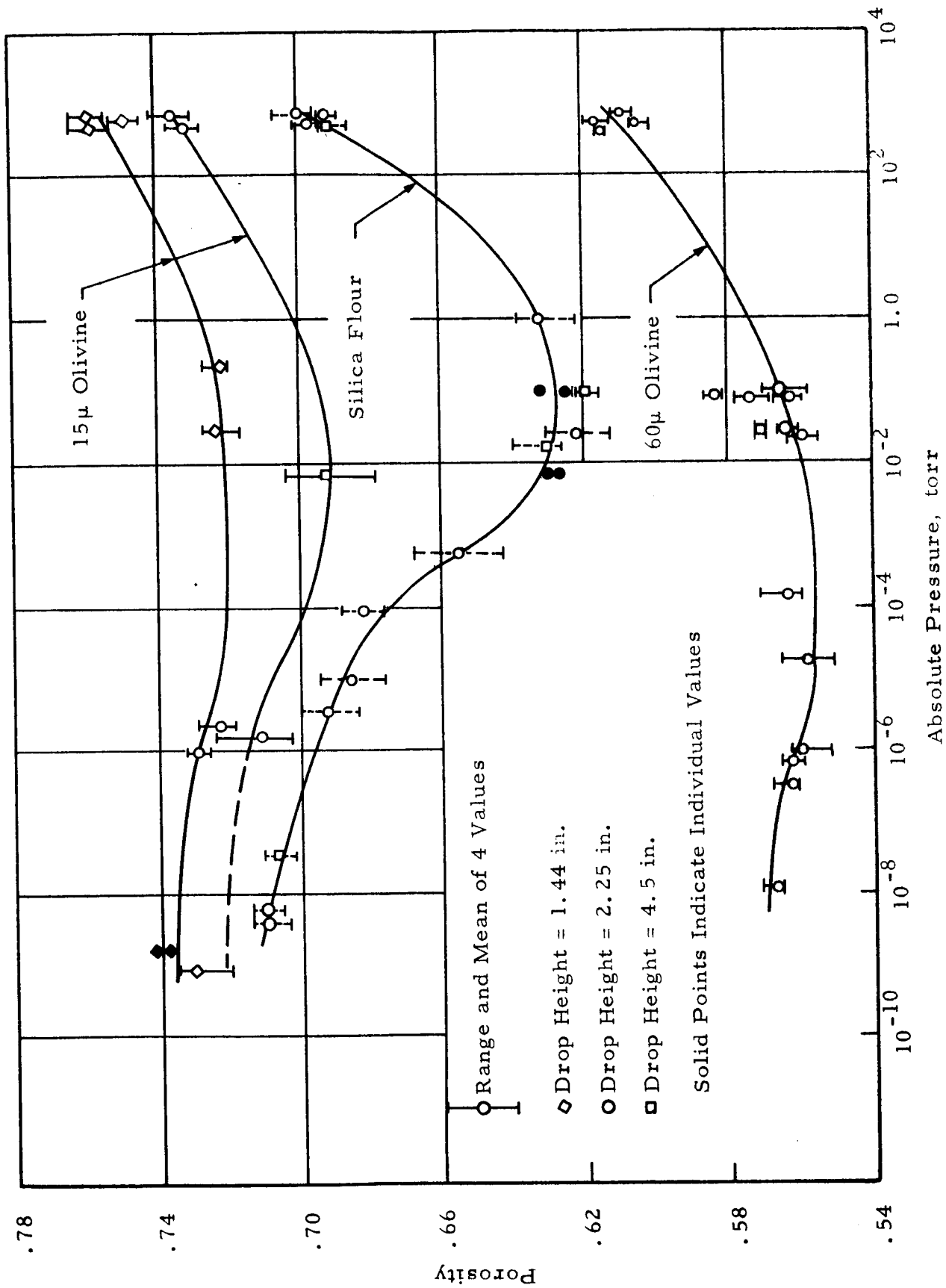
Fig. 12 POROSITY ATTAINED BY SOIL AS A FUNCTION OF VACUUM

Slightly higher porosities were obtained than in the previous
atmospheric tests, because of the use of a different drop height in the oven
than in the vacuum chamber. The porosity which was attained in each case
is shown graphically in Fig. 13. It is evident that the removal of the
hygroscopic moisture did cause a small decrease in the porosity. However,
deposition in low vacuum produced a decrease in porosity of approximately
0.07 which is relatively large in comparison to that shown in Fig. 13 and
hence it appears that hygroscopic moisture (1 percent) had little effect on
the grain structure of the quartz powder.
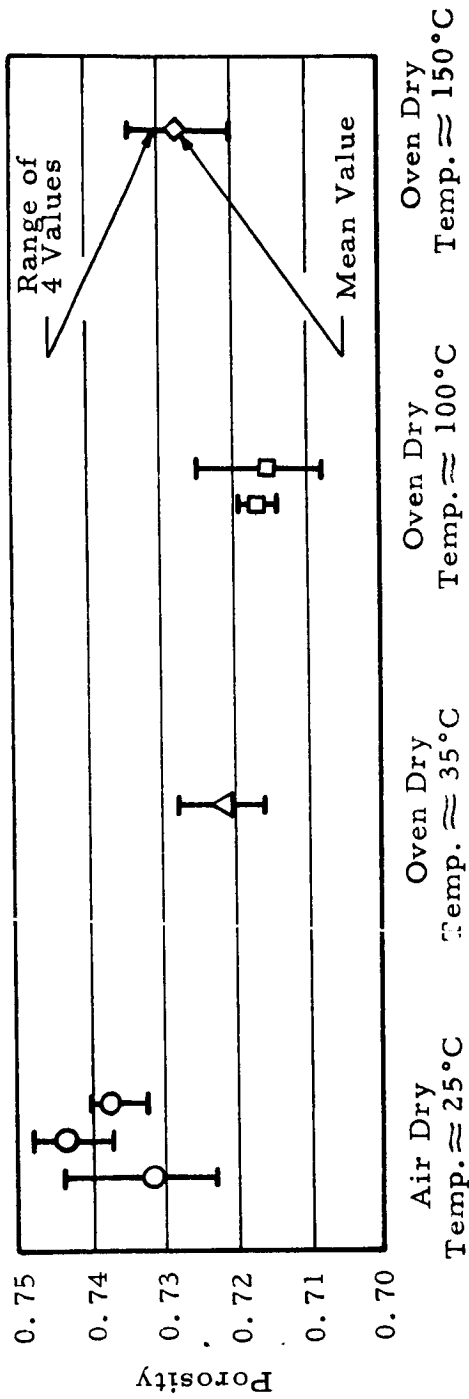
Fig. 13 POROSITY OF SILICA FLOUR DEPOSITED UNDER VARYING ENVIRONMENTS

V. DETERMINATION OF SHEAR STRENGTH PARAMETERS

The shear strength of a soil is generally referred to as the maximum shear stress which the soil is capable of resisting. This stress is a function of the soil cohesion and the normal stress on the plane of failure and in most cases may be represented approximately by the linear relationship

$$\tau = c + \sigma \tan \phi \qquad (8)$$

in which τ is the maximum shear stress

σ is the normal stress on the failure plane

c is the cohesion

ϕ is the angle of internal friction.

Equation (8) defines a straight line which is termed Mohr's rupture diagram, the intercept on the τ axis defining c and the slope defining ϕ. Thus, the cohesion or apparent cohesion represents the shear stress which the soil is capable of resisting with no normal stress on the failure plane and is due generally to interparticle forces and/or interlocking of the soil grains. Tan ϕ is analogous to the coefficient of friction between the soil grains and thus represents the contribution of the normal stress to the shear strength. It follows, therefore, that the shear strength of soil can be defined by the two parameters ϕ and c.

The most direct means of measuring these parameters is by triaxial or direct shear testing. Because of possible limitations imposed on the vacuum level by the outgassing of membranes required in the triaxial test, direct shear tests were used in these investigations. A complete discussion of the direct shear test and its limitations is presented in the final report on Phase I of this program and, therefore, only a brief description of the experiment and apparatus will be presented here.

The direct shear test consists of applying a normal stress on a prescribed failure plane and measuring the shear stress required to cause failure of the soil. The apparatus used in this investigation is shown schematically in Fig. 14. To minimize outgassing the entire equipment except for the force transducer and the heat shield was fabricated of stainless steel. The apparatus consisted basically of a two piece cylindrical mold in

IIT RESEARCH INSTITUTE

which the soil was placed and vertical and horizontal forces applied as indicated in Fig. 14. The upper half of the mold was supported on ball bearings with a maximum clearance between the two parts of 0.005 inch. A series of tests were performed in vacuums ranging from 1.1 to 2.8×10^{-8} torr with no soil in the apparatus and a normal load of 1.7 lb applied directly to the upper half of the shear box (this load would produce a normal stress of approximately 0.5 psi on a soil sample in the apparatus). The force required to displace the upper half of the box was found to be approximately 0.05 lb (corresponding to an average shear stress of approximately 0.01 psi). When no vertical force was applied to the box the force required to cause displacement was not measurable. Consequently, the friction in the apparatus may be considered negligible in comparison to the soil shear strength.

Experiments were performed using fine grained olivine, quartz powders and fine grained sand. Vacuum levels in the chamber ranged from atmospheric pressures to approximately 1×10^{-9} torr. As was discussed previously, however, the actual environmental vacuum (i.e., the vacuum in the soil pores) was probably less than that recorded in the chamber. In order to aid in outgassing the sample the top and bottom of the shear box were perforated and the sample was baked out. It was noticed in these experiments, as in others, that a considerably longer period of time was required to reach the ultimate vacuum when olivine was in the chamber than was the case for the quartz. Also, the ultimate vacuum was generally somewhat less for the olivine than the quartz.

Thus, considering the sample size and confinement and based on the results presented in Section III of this report, it was estimated that the actual vacuum level in the quartz powder was approximately one to two orders of magnitude lower than the chamber vacuum and even lower for the olivine. Because of the lower specific surface area of the sand it was estimated that the vacuum level in the pores was greater than for the powder but nevertheless, lower than that in the chamber. Because of the inability to accurately determine the actual vacuum in the soil pores the vacuum levels reported are those recorded in the chamber prior to performing the experiment.
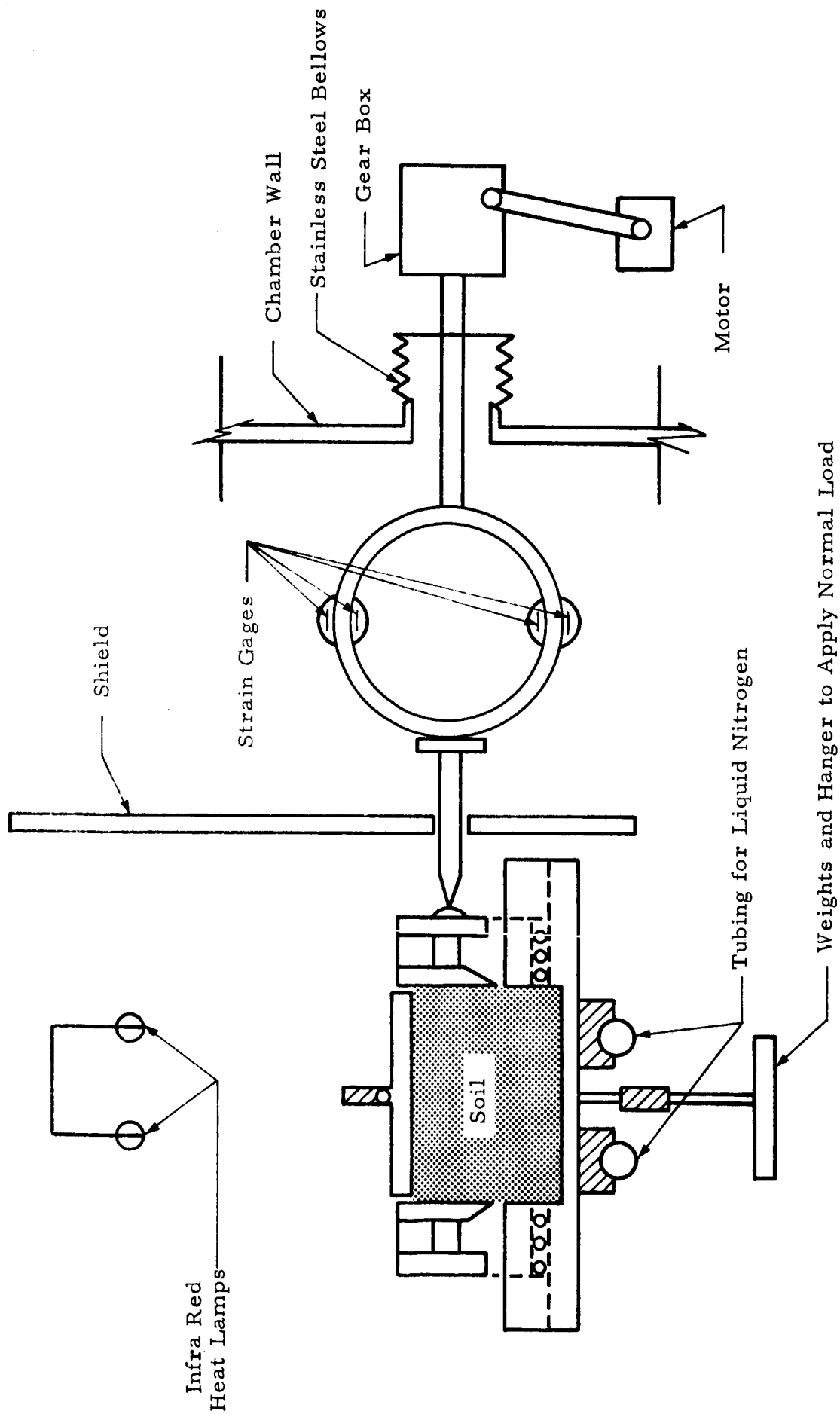
Fig. 14   DIRECT SHEAR APPARATUS

Chamber Wall

Stainless Steel Bellows

Gear Box

Motor

Shield

Strain Gages

Tubing for Liquid Nitrogen

Weights and Hanger to Apply Normal Load

Soil

Infra Red
Heat Lamps

The porosity of the powder samples was controlled by depositing the soil in the shear box by means of a sieve and then consolidating the sample under a normal stress equal to the greatest used in any experiment. This technique resulted in porosities ranging from 0.536 to 0.555 with an average value of 0.547 for 34 tests on quartz and from 0.618 to 0.640 with an average value of 0.631 for 35 tests on olivine. The sand samples were deposited by pouring through a tube with a slotted end piece to insure that the velocities of the sand grains were close to zero as they left the tube. The porosity was controlled by maintaining the bottom of the tube at a constant height above the surface of the deposited soil (in this case approximately 0.25 in.) and preconsolidating the sample by the same procedure used for the powder. The resulting porosities ranged from 0.410 to 0.422 with an average of 0.415 for 6 tests. For a small number of tests in which the porosities were not within the indicated range, the direction in which a correction for porosity would move the points is indicated in the figures.

Direct shear experiments were performed at room temperature and at elevated temperatures of approximately 250 deg F over a range of vacuum levels for the three soil types. The elevated temperatures were achieved by placing tubular quartz infrared lamps directly over the shear boxes as shown in Fig. 14. The shield shown in the figure was necessary to maintain a temperature close to room temperature at the load cells. This temperature never exceeded 130 deg F. As each strain gage bridge on the load cells consisted of four active arms they were temperature compensating except for possible effects on the gage factor. Calibrations were performed under various temperatures and it was found that the calibration factor did not vary significantly within the range from room temperature to 130 deg F.

A limited number of experiments were also performed on the quartz powder at low temperatures. The samples were cooled by passing liquid nitrogen through stainless steel tubing fastened to the bottom of the shear boxes. In order to increase the area of contact between the tubing and the shear boxes, aluminum spacers were placed between the tubing and the apparatus as shown in Fig. 14. To assure a high vacuum level in the pores,

it was necessary to bake the soil during pumpdown. Consequently, while the bottom of the soil could be cooled to a temperature of -120 deg F, the thermal conductivity of the soil and the stainless steel was such that the temperature at the top of the sample (approximately 1 inch in height) was approximately 10 deg F. The average temperature of the soil at the shear surface in all experiments, therefore, was approximately 0 deg F for the low temperature experiments.

A. Results of Direct Shear Tests on Quartz Powder

Direct shear tests on the quartz powder at room temperature were performed in Phase I and, hence, the results of those tests will be presented only where needed for comparative purposes. To briefly summarize the results, both the stiffness (i.e., resistance to shear displacement) and the shear strength were observed to increase at vacuum levels greater than approximately 10^{-7} torr. The increase in the shear strength was attributed mainly to an increase in the apparent cohesion while the angle of internal friction increased only slightly.

Representative curves showing the shear stress as a function of the displacement at elevated temperatures in atmosphere and ultra-high vacuum are presented in Fig. 15 and 16 along with results at room temperature. In Fig. 15 (σ = 2.03 psi) it can be seen that for small displacements the curves are very nearly linear up to a point at which the slope changes and the stress-displacement curve becomes nonlinear. For room temperatures the stress at which this change takes place is greater in vacuum than in atmosphere and even greater at elevated temperatures, while the temperature has a negligible effect on the shape of the curve under atmospheric conditions. Thus, it is evident that under these normal stresses the stiffness of the soil increased under vacuum with an increase in temperature causing a further increase in stiffness.

Figure 16 shows the stress-displacement curves for lower normal stresses in which it can be seen that a peak shear stress is reached at a displacement of approximately 0.002 inch under all conditions. This peak, however, is quite small under atmospheric conditions but increases at ultra-high vacuum and is largest under both elevated temperature and vacuum.
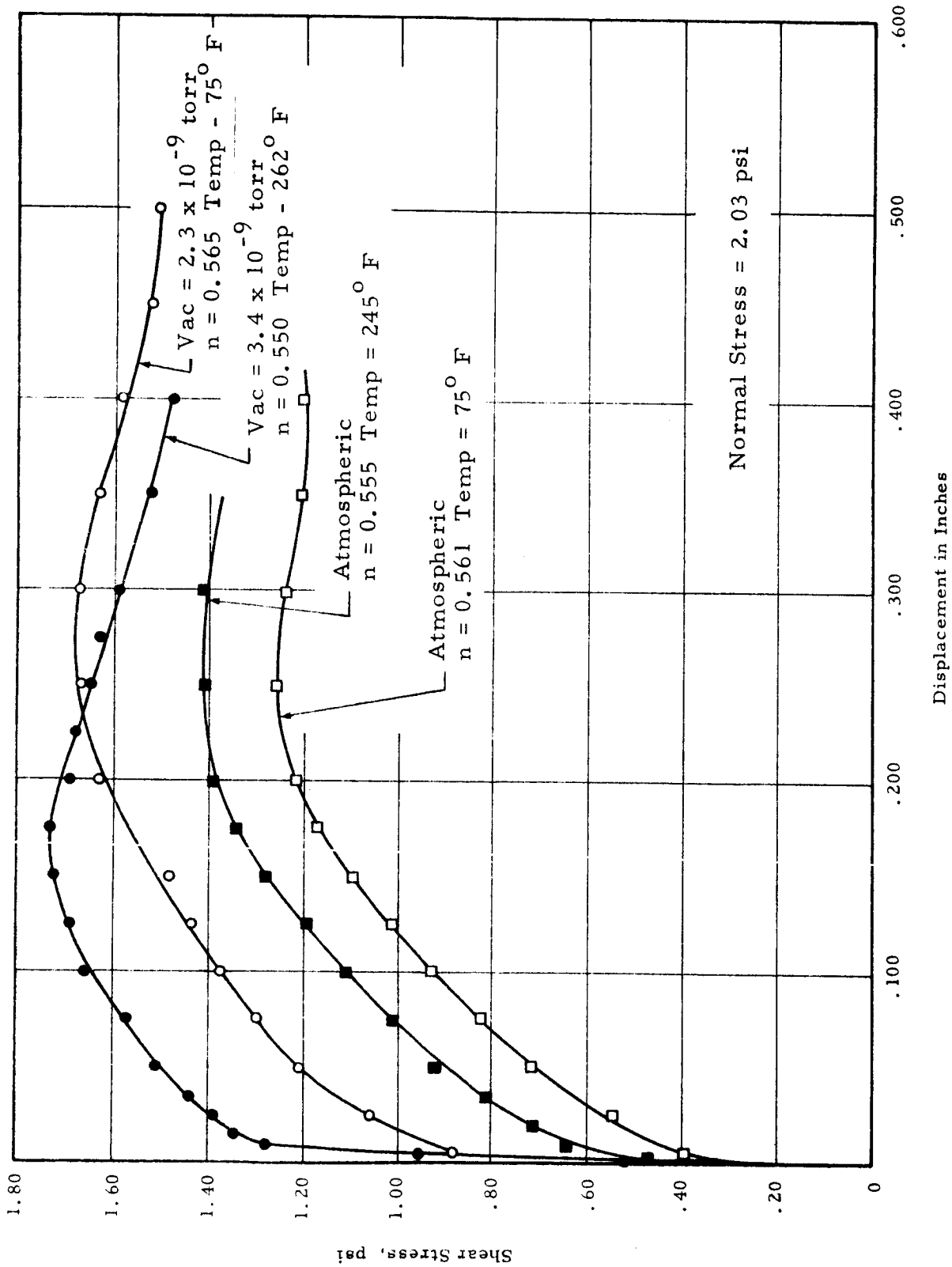
IIT RESEARCH INSTITUTE

Fig. 15 SHEAR STRESS AS A FUNCTION OF DISPLACEMENT IN DIRECT
SHEAR TESTS ON QUARTZ POWDER

0.600

0.500

0.400

0.300

0.200

0.100

0

Displacement, in.

○ Vac = 8 x 10⁻¹⁰ torr σ = 0.40 psi
  n = 0.549   Temp = 75° F

□ Atmospheric   σ = 0.40 psi
  n = 0.575   Temp = 75° F

● Vac = 3.3 x 10⁻⁹ torr σ = 0.54 psi
  n = 0.550   Temp = 75° F

■ Atmospheric   σ = 0.54 psi
  n = 0.548   Temp = 236° F

0.7
0.6
0.5
0.4
0.3
0.2
0.1
0
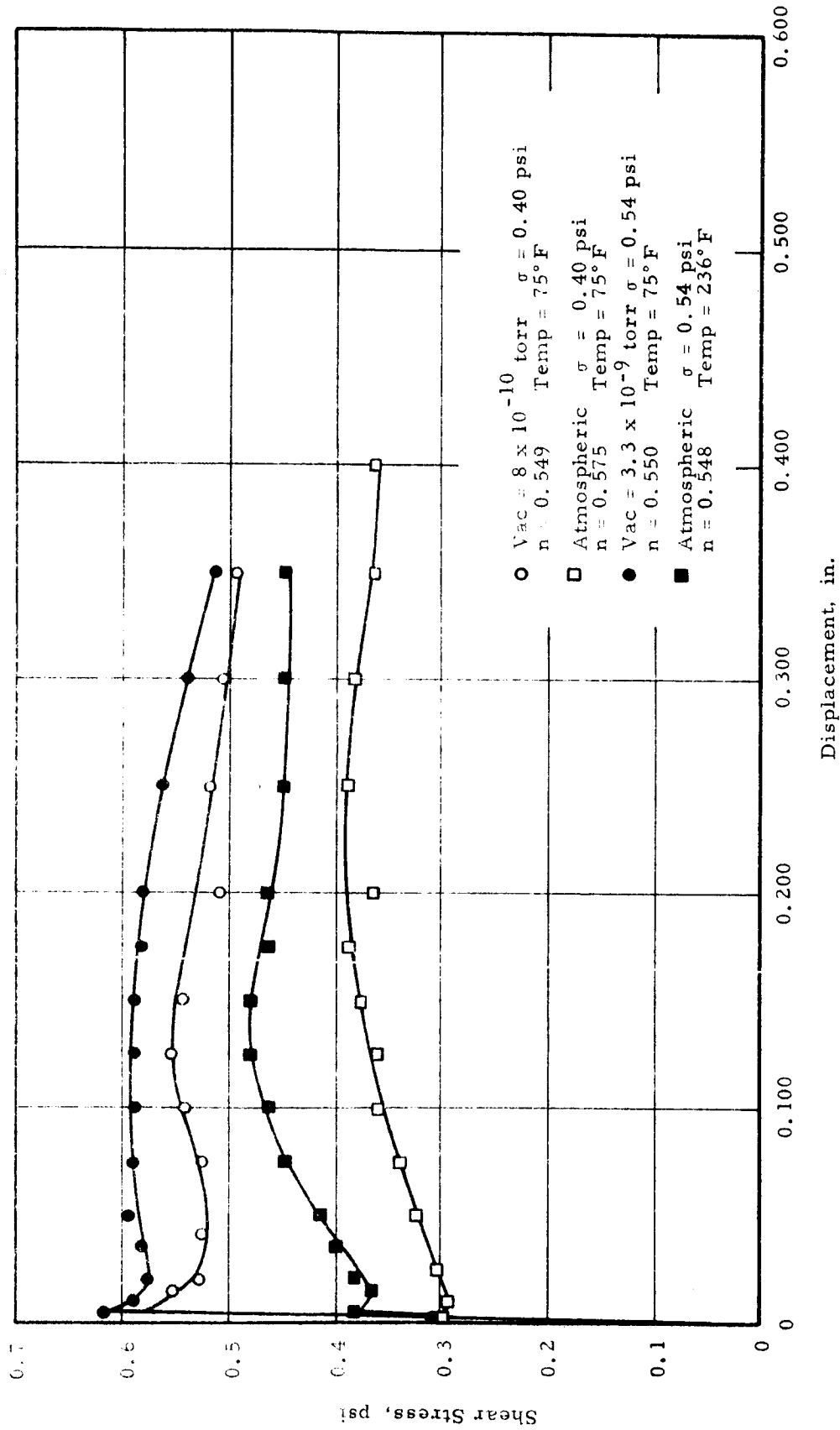
Shear Stress, psi

Fig. 16 SHEAR STRESS AS A FUNCTION OF DISPLACEMENT IN DIRECT
SHEAR TESTS ON QUARTZ POWDER

Subsequent to reaching this peak the shear stress decreased and then increased to another maximum point at considerably larger values of displacement. It should be noted also that under vacuum this initial peak was of approximately the same magnitude as the maximum stress developed at the higher displacements, whereas in the atmosphere it was generally smaller. Thus, an increase in stiffness under vacuum is apparent at lower normal stresses also.

Since the apparatus consisted of two shear boxes mounted in the vacuum chamber it was possible to obtain two points on the rupture envelope under identical conditions. This would then define the rupture line assuming it to be a straight line. In order to ascertain the true shape of the rupture line a number of experiments were performed under various normal stresses in atmosphere and ultra-high vacuum. As shown in Section III the drawdown history has a pronounced influence on the actual vacuum in the soil pores and consequently, care had to be taken to duplicate the drawdown curves for these experiments as closely as possible in order to insure identical environmental conditions. The rupture diagrams so determined in atmosphere and vacuum are shown in Fig. 17 from which it is evident that the rupture line is a straight line under all conditions. However, there does exist some experimental scatter in the data particularly at the higher normal stresses and consequently the determination of $\emptyset$ and c based on only two points could result in somewhat anomalous results. To show the effect of vacuum on the shear strength, therefore, the maximum shear stress was plotted as a function of the vacuum level in Fig. 18 for various normal stresses. For the lower normal stresses, the maximum shear stress was taken as the second maximum point, since the displacement at which this shear stress was developed was more consistent with those for the higher normal stress. Although there is some scatter in the data a definite increase in shear resistance under vacuum is evident.

The shear strength parameters may then be determined from the values given by the curves in Fig. 18 and are shown in Fig. 19. It must be recognized that the values at room temperature are based on a relatively small number of points. The apparent cohesion is not affected

appreciably by elevated temperatures whereas the angle of internal friction is considerably greater at elevated temperatures.

It should be remembered that Fig. 17 thru 19 are based on the second maximum point for the lower normal stresses and do not consider the initial peak stress. It is possible that the cohesion and the friction may be developed at different displacements and, hence, the initial peak may be attributed to cohesion which was developed at relatively low values of displacement. However, to determine what portion of this peak stress is due to cohesion would be difficult. It is probably due to bonds developed at the asperity contacts in the soil and, hence, would be principally a cohesive stress. The effect of vacuum on this peak stress is shown in Fig. 20. Consistent with previous results a definite increase in peak stress is seen to occur under vacuum.

A limited number of experiments were performed on the quartz powder at low temperatures under ultra-high vacuum for representative stress-displacement curves which are shown in Fig. 21. Comparison with Fig. 15 and 16 shows the curves to be similar to those under elevated temperatures. Therefore, it appears that the stiffness is somewhat greater than at room temperature. Experiments were not performed in the atmosphere at these low temperatures because of the extensive formation of frost on the shear boxes and within the soil mass under such conditions. The rupture diagram is shown in Fig. 22 from which increase in shear strength over that at ambient conditions is evident. It differs little, however, from that at ultra-high vacuum and ambient temperatures.

Thus, the effect of vacuum on the shear strength of the quartz powder was to increase both the cohesion and angle of internal friction. While temperatures of approximately 0 deg F appear to have little influence on the shear strength under vacuum, an increase in the temperature produces a further increase in shear strength, due to an increase in the angle of internal friction.

B. Results of Direct Shear Tests on Olivine Powder

Representative curves of the shear stress as a function of the displacement for the olivine powder are shown in Fig. 23 and 24. For the higher

IIT RESEARCH INSTITUTE

-34-

normal stress (Fig. 23) the stiffness of the soil is essentially the same under vacuum as in atmosphere except for a small increase in stiffness under elevated temperature and ultra-high vacuum. At the lower normal stress, there appears to be an increase in stiffness under vacuum at both temperatures and in atmosphere at elevated temperature. As in the quartz powder an initial peak may be seen to occur under vacuum at both room temperature and elevated temperature. In atmosphere such a peak is also shown for the elevated temperatures although this did not occur in all cases.

The rupture diagram for the olivine powder is shown in Fig. 25. It is evident that this is a straight line at least within the stress levels used. The maximum shear stress is shown as a function of vacuum level in Fig. 26. Again it should be noted that the maximum stress was taken as the second peak which developed and does not consider the initial peak. It can be seen that for the higher normal stress there exists a considerable amount of scatter and the data does not clearly define a relationship between shear stress and vacuum level. At the lower normal stress there appears to be a small increase in stress at the higher vacuum levels for elevated temperatures but at room temperature the effect of vacuum is negligible.

Because of the wide scatter in the data at the higher normal stress it is not possible to determine meaningful values of $\emptyset$ and c based on Fig. 26. However, from Fig. 25 it appears that the shear strength of the olivine is essentially the same at all temperatures under atmospheric conditions. At room temperature the vacuum has little, if any, effect on the shear strength; however, there is a rather definite increase in the shear strength at elevated temperatures under vacuum due mainly to an increase in the apparent cohesion.

The initial peak which developed in the olivine is shown as a function of vacuum level in Fig. 27. A very definite increase takes place under vacuum at room temperature with a somewhat smaller increase under elevated temperature. However, it should be noted that the peak stress was always greater at the higher temperatures than at room temperature.

IIT RESEARCH INSTITUTE

Fig. 17   MOHR'S RUPTURE DIAGRAM FOR QUARTZ POWDER

□ Ambient Conditions

○ 2 to 7 x 10^{-9} torr ambient temperature

■ 760 torr   250° F

● 3 to 6 x 10^{-9} torr   250° F

Normal Stress, psi
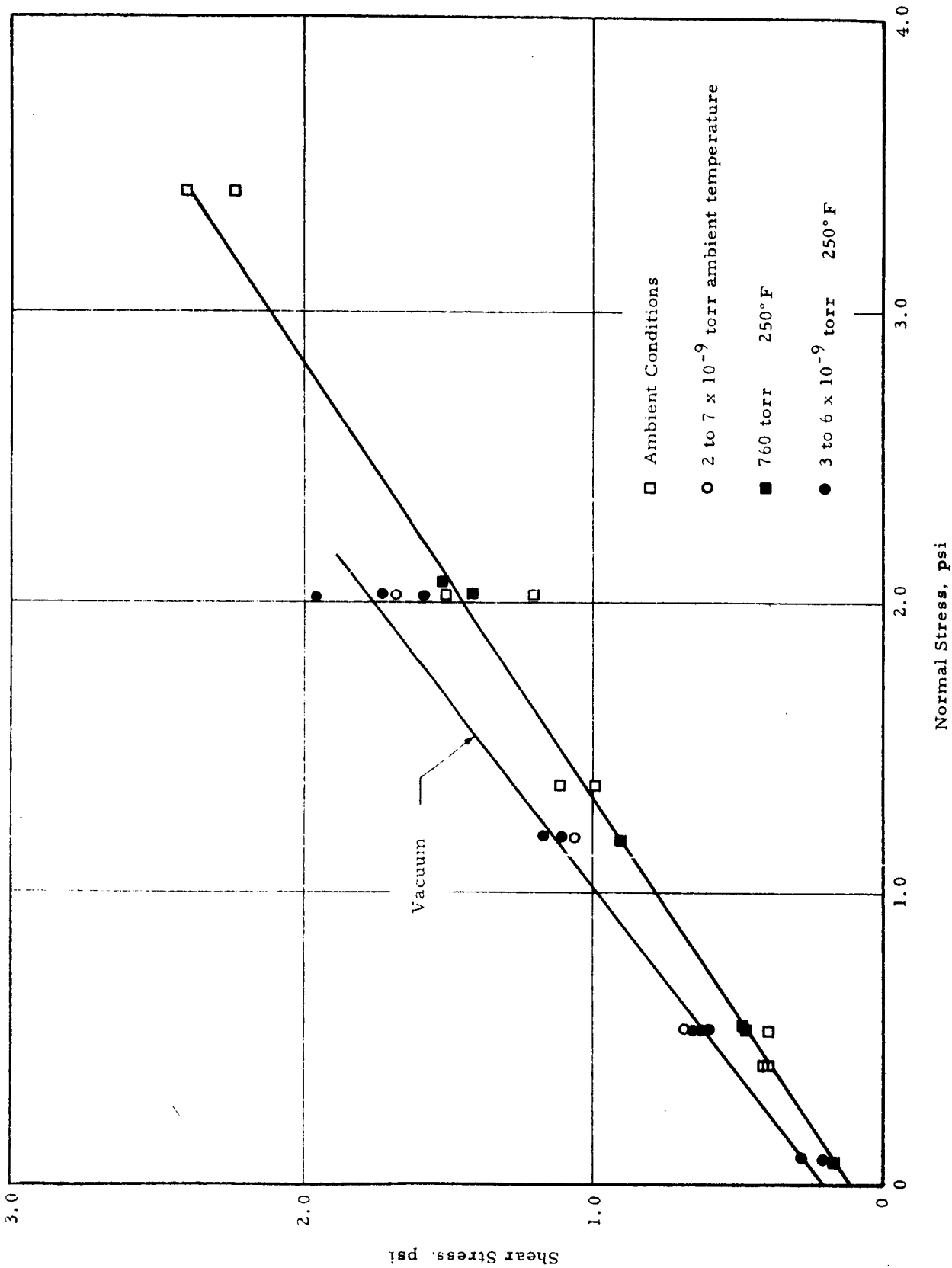
Shear Stress, psi
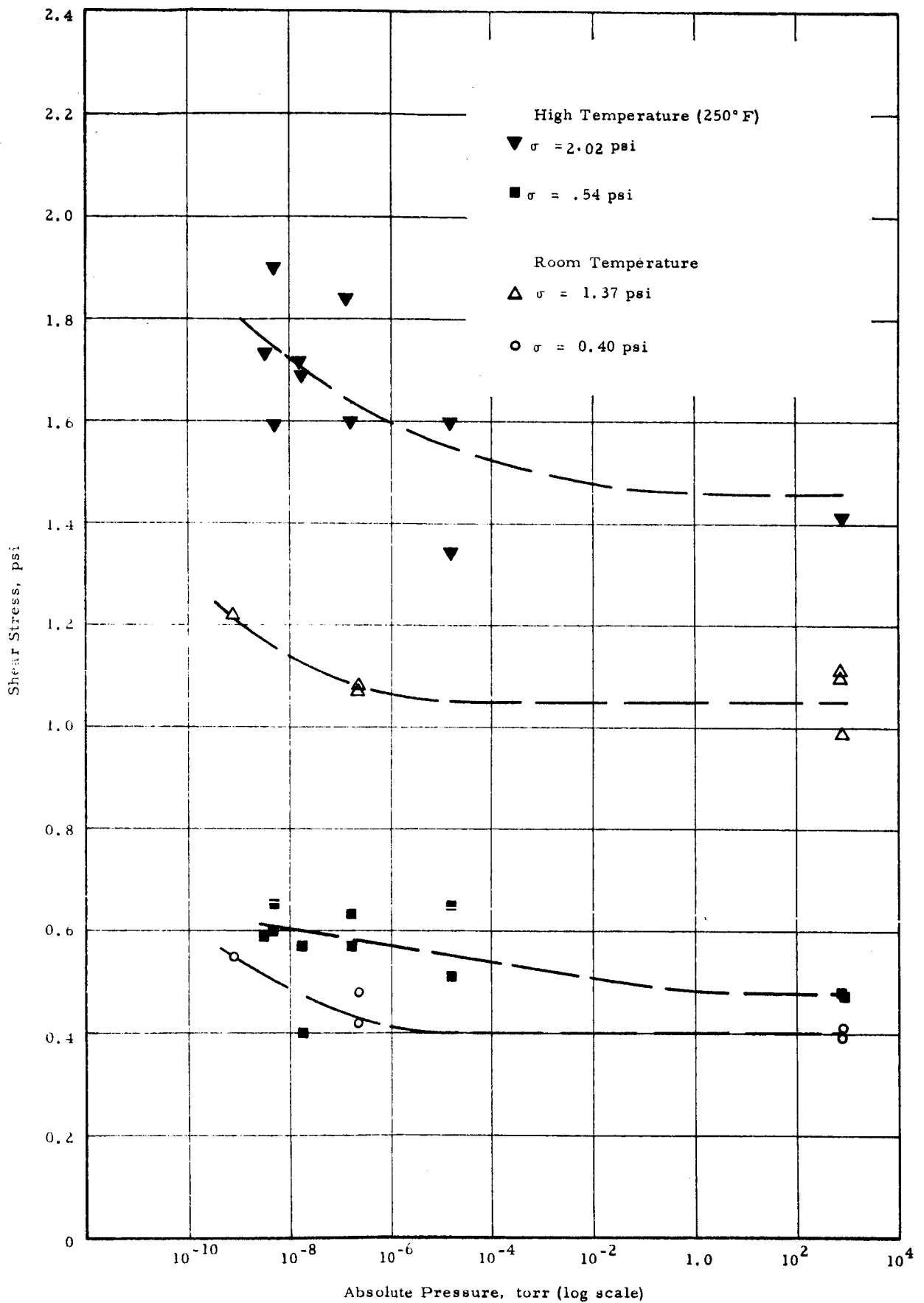
Vacuum

Fig. 18 EFFECT OF VACUUM ON MAXIMUM SHEAR STRESS
OF QUARTZ POWDER
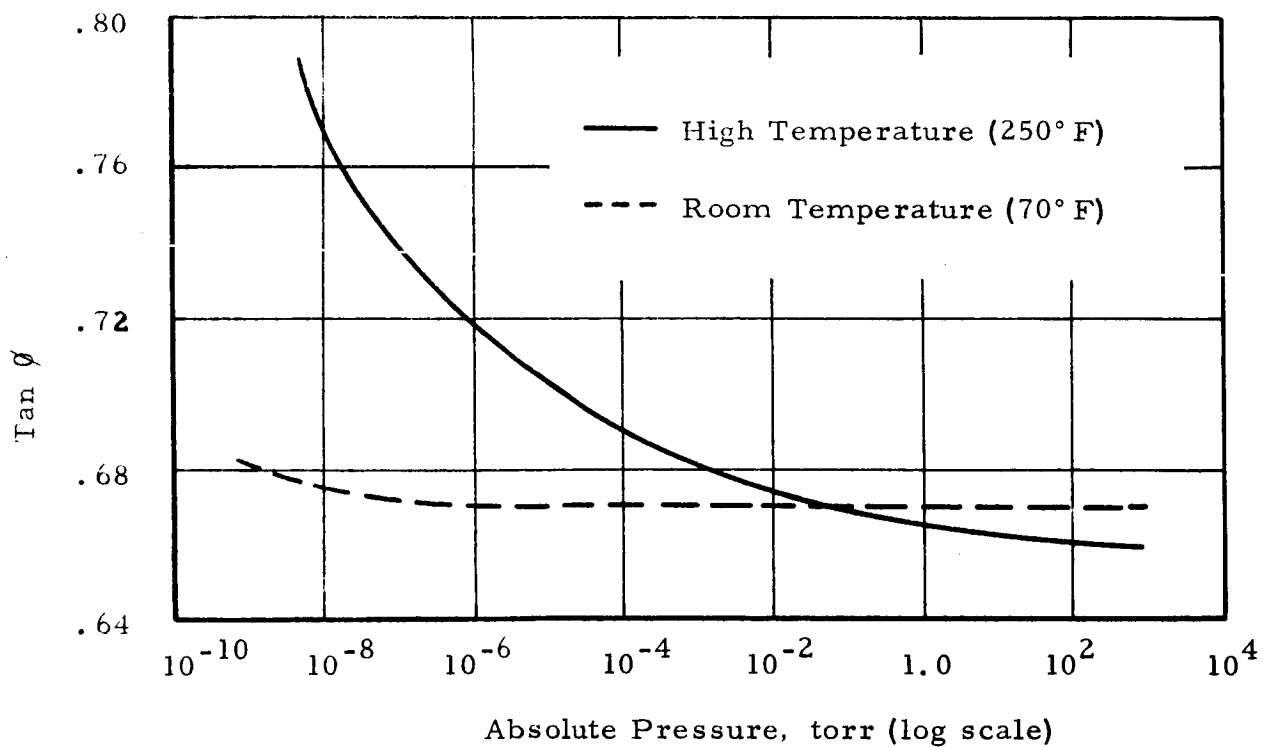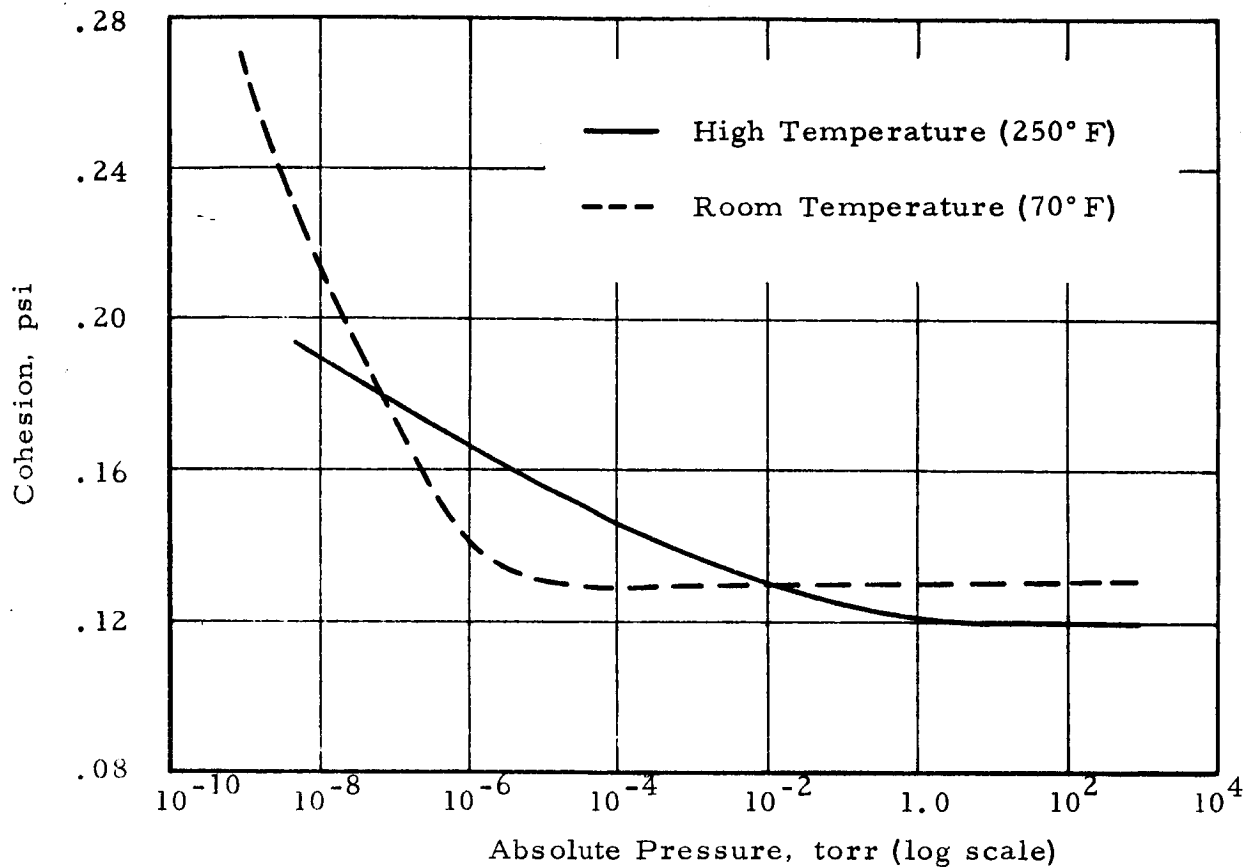
Fig. 19 EFFECT OF VACUUM ON SHEAR STRENGTH PARAMETERS
OF QUARTZ POWDER
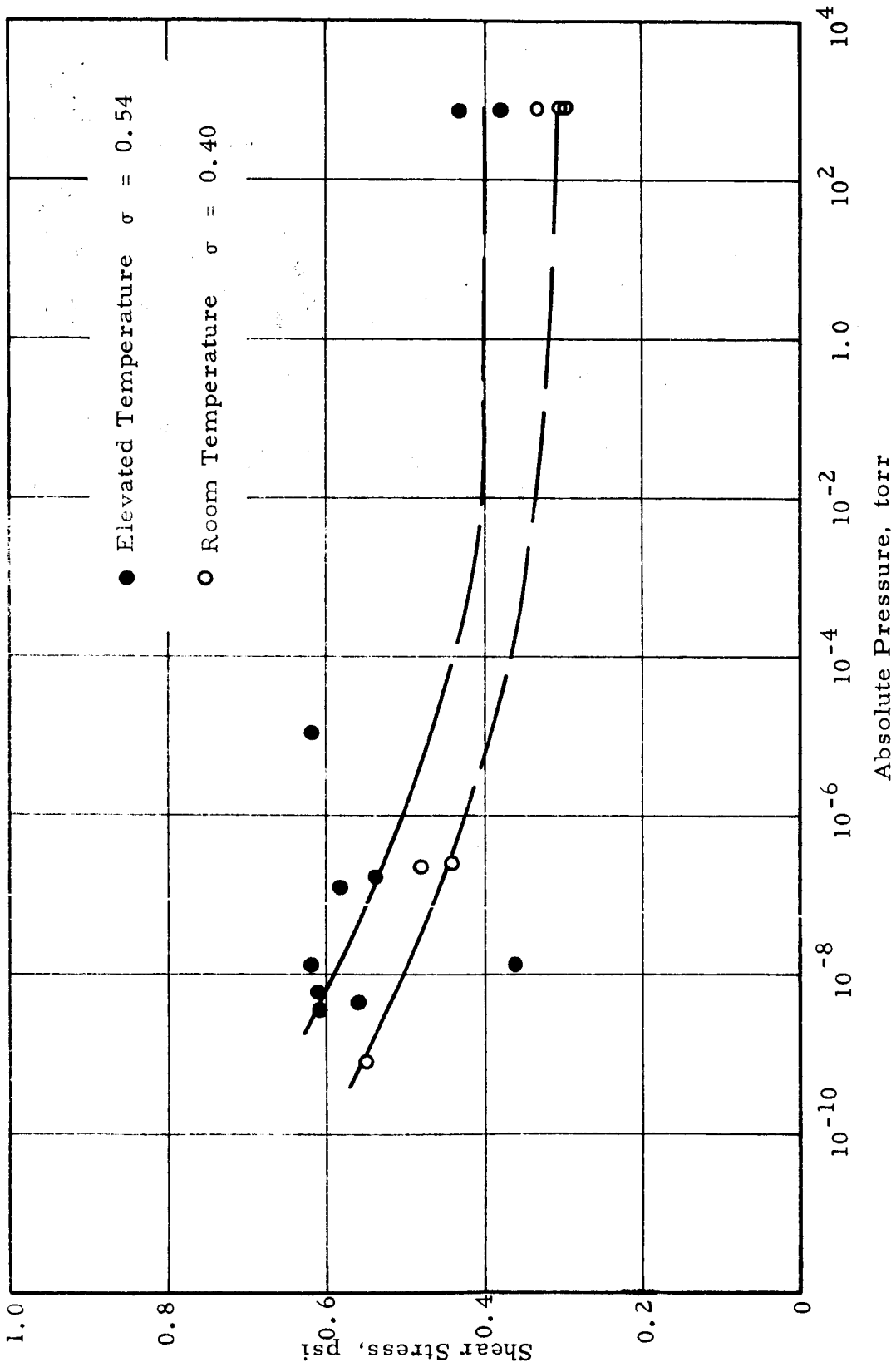
Fig. 20   EFFECT OF VACUUM ON INITIAL PEAK SHEAR STRESS (τ_1)
           IN SILICA FLOUR
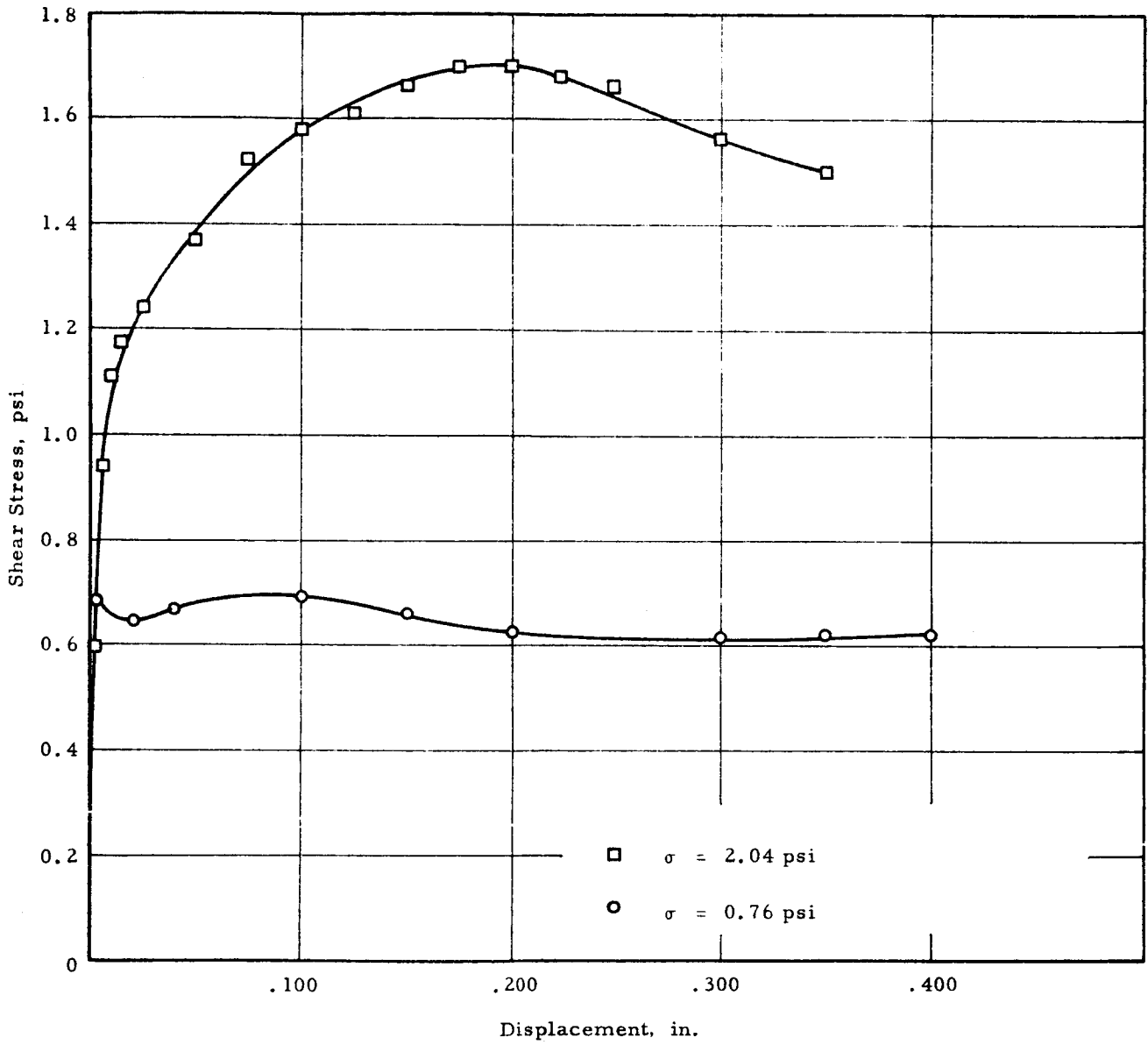
Fig. 21   SHEAR STRESS VERSUS DISPLACEMENT IN DIRECT SHEAR TESTS
ON QUARTZ POWDER AT LOW TEMPERATURES
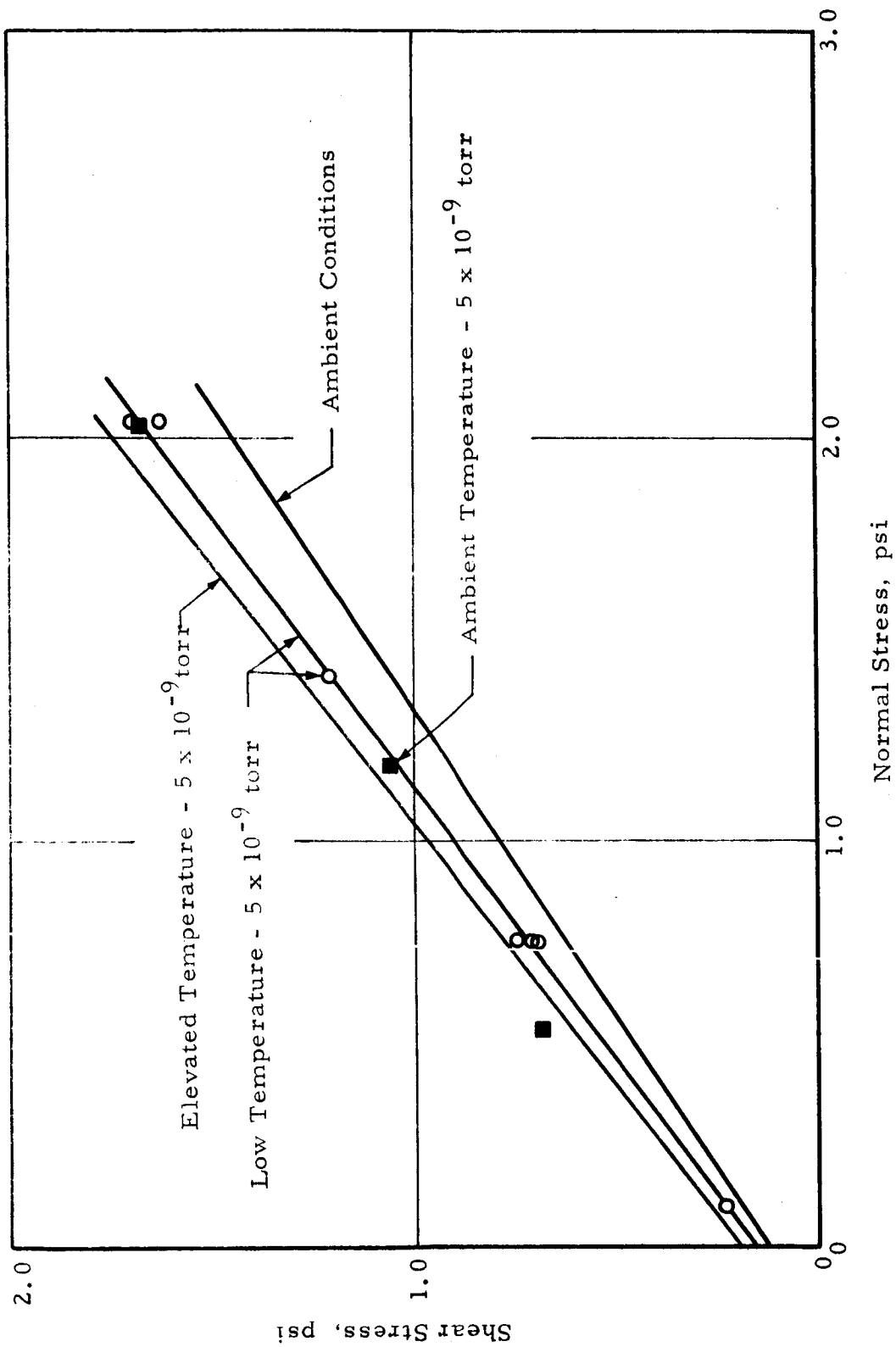
Fig. 22   RUPTURE DIAGRAM FOR QUARTZ POWDER UNDER LOW
TEMPERATURES
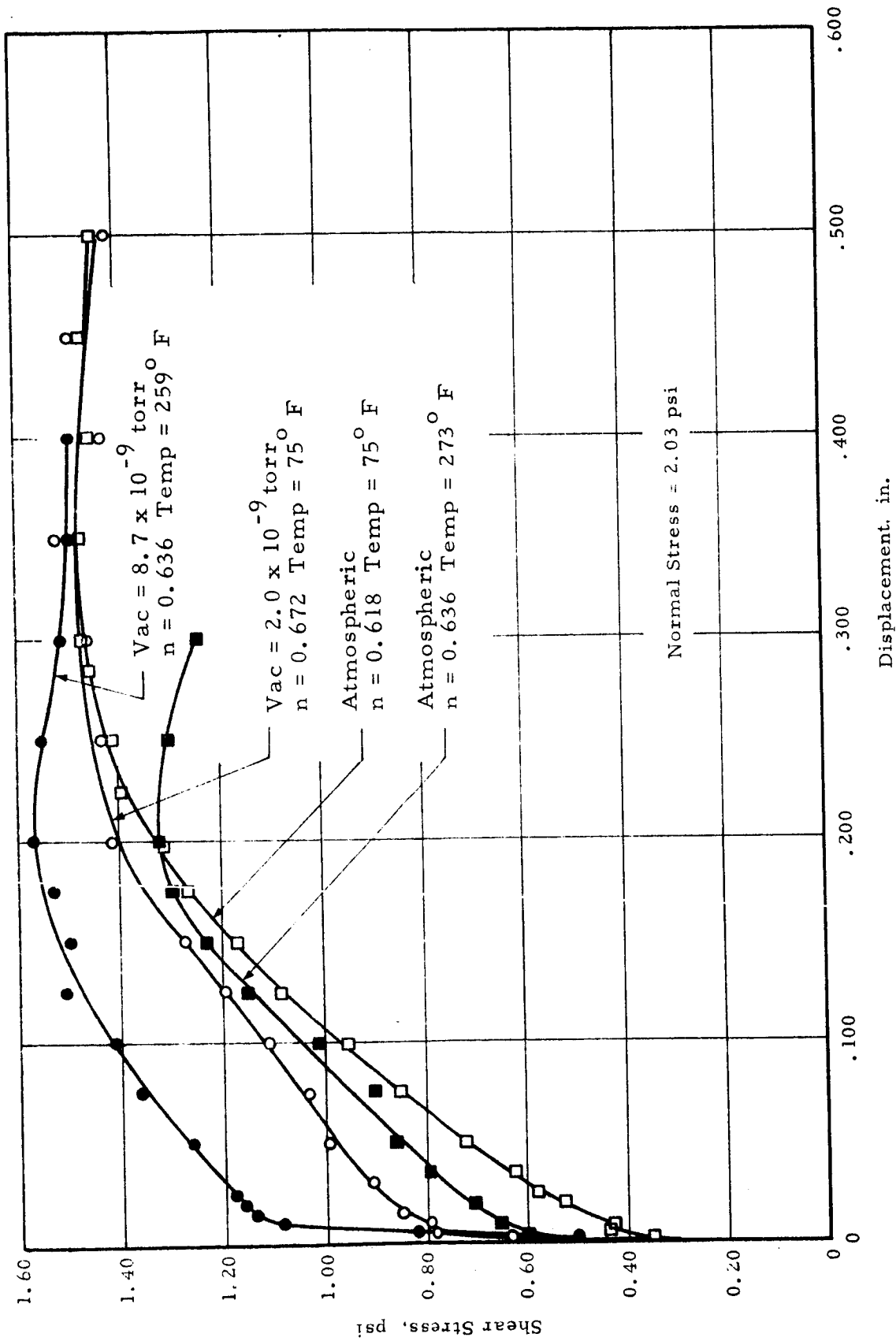
Fig. 23   SHEAR STRESS AS A FUNCTION OF DISPLACEMENT IN DIRECT SHEAR TESTS
ON OLIVINE POWDER
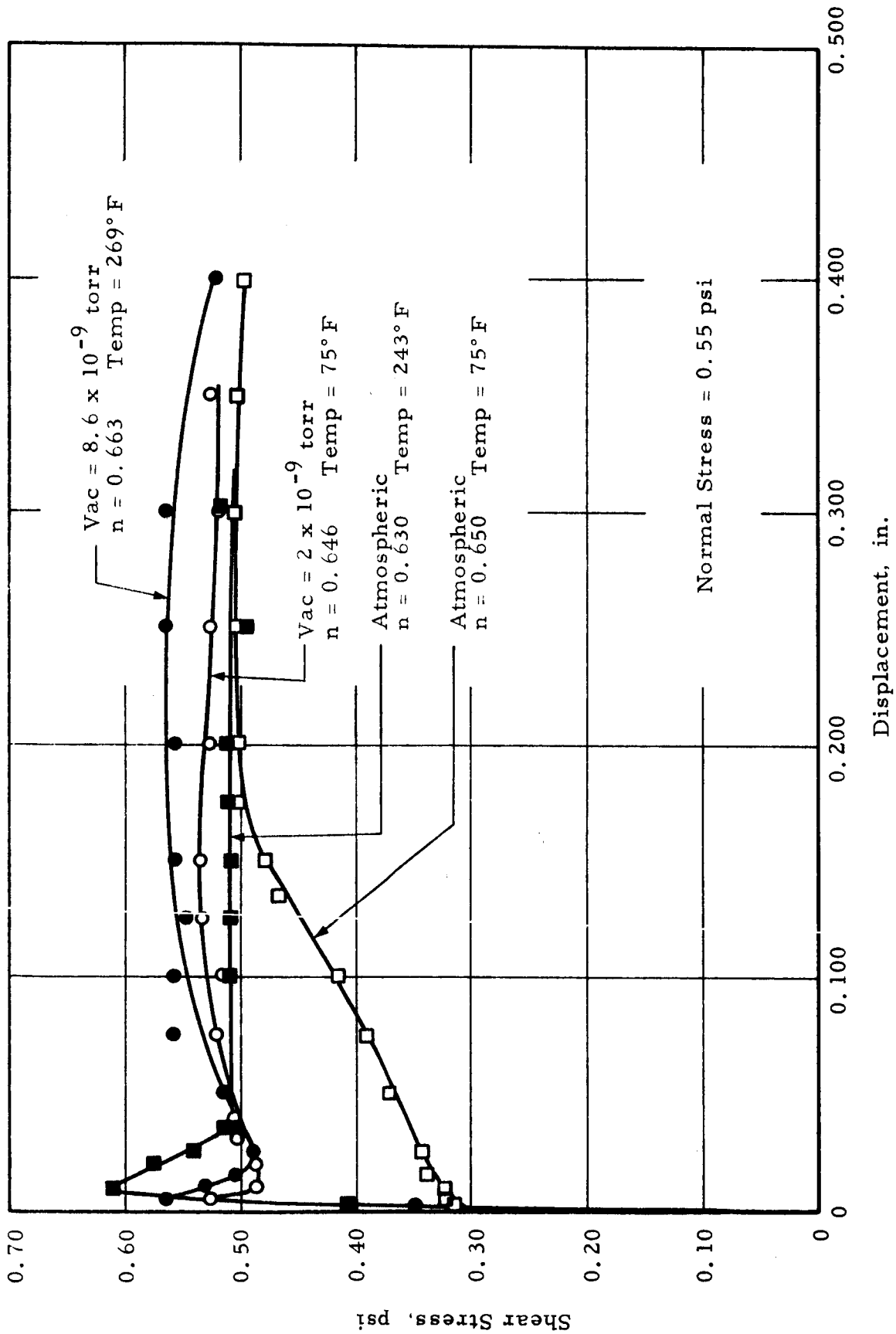
Fig. 24 SHEAR STRESS AS A FUNCTION OF DISPLACEMENT IN DIRECT SHEAR TESTS ON OLIVINE POWDER

- 43 -
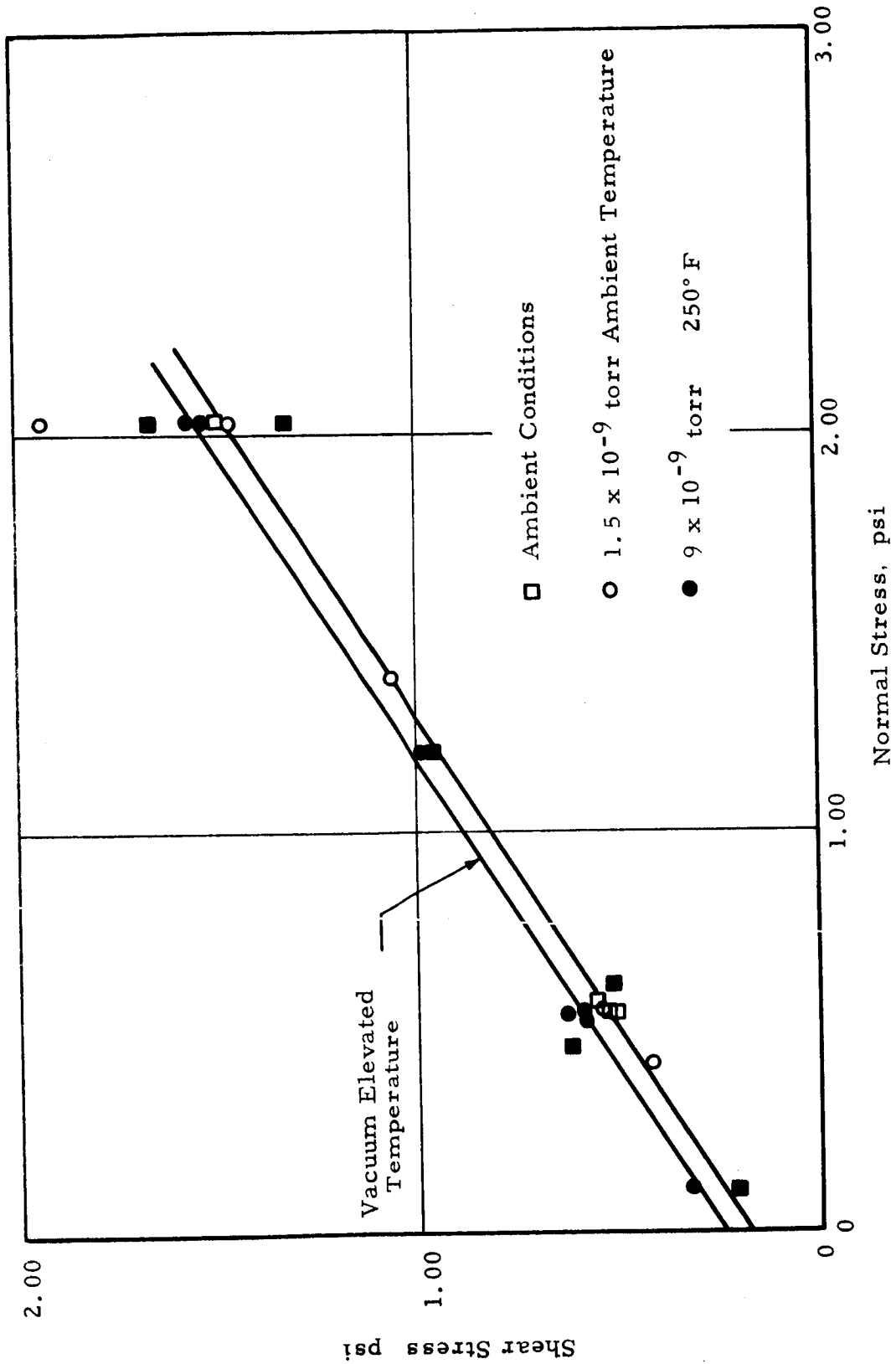
Fig. 25   MOHR'S RUPTURE DIAGRAM FOR OLIVINE POWDER
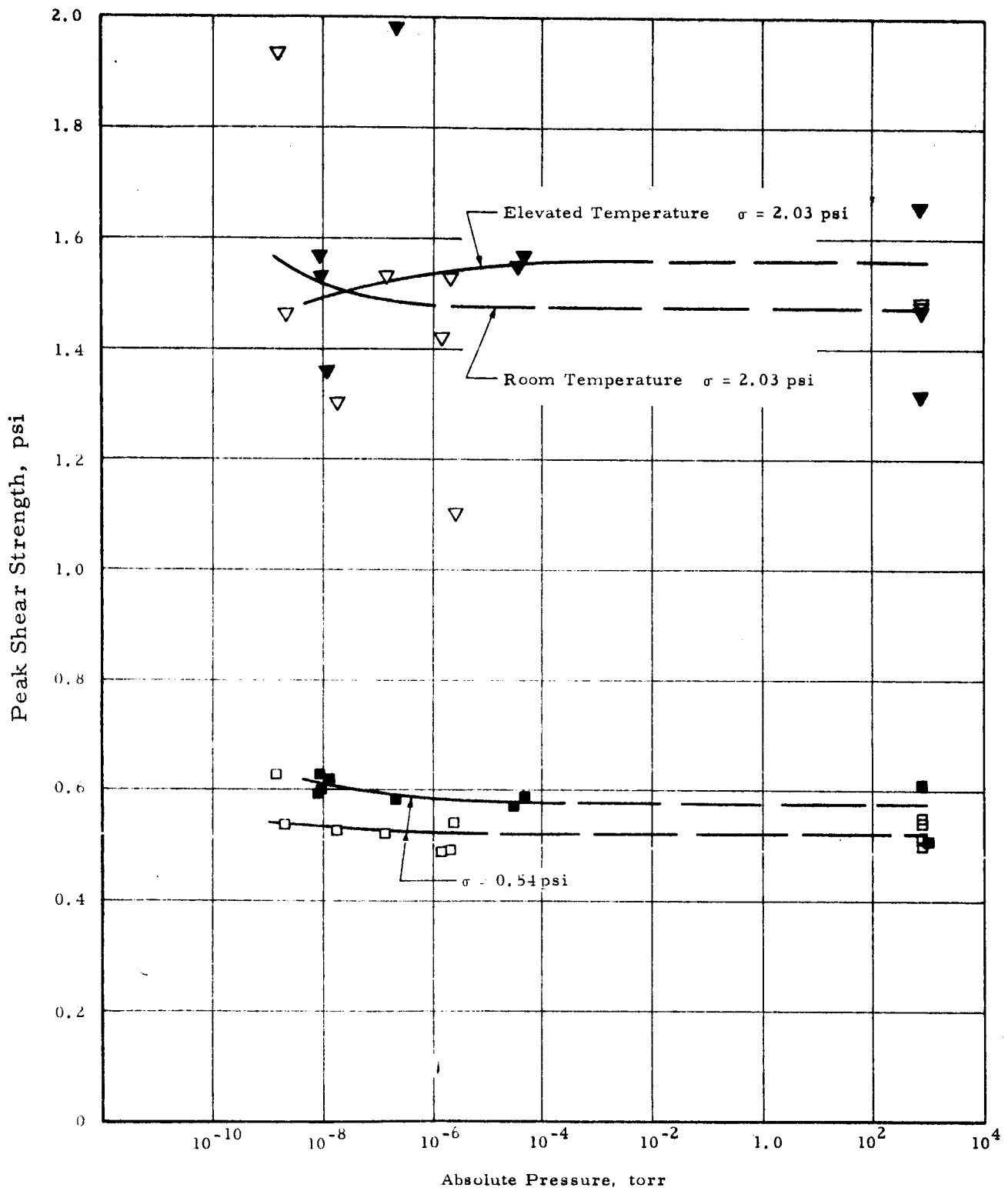
Fig. 26   EFFECT OF VACUUM ON MAXIMUM SHEAR STRESS IN OLIVINE
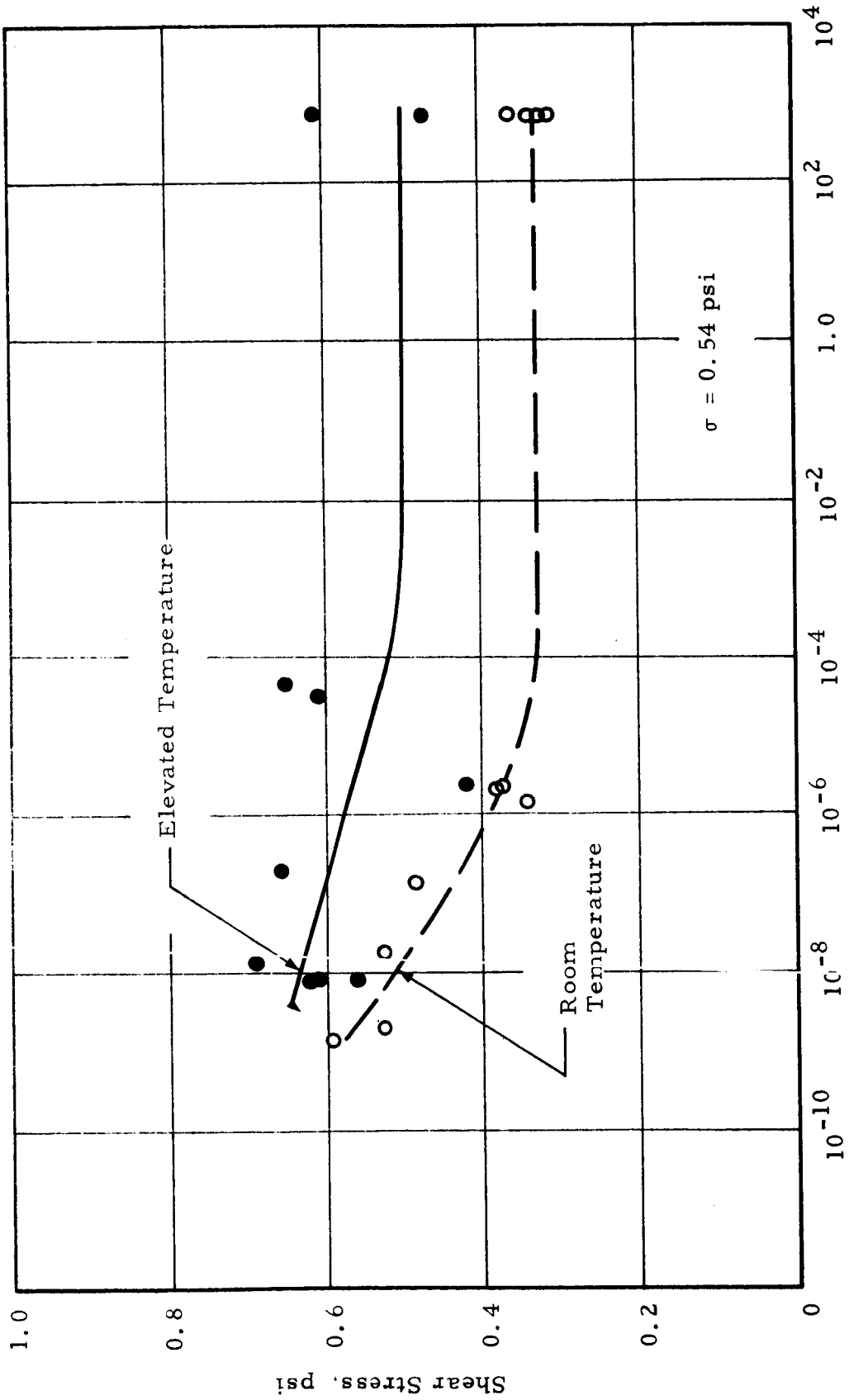
Fig. 27   INITIAL PEAK SHEAR STRESS (τ_1) AS A FUNCTION OF VACUUM LEVEL (OLIVINE)

- 46 -

C.   Results of Direct Shear Tests on Fine Sand

A limited number of experiments were also performed on fine grained sand the results of which are shown in the form of stress versus displacement curves in Fig. 28. It can be seen that the general shape of the curves in atmosphere is independent of temperature. Under vacuum and elevated temperature, however, the stiffness appears to be greater than in atmosphere.

The rupture diagram for the sand is shown in Fig. 29. In view of the fact that vacuum and high temperatures were observed previously to have no effect on the shape of the rupture diagram the assumption of a straight line in Fig. 29 is believed to be valid. Although the data is rather limited it appears that the effect of vacuum and elevated temperature is to cause an increase in angle of internal friction with little, if any, change in the apparent cohesion.
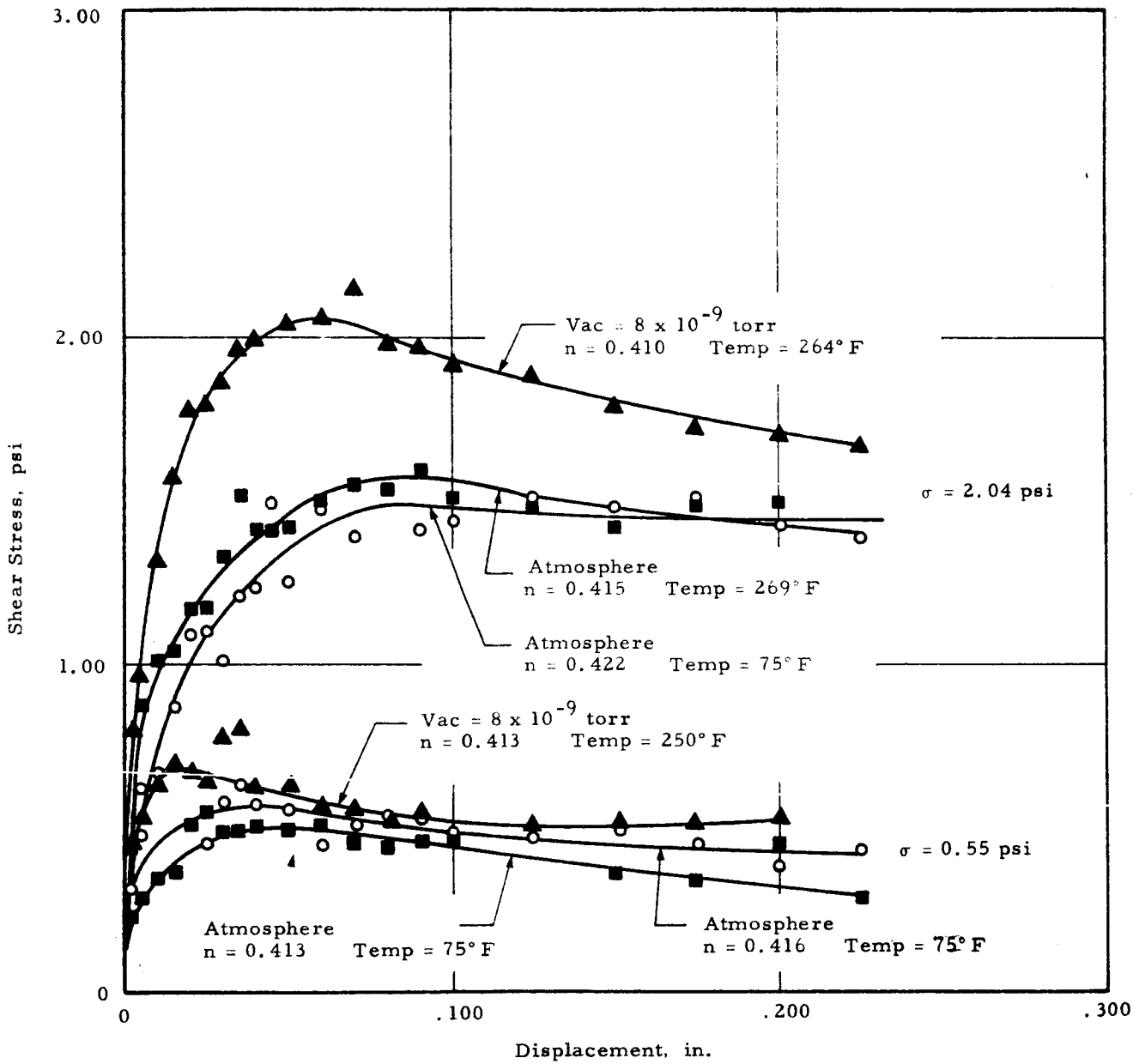
Fig. 28   SHEAR STRESS AS A FUNCTION OF DISPLACEMENT ON DIRECT
SHEAR TESTS ON FINE SAND
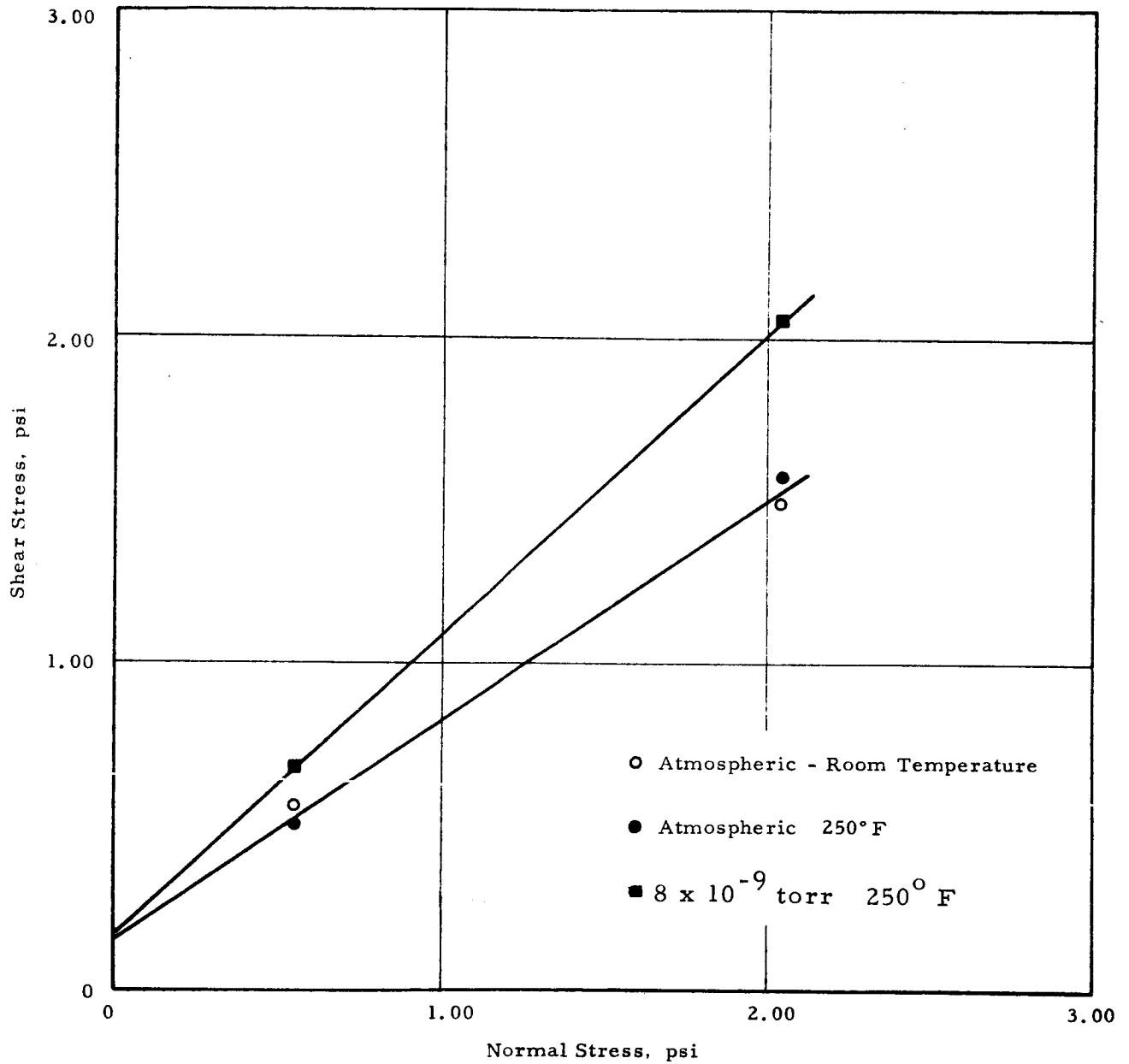
Fig. 29   MOHR'S RUPTURE DIAGRAM FOR FINE SAND

VI.   STATIC BEARING CAPACITY OF SMALL FOOTINGS

Experiments were performed to determine the effect of vacuum on the bearing capacity of small loaded footings. Measurements were made of the load-penetration relationships of 1 inch and 2 inch diameter circular footings on quartz powder in atmosphere and at vacuum levels of approximately 1×10^{-7} torr.

In order to aid in outgassing the sample during drawdown, holes were drilled in the bottom and sides of the container as indicated in Fig. 30. Quartz infrared heat lamps were suspended below the soil to permit efficient bakeout of the sample. Prior to placing it in the vacuum chamber, the soil was heated to approximately 350 deg F in the atmosphere for a period of 16 hours.

Because of the large amount of soil and, hence, the large pumping speed necessary to achieve high vacuum levels, a 35 inch oil diffusion pump was used to evacuate the chamber. Backstreaming was minimized by placing a chevron baffle between the chamber and the pump and cooling the system with liquid nitrogen.

The apparatus used in the investigation is shown schematically in Fig. 30. The soil container consisted of a stainless steel cylinder having a diameter of 28 inches and a false bottom permitting a soil depth of approximately 17 inches.

The effect of container size on bearing capacity was investigated previously in Phase I. It was found that the width of container should be approximately eight times the footing diameter and have a depth of three times the footing diameter. It was observed, however, that the actual size of the container must also be considered and for large containers (width greater than approximately 2 ft), smaller ratios of container width to footing diameter could be used.

In this investigation a number of experiments were performed in the same soil bin at different positions on the surface. The minimum distance from any footing side to that of the container was approximately 8 inches and the distance between any two footing locations was greater than
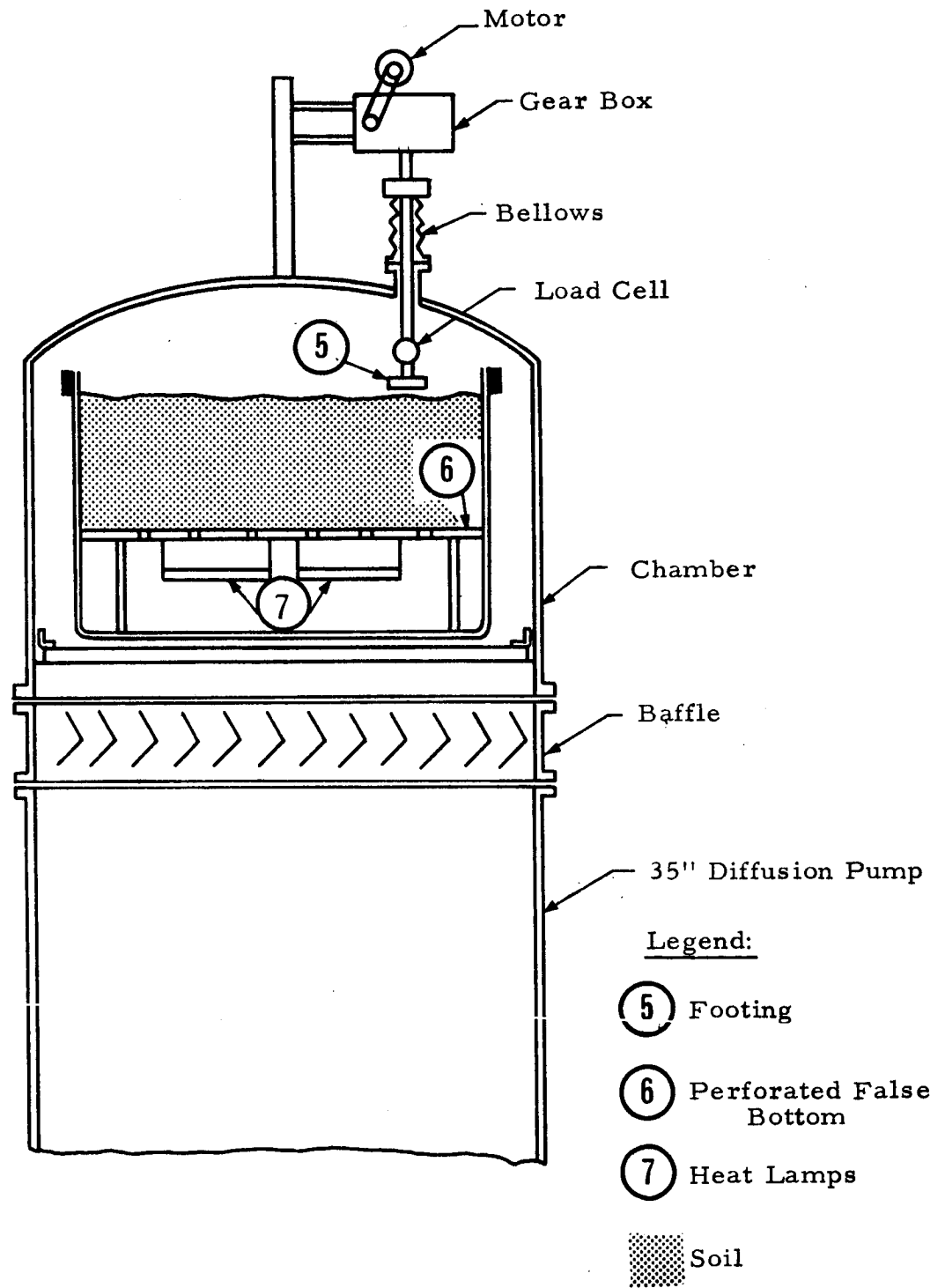
Fig. 30 APPARATUS FOR BEARING CAPACITY EXPERIMENTS

approximately 6 inches for the smaller footings. While the ratio of the distance from footing to container wall to the footing diameter was less than eight, the large diameter of the container was sufficient to prevent any arching in the soil below the footing. Hence, the container effects were believed to be minimal.

Vacuum levels recorded in the chamber varied from 9×10^{-8} torr to 1.1×10^{-7} torr but the vacuum level in the soil was undoubtedly somewhat less than this. On the basis of the results presented in Section III and in view of the extensive bakeout period, the high pumping speed, the fact that the sample was pumped through the bottom of the container as well as the top surface and the long drawdown time (approximately 2 weeks), it is believed that the vacuum in the soil pores was at least in the high 10^{-7} torr range during the experiments.

The soil was deposited in the container by sifting through a large No. 10 sieve 18 inches in diameter with walls 23 inches high. The sieve was vibrated by a small vibrator mounted on the top which caused the soil to be deposited in the container placed below. In this manner a uniform porosity of 0.60 was achieved.

The results of the experiments in the form of the average bearing pressure as a function of penetration for the 1 and 2 inch footings in atmosphere and vacuum are shown in Fig. 31 along with the results for a 3 inch footing which were obtained in a previous program.[3] The effect of footing size is evident in Fig. 31 in that under both atmospheric and vacuum conditions the average bearing pressure at any particular value of penetration decreased with an increase in footing size. As would be expected because of the observed increase in shear strength under vacuum, the bearing capacity of each footing was greater under vacuum than in the atmosphere.

The experiments on the 1 and 2 inch footings were performed at two different rates of penetration, 0.05 inch per min. and 0.50 inch per min.

---

[3] "Penetration Subsystem for the Surveyor Lunar Roving Vehicle", IITRI Project M6073, Final Report for Bendix Systems Division, April 3, 1964.
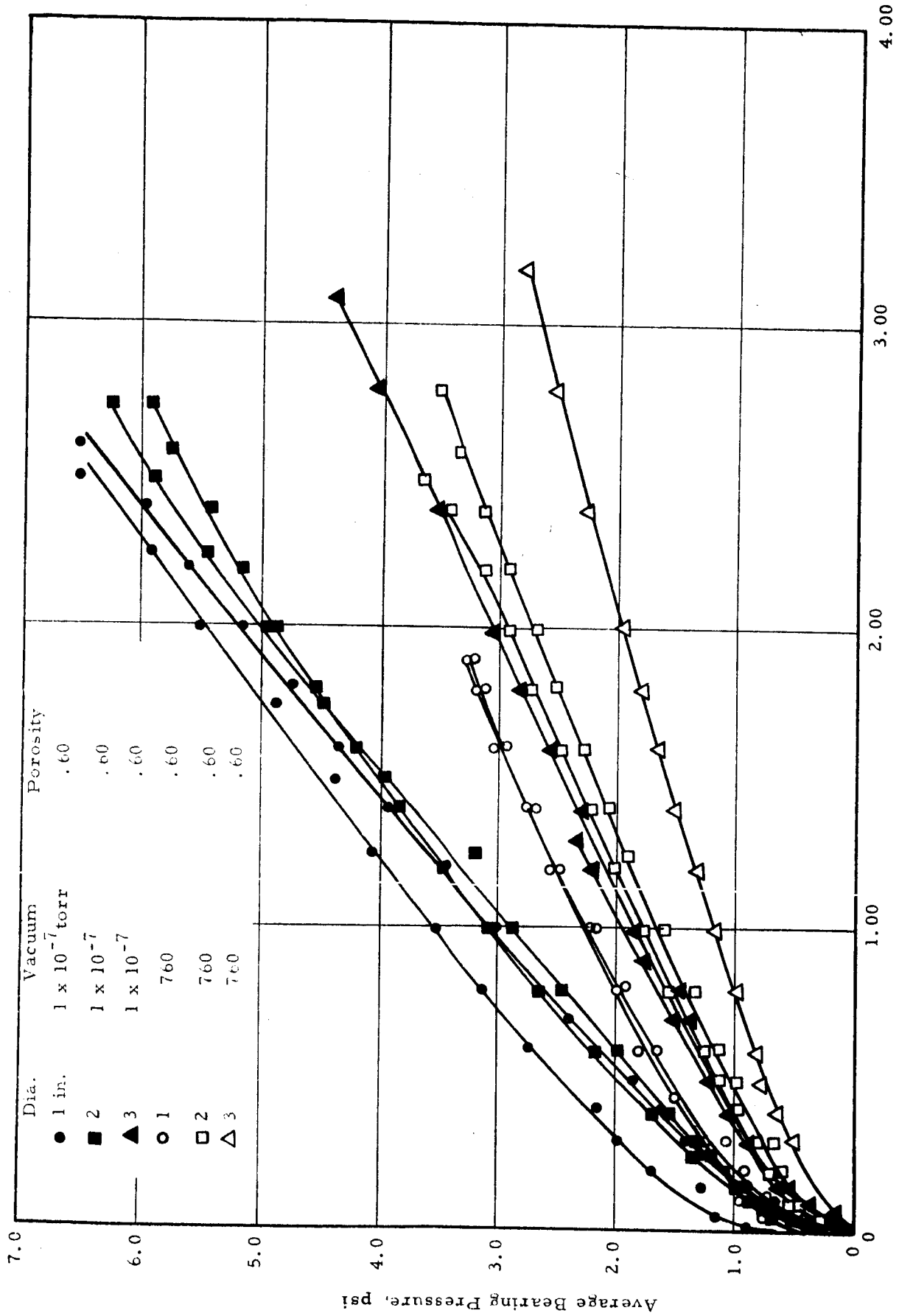
Fig. 31 BEARING CAPACITY OF SMALL FOOTINGS ON QUARTZ POWDER

While the bearing pressure for the higher penetration rate is greater than that for the lower rate in the case of the 1 inch footing in vacuum, the rate appears to have little, if any, effect on any of the other curves. The data is too limited to permit any definite conclusions to be drawn but it is believed that this difference in bearing pressure is largely experimental scatter rather than strain rate effects.

Various methods of analysis have been used in the past to interpret the results of bearing capacity experiments in soil. The problem is primarily one of getting a mathematical expression for the load-penetration curve which takes into account the influencing parameters such as footing size and geometry and soil strength. One method of analysis which appears to be applicable to the quartz powder assumes the bearing pressure to be related to the penetration by a hyperbola.[4,5]

The data was plotted in the form of the dimensionless parameters $\frac{xAq}{FC}$ as a function of x/C in which F is the total force on the footing, x is the penetration, q is the unconfined compressive strength of the soil and A and C are the area and circumference respectively of the footing. For most soils this form of representing the data resulted in the straight line relationship given by the equation

$$\frac{xAq}{FC} = a + b\,x/C \qquad (9)$$

which may be rewritten as

$$\frac{F}{Aq} = \frac{x/C}{a + b\,x/C} \qquad (10)$$

In the above equation a and b are constants and for cohesive soils dependent only upon the soil properties. The physical significance of the constants a and b can be seen from Eq. (10) where the initial tangent modulus or slope of the $\frac{F}{Aq}$ vs. x/C curve at the origin is given by the

_____

[4] Kondner, R. L. and R. J. Kriezek, "Correlation of Load Bearing Tests on Soils", Proc. Highway Research Board, Vol. 41, January 1962.

[5] Nelson, J. D. and E. Vey, "Bearing Capacity of the Lunar Soil", ASME Winter Annual Meeting, Paper No. 64-WA/AV-13, December 2, 1964.

value of 1/a and since

$$\text{Lim} \ \frac{F}{Aq} \ = \ 1/b \hspace{4cm} (11)$$

$$x \rightarrow \infty$$

the ultimate bearing pressure is given by the value of q/b.

Typical results obtained by plotting the data given in Fig. 31 in this form are shown in Fig. 32. Because of the uncertainty of the actual value of q for the soil under vacuum, the ratio $\frac{xA}{FC}$ was plotted in Fig. 32 instead of the ratio $\frac{xAq}{FC}$. This should have no effect on the shape of the curves. However, differences in q would displace the curves for the data under vacuum relative to those in atmosphere.

For values of x/C greater than approximately 0.15 the data may be represented by a straight line, whereas below this the relationship becomes nonlinear. For values of x/C less than approximately 0.075 the data may also be represented by a straight line but the slope and intercept are different from those at the greater penetrations.

Thus, the bearing capacity may be represented by the equation

$$F/A \ = \ \frac{x/C}{\alpha + \beta \ x/C} \hspace{4cm} (12)$$

where α and β are the intercept and slope respectively of the data in Fig. 32. To determine the initial tangent modulus of the F/A vs. x/C curve the value of α must be taken as the intercept of the straight line in the region of x/C less than 0.075. It should be noted, however, that for x/C = 0 the force on the footing is also zero and, hence, the value of $\frac{xA}{FC}$ at x/C = 0 is undefined. Consequently, α must be determined by extrapolation of the data shown in Fig. 32. Also for very small values of x/C (<0.01) it was observed that the data exhibited considerable scattering. This can be attributed to "seating" of the footing and does not, therefore, reflect on the validity of the relationships for larger x/C values.

The ultimate bearing pressure on the footing may be determined from the slope of the curve in the region of x/C greater than 0.15. Average
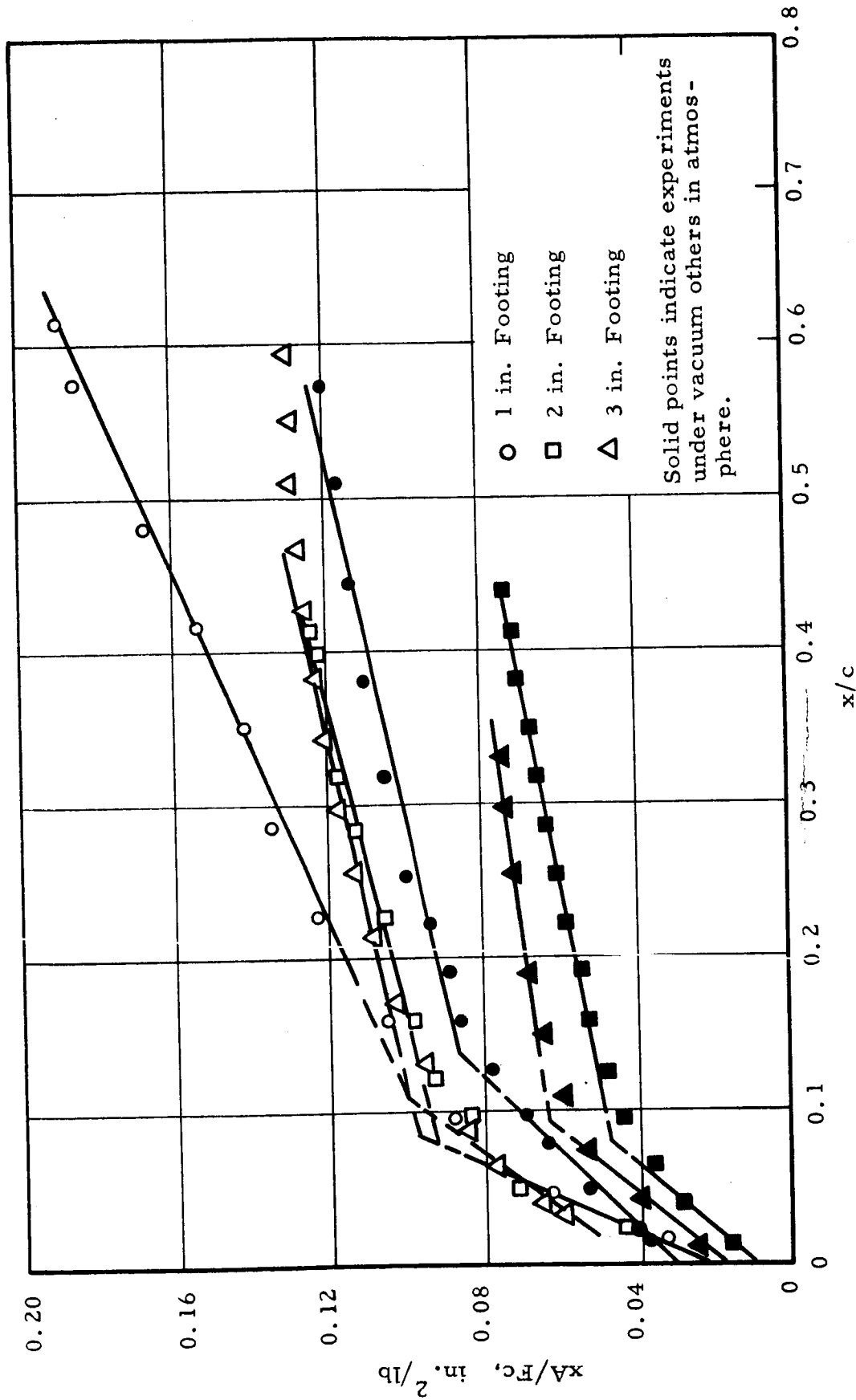
Fig. 32 xA/Fc VS. x/c FOR SMALL FOOTINGS ON QUARTZ POWDER

- 56 -

values of α and β for the appropriate regions as determined from the data shown in Fig. 31 are presented in Table 1 for the various footings and environmental conditions.

Table 1

VALUES OF α AND β FOR FOOTINGS ON QUARTZ POWDER

Footing Diameter	Environmental Conditions	α	β
1 in.	Atmospheric	0.040 in.^{2}/lb	0.177 in.^{2}/lb
2	Atmospheric	0.030	0.118
3	Atmospheric	0.042	0.105
1	Vacuum	0.026	0.126
2	Vacuum	0.010	0.064
3	Vacuum	0.021	0.052

While it can be seen that β decreased with an increase in footing size this does not necessarily imply that the bearing capacity of a larger footing is greater than that of a smaller one. Rather the value of β is largely a measure of the amount of curvature of the F/A versus x/C curve. For example, if $\beta = 0$, Eq. (12) reduces to

$$F/A = (1/a)\ x/C \qquad (13)$$

$$\lim_{x \to \infty} F/A = \infty$$

In this case the ultimate bearing pressure could be greater than for a stiff soil exhibiting a large positive value of β. While this would be true at large values of penetration, the bearing capacity of the soil with β greater than zero may very well be larger at smaller and more reasonable values of penetration. Thus, while β decreased with an increase in footing size, α was essentially constant and as was seen previously, the bearing pressure for values of x/C at which the experiments were performed was less for the larger footings.

IIT RESEARCH INSTITUTE

From Fig. 32, however, it may be seen that in general both the intercept and slope (α and β) throughout the range of values of x/C are less in vacuum than in atmosphere for a particular footing. Under vacuum conditions the load-penetration curve was somewhat steeper than in atmosphere and exhibited less curvature. The initial tangent modulus and ultimate pressure in atmosphere and vacuum for the different footing sizes are given in Table 2.

Table 2

EFFECT OF VACUUM ON INITIAL TANGENT MODULUS (E)
AND ULTIMATE BEARING PRESSURE (P)

Footing Diameter (in.)	$\dfrac{\alpha_{atm}}{\alpha_{vac}} = \dfrac{E_{vac}}{E_{atm}}$	$\dfrac{\beta_{atm}}{\beta_{vac}} = \dfrac{P_{vac}}{P_{atm}}$
1	1.54	1.41
2	3.00	1.85
3	2.00	2.02

It is evident that the effect of vacuum was to increase the bearing capacity by increasing the slope of the load-penetration curve for small values of penetration and decrease the curvature. The result was an increase in bearing capacity at all values of penetration.

Also, it appears that the increase in ultimate bearing pressure under vacuum was greater for the larger footings than the smaller ones.

VII. PENETRATION RESISTANCE UNDER DYNAMIC LOADING

In order to investigate the effect of vacuum on the penetration resistance of soils under conditions of dynamic loading, experiments were performed in which the deceleration-time history of projectiles was measured during penetration of the soil. This method of determining soil properties has also been suggested as being particularly applicable for the investigation of the lunar surface from a remote position,[6] such as an orbiting vehicle.

The experiments consisted of measuring the deceleration-time history or signature of a projectile under vacuum levels ranging from atmospheric to 2×10^{-9} torr and at impact velocities ranging from approximately 2 to 5 ft per second.

The penetrometers consisted of hollow aluminum cylinders 0.73 inches in diameter in which were mounted accelerometers (Fig. 33). They were designed with interchangeable tips so that both a 60 deg cone and a flat end could be used. Piezoelectric accelerometers were selected for use primarily because of their wide range of allowable temperatures, and desirable frequency response characteristics.

Experiments were performed on samples of quartz and olivine powders (Fig. 1 and curve b Fig. 2) and fine coarse grained Ottawa sand (Fig. 3) under vacuum levels up to 2×10^{-9} torr. Impact velocities were varied by changing the height from which the penetrometers were dropped.

A series of preliminary experiments were performed in order to determine the minimum size of soil container which would have no effects on the results. Maximum effects of container diameter were observed under atmospheric conditions in containers with small diameters (1.50 to 3.75 inches). During penetration, pore air pressures were developed in the soil which caused a reduction in penetration resistance. In small containers

---

[6] McCarty, J. L. and Carden, H. D., "Impact Characteristics of Various Materials Obtained by an Acceleration-Time History Technique Applicable to Evaluating Remote Targets", NASA-LRC, TN D-1269, June 1962.

Release Pin

To Recording Instrumentation

Accelerometer

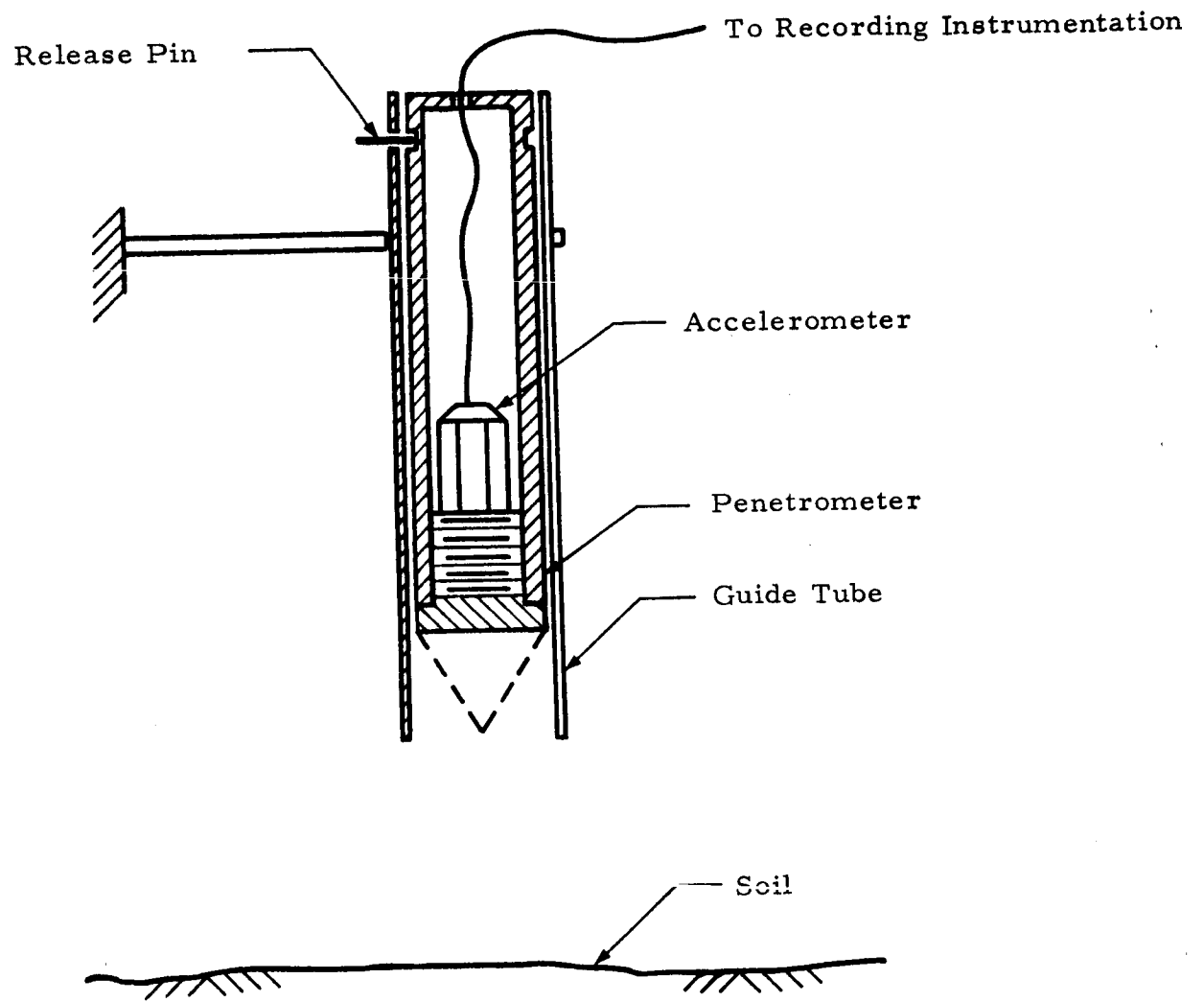Penetrometer

Guide Tube

Soil

Fig. 33 DYNAMIC PENETRATION APPARATUS

these pressures could not be dissipated radially and as a result the soil shear strength was influenced considerably by the proximity of the container walls. In the small containers, therefore, the penetrometer penetrated the entire depth of soil (7.0 inches) even at very low impact velocities. Containers having diameters of 4.50, 5.50, 6.50 and 8.50 inches were also used and it was observed that the container effects decreased as the diameter increased. The signature obtained in the 8.50 inch container was the same as that obtained in the 6.50 inch container indicating that at diameters greater than 6.5 inches the container walls had a negligible effect.

The depth of soil was also varied until the container bottom effects were minimized. When the depth was too shallow it was observed that the deceleration increased rapidly near the end of the signature. At depths greater than approximately 6 inches this effect was not observed.

The size selected for the penetration experiments, therefore, was a cylindrical container 10 inches in diameter and 8 inches deep. This permitted four experiments to be performed in the same soil sample at a minimum distance of 3 inches from the container wall.

A.   Experiments on Quartz Powder

Typical signatures obtained by the flat end penetrometer in the quartz powder are shown in Fig. 34. The scale of these and following signatures may be determined by noting that the difference in accelerations prior to impact and after the penetrometer had come to rest was approximately 32 ft per sec^2. A feature of particular interest in the loose soil under atmospheric conditions is the sharp "spike" which occurred in the initial portion of the signature. This spike was previously attributed to pore air effects. However, although the spike did not occur under vacuum it can be seen in Fig. 34b that the deceleration increased rapidly at first then leveled off slightly and finally increased again. It is believed that the spike and the sharp rise in deceleration at the initial point was due to the inertia of that portion of the soil being accelerated.

In the dense soil it is evident that some shear took place in the soil under atmospheric conditions whereas under vacuum conditions the penetrometer
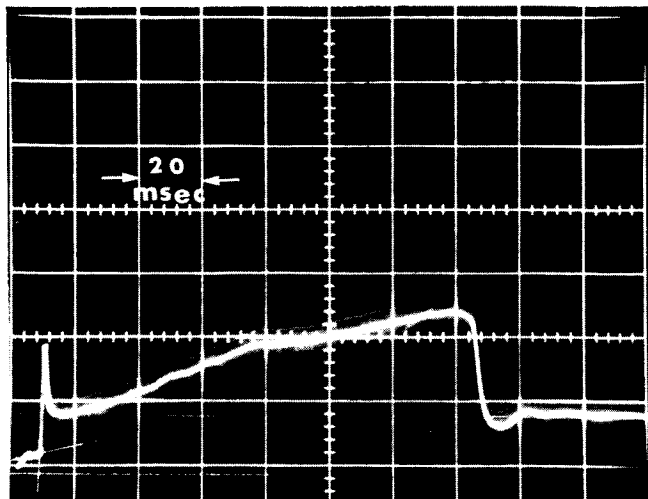
a) Loose-Atmospheric
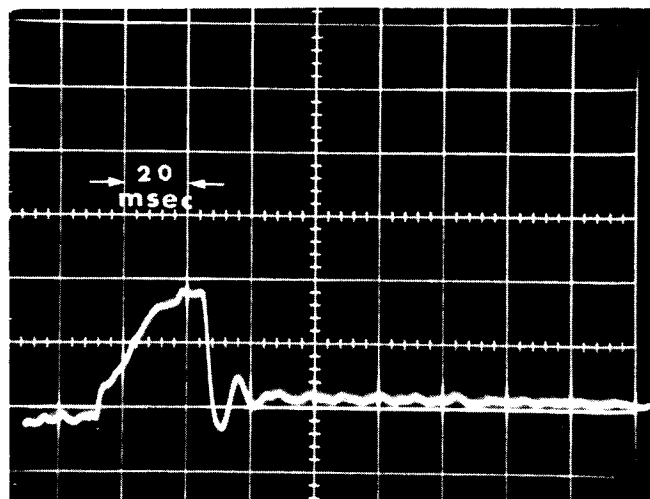
b) Loose - Vac = 8.2×10^{-9} torr
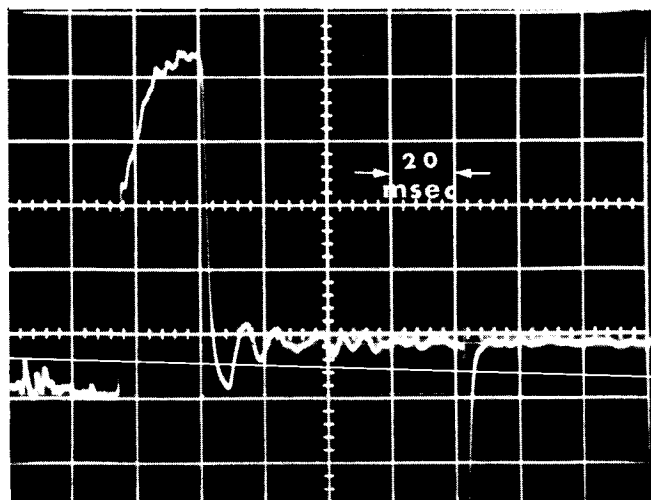
c) Dense-Atmospheric
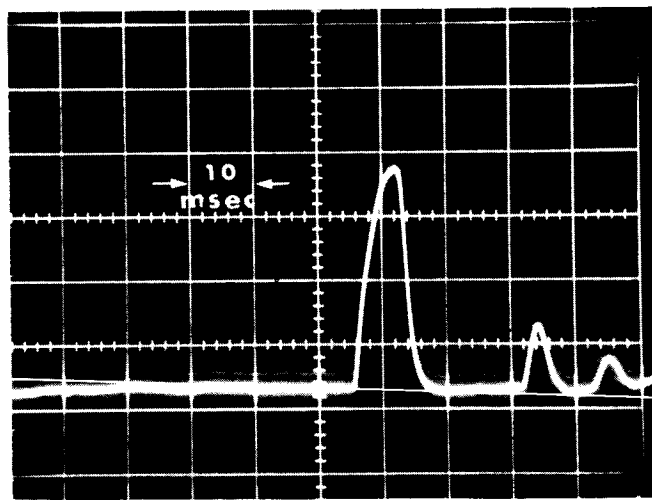
d) Dense - Vac = 2×10^{-9} torr

Fig. 34   TYPICAL SIGNATURES FOR FLAT END PENETROMETER
IN QUARTZ POWDER

decelerated rapidly and then stopped, indicating only compression and no shear failure. It should be noted that in all cases the signature crossed below the base line at the end indicating an acceleration of the penetrometer followed again by a deceleration. This was due to some elasticity of the soil causing oscillation of the penetrometer. Of particular interest in this regard is the signature in dense soil under vacuum. After the first impact it can be seen that the penetrometer reached an acceleration of 32 ft per $\sec^2$ and held it for a considerable period of time. This was followed by a second impact and another acceleration of 32 ft per $\sec^2$ for a shorter period. Thus, it is apparent that the soil was elastic enough under these conditions to cause the penetrometer to leave the soil surface twice after the initial impact.

Figure 35 shows signatures obtained in the quartz powder using a 60 deg cone on the tip of the penetrometer under atmospheric conditions. Except for the initial spike in the loose soil with the flat end penetrometer the cone tip had little effect on the total pulse time or the maximum deceleration. The absence of the initial peak may be attributed to the fact that with the cone a smaller area is in contact in the beginning of the penetration and, hence, the mass of soil being accelerated initially is smaller than for the flat end.

By integrating the deceleration-time curve twice with respect to time the displacement can be determined as a function of time. Also the resistance offered by the soil to the penetrometer can be determined from the equation

$$R = m \ (g - a) \tag{14}$$

where

R is the soil resistance

m is the mass of the penetrometer

a is the acceleration of the penetrometer

g is the gravitational constant.

Representative curves showing the resistance as a function of the penetration in loose quartz powder are shown in Fig. 36 for different vacuum levels. Under atmospheric conditions the total penetration was
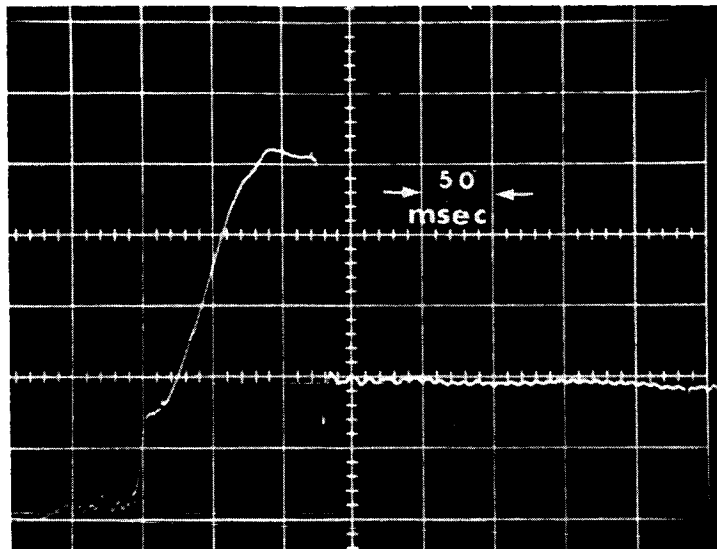
a) Loose
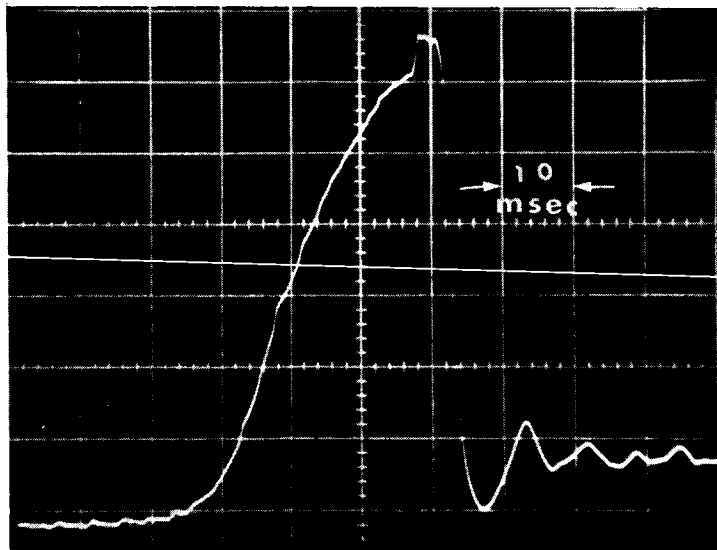
b) Dense

Fig. 35   TYPICAL SIGNATURE OF 60° CONE IN QUARTZ POWDER
UNDER ATMOSPHERIC CONDITIONS

Vac = 9.2 x 10^{-9} torr
n = C.641 v$_o$ = 3.36 fps

Vac = 7 x 10^{-6} torr
n = 0.648 v$_o$ = 3.45 fps

Static Penetration in Atmosphere n = 0.646

Vac = 4 x 10^{-2} torr
n = 0.646 v$_o$ = 2.76 fps

Atmosphere
n = 0.656 v$_o$ = 3.73 fps

.8

.7

.6

.5

.4

.3

.2

.1

0

Resistance, lb

0   1.0   2.0   3.0   4.0   5.0

Penetration, in.

Fig. 36   RESISTANCE AS A FUNCTION OF PENETRATION FOR DIFFERENT
VACUUM LEVELS IN QUARTZ POWDER

quite large relative to that under even low vacuum. This is due to the fact that during failure of the soil the void ratio decreased, causing pore air pressures to be developed which produced a decrease in the effective stress and hence a decrease in the shear strength. When the pore air is removed under rough vacuum, all stresses in the soil mass appear as effective stresses and, hence, there is no reduction in shear strength. The penetration-resistance curve for dynamic penetration under rough vacuum is very nearly the same as that obtained under static loading after the initial peak resistance has been overcome. This would indicate that in the absence of pore air the loading rate has a small effect on the shear strength. The fact that the initial peak occurs under both rough vacuum and atmospheric conditions and has approximately the same magnitude in both cases indicates that it is due to inertia of the soil and is not due to pore air effects.

A reduction in vacuum level from rough vacuum to high and ultra-high vacuum is seen to produce a further increase in penetration resistance probably due to an increase in shear strength. Also the curve rises quite rapidly at first and then begins to level off. The high point represents the force necessary to overcome the inertial resistance of the soil wh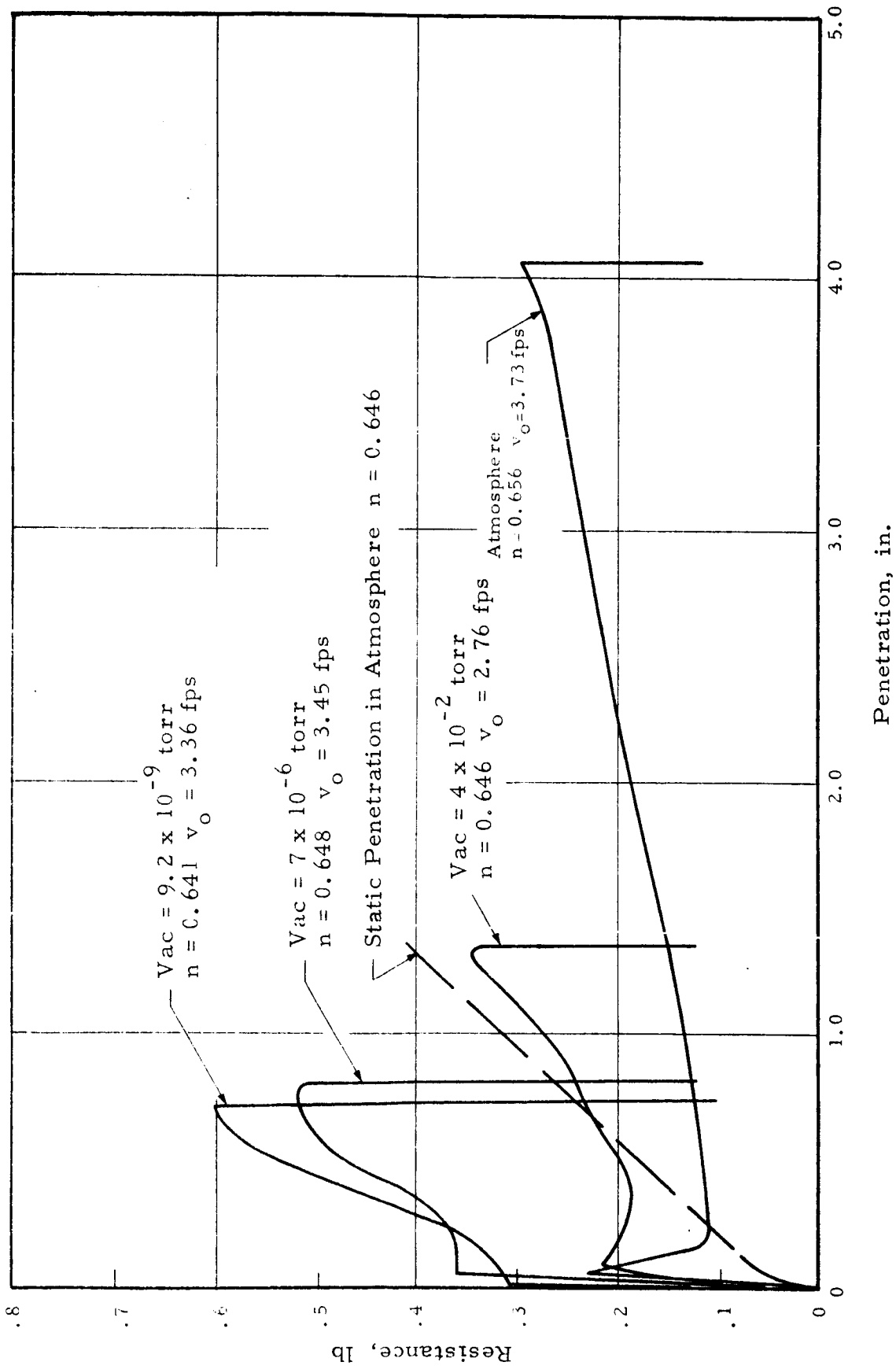ich is caused by bonding at the asperity contacts and the acceleration of the displaced soil. As would be expected, the magnitude of this force is greater under high vacuum than at low vacuum or atmospheric conditions.

Experiments were performed at different impact velocities, representative results of which are shown in Fig. 37. Under atmospheric conditions it is evident that the effect of increasing the impact velocity was to increase the total penetration, but this had little, if any, effect on the magnitude of the resistance as a function of penetration. Under ultra-high vacuum, however, it appears that the impact velocity had little effect on the total penetration but did produce an increase in the resistance offered by the soil.

The effect of impact velocity on the penetration resistance can be seen in Fig. 38 in which the penetration caused by 0.3 in.-lb of work done on the soil is shown as a function of the impact velocity. Since the work is
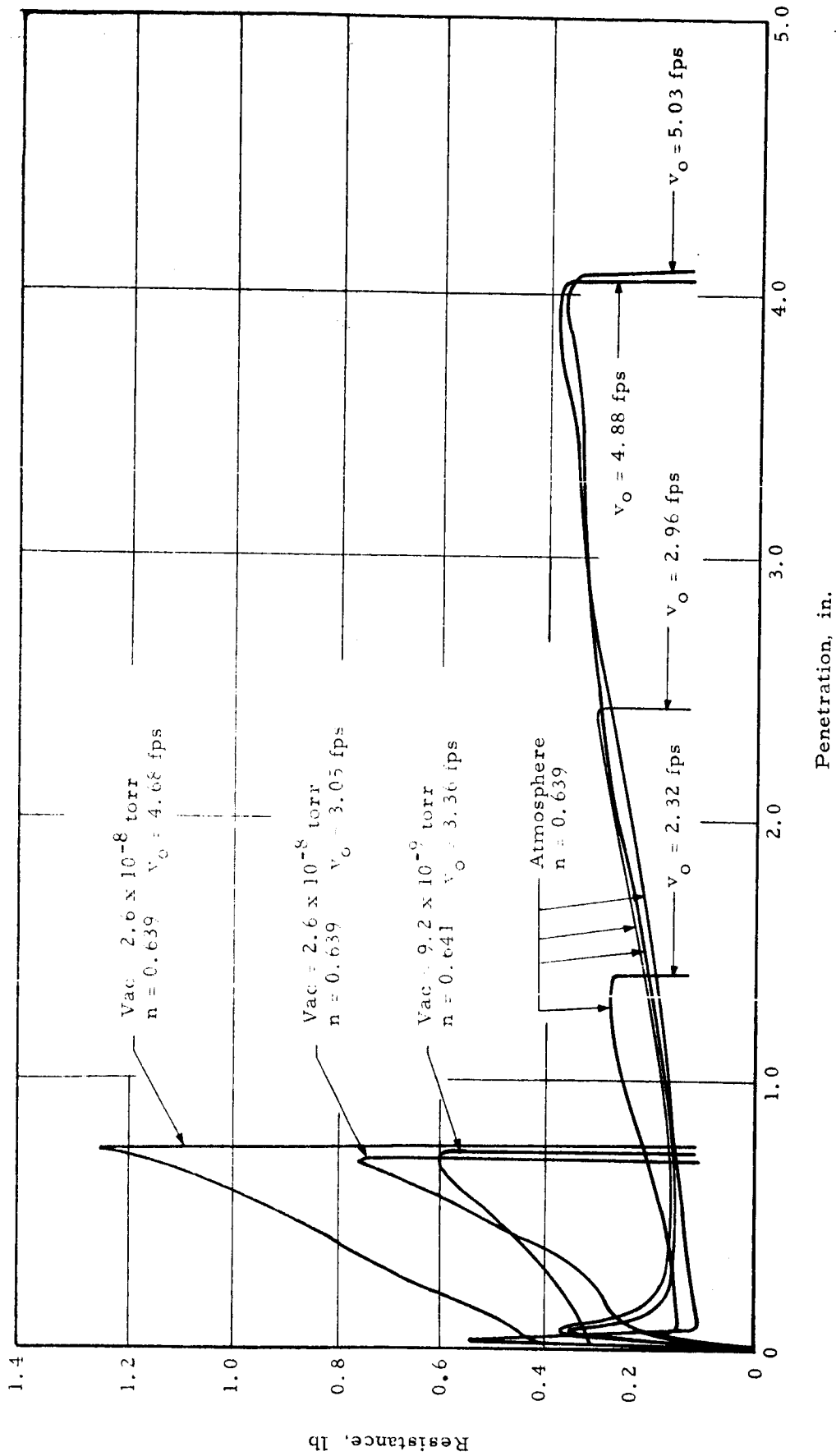
Penetration, in.

Fig. 37   RESISTANCE AS A FUNCTION OF PENETRATION FOR VARIOUS IMPACT
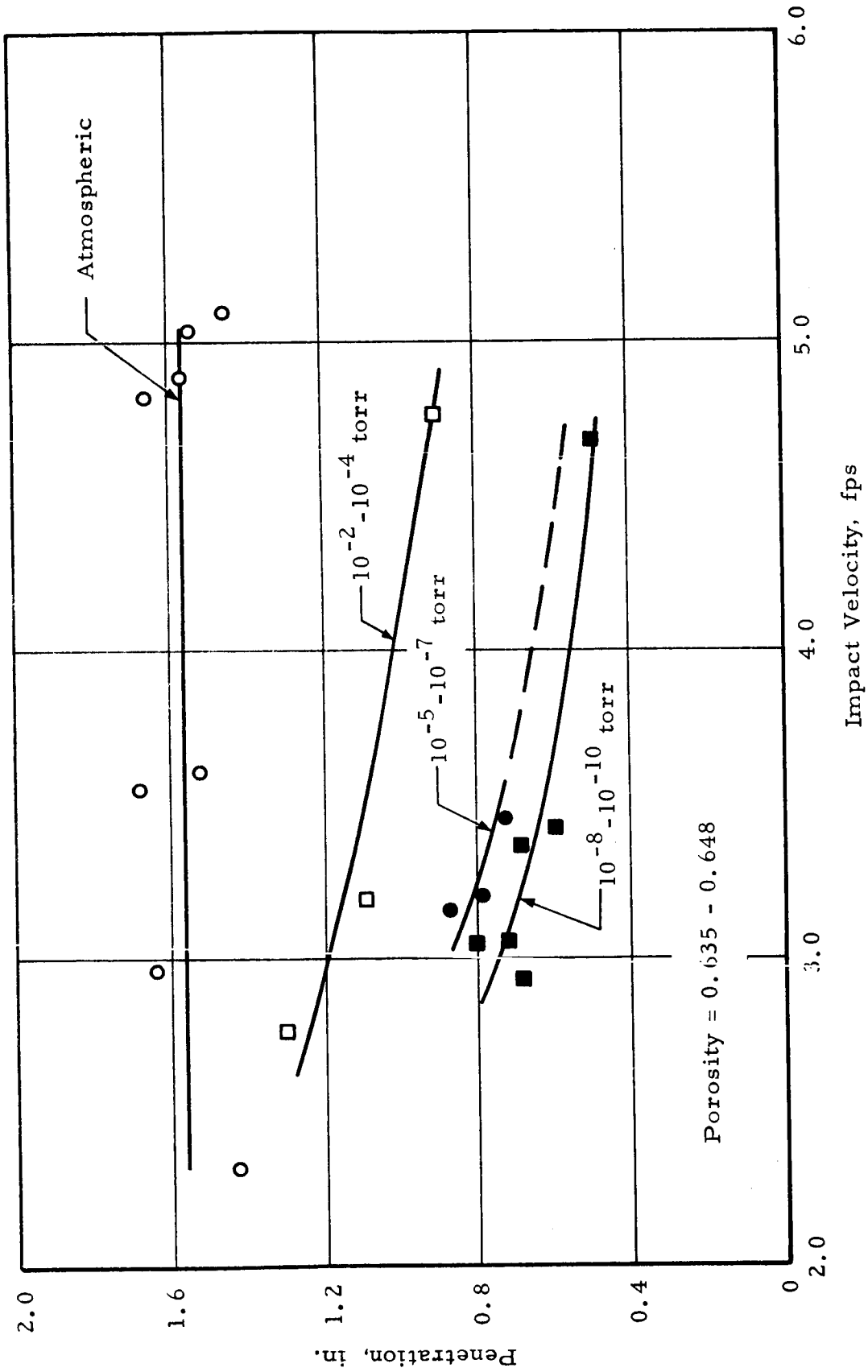VELOCITIES IN QUARTZ POWDER

-67-

Fig. 38   EFFECT OF IMPACT VELOCITY ON PENETRATION AT 0.3 IN.-LB
WORK IN QUARTZ POWDER

the integral of the resistance as a function of the penetration, the penetration produced by a particular amount of work will be the same for all curves which follow the same path. The particular value of 0.3 in.-lb was chosen for use in the following figures because this was approximately equal to the maximum amount of work the penetrometer was capable of doing at the lowest impact velocities. As would be expected from the results shown in Fig. 37 this penetration appears to be independent of impact velocity for atmospheric conditions. However, under even low vacuum levels, an increase in impact velocity caused a decrease in the penetration indicating an increase in resistance.

The results of experiments on samples having different porosities are shown in Fig. 39 in the form of the penetration at 0.3 in.-lb of work as a function of porosity. As would be expected a decrease in porosity resulted in a decrease in penetration. However, the degree to which the penetration was influenced by porosity depended upon the vacuum level, the soil under high and ultra-high vacuum levels being influenced less than that under rough vacuum or atmospheric conditions. It should be noted also that the curves tend to converge at the lower porosities.

In Fig. 38 and 39 it can be seen that some increase in resistance was produced by rough vacuum with further increases in vacuum causing even further increases in the resistance. In Fig. 40 the penetration at 0.3 in.-lb of work is shown as a function of vacuum level. Only those points corresponding to porosities and impact velocities within the ranges indicated on the figure were plotted in order to eliminate as much as possible the effect of these parameters. A relatively large increase in resistance occurred up to vacuum levels of approximately 10^{-5} or 10^{-6} torr, whereas an increase in vacuum level above this caused a relatively smaller increase in resistance. While the increase in resistance at rough vacuum levels may be attributed to pore air pressures they would be expected to have a negligible effect on the effective stresses at vacuum levels higher than approximately 10^{-2} or 10^{-3} torr. This indicates a relatively large increase in the shear strength under high vacuum.
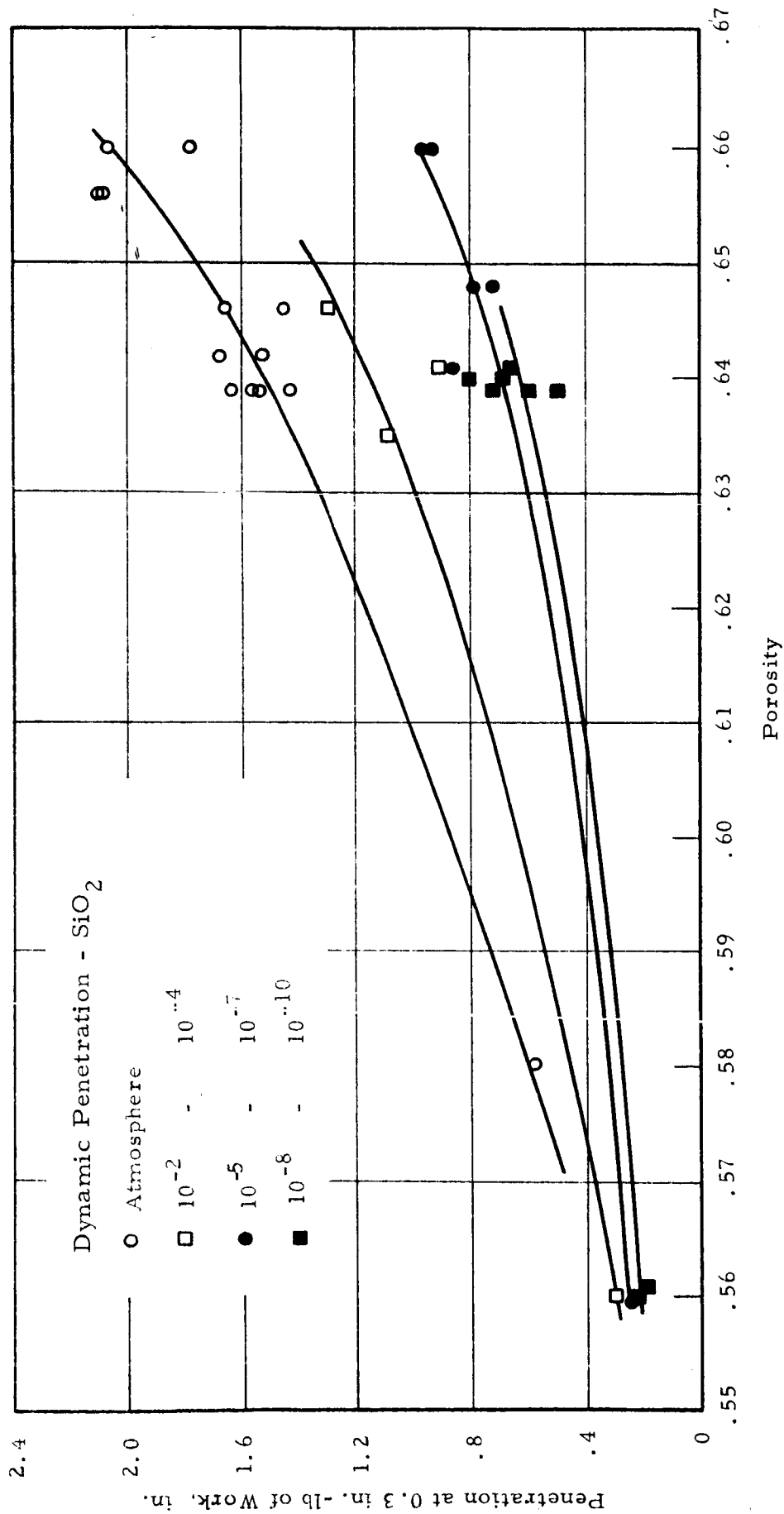
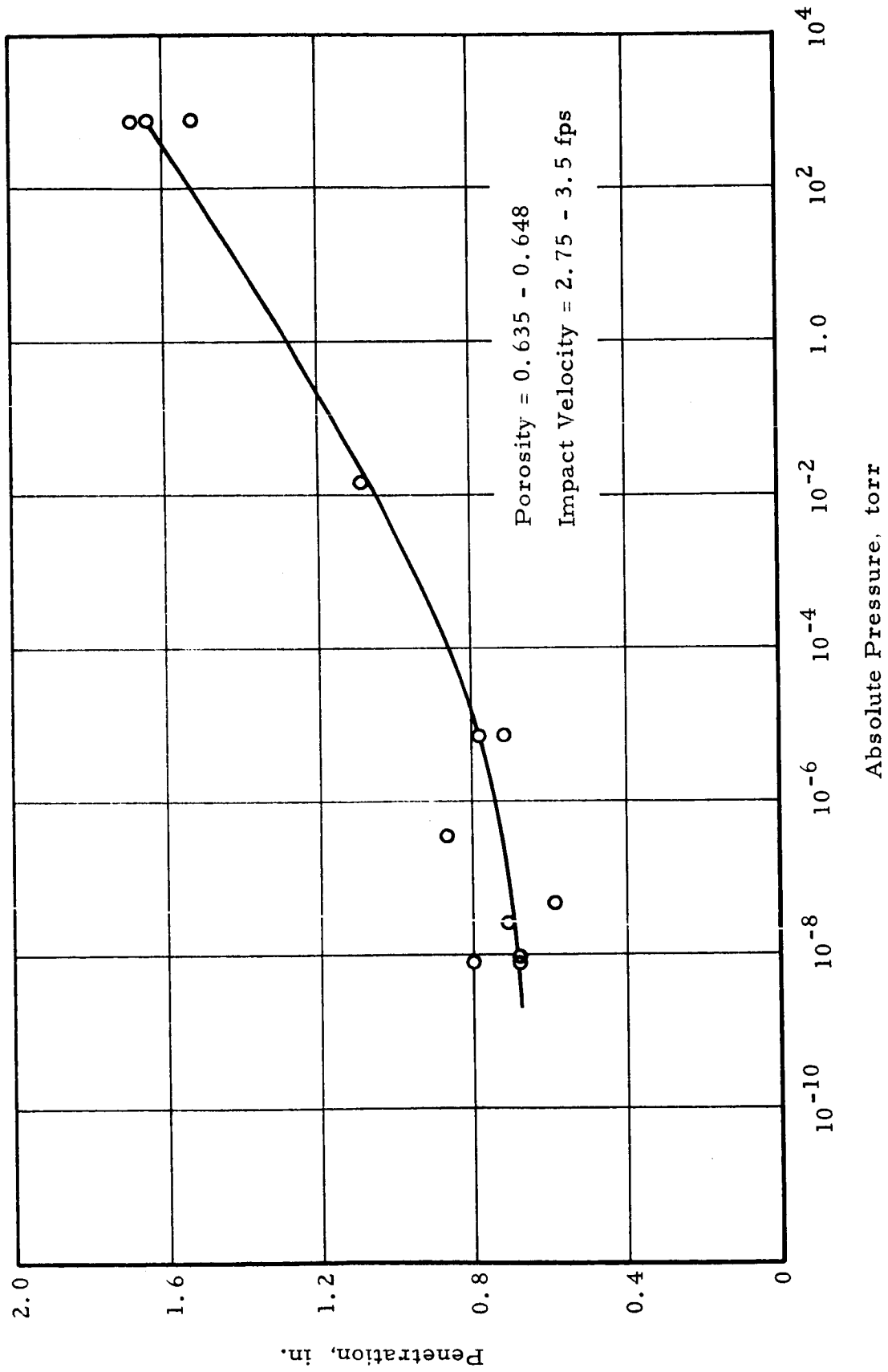Fig. 39   EFFECT OF POROSITY ON PENETRATION AT 0.3 IN. -LB WORK
IN QUARTZ POWDER

Fig. 40   EFFECT OF VACUUM ON PENETRATION AT 0.3 IN.-LB WORK
IN QUARTZ POWDER

Porosity = 0.635 - 0.648

Impact Velocity = 2.75 - 3.5 fps

Absolute Pressure, torr

Penetration, in.

B.   Experiments on Olivine Powder

Typical signatures obtained in the olivine powder in atmosphere and vacuum in both the loose and dense states are shown in Fig. 41. They are similar in all respects to those obtained in the quartz powder except that under ultra-high vacuum the initial spike is slightly more pronounced than in the quartz. In the dense soil in vacuum, the penetrometer also bounced off the surface after the initial impact as was true in the case of the quartz powder.

The resistance as a function of penetration for various vacuum levels is shown in Fig. 42. Again a distinct difference in the penetration resistance can be seen between experiments in atmosphere and in rough vacuum. However, the curves obtained under high and ultra-high vacuum had essentially the same shape as those obtained at rough vacuum. In addition, the initial spike had approximately the same magnitude under all vacuum levels as it had in atmosphere.

The penetration at 0.3 in.-lb work is shown as a function of the impact velocity in Fig. 43. The data in atmosphere is rather limited but it appears that under vacuum an increase in impact velocity caused some increase in resistance.

Figure 44 shows the penetration at 0.3 in.-lb work as a function of porosity. The resistance increases with a decrease in porosity with the curves tending to converge at the lower values of porosity as for the quartz.

The effect of vacuum on the penetration resistance can be seen in Fig. 45. Although the data is somewhat limited it appears that the vacuum caused a definite increase in penetration resistance up to the 10^{-5} torr range while a further increase to the 10^{-8} torr range had a small effect. The two points at 10^{-1} torr were obtained in samples having a porosity of 0.675 and hence, should be higher than shown to compare with results at higher porosities. However, in both Fig. 43 and 44 the curves for rough vacuum and for vacuum levels of approximately 10^{-6} torr are essentially the same. Thus, it appears that the major effect of the vacuum on the penetration resistance of the olivine is due to the removal of pore air with little, if any, increase attributable to an increase in the shear strength.
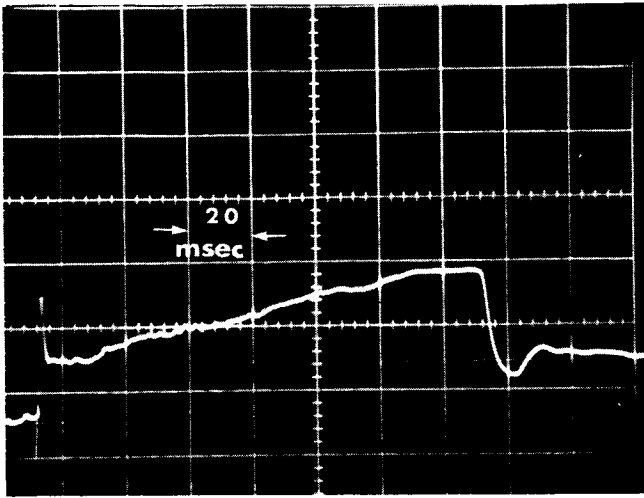
a) Loose-Atmospheric
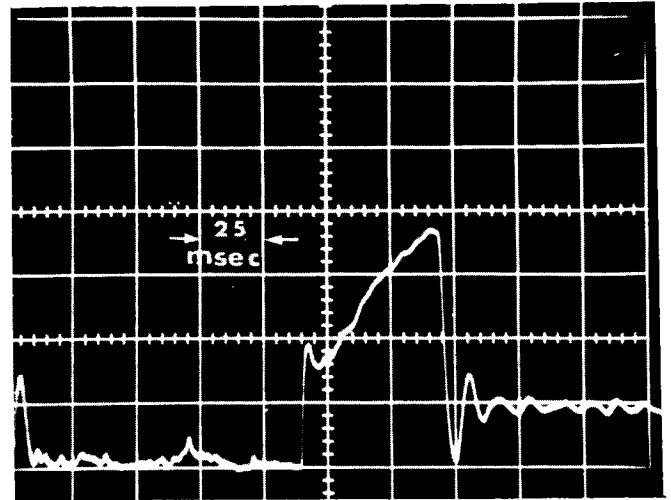
b) Loose-Vac = 2.8 x 10^{-8} torr
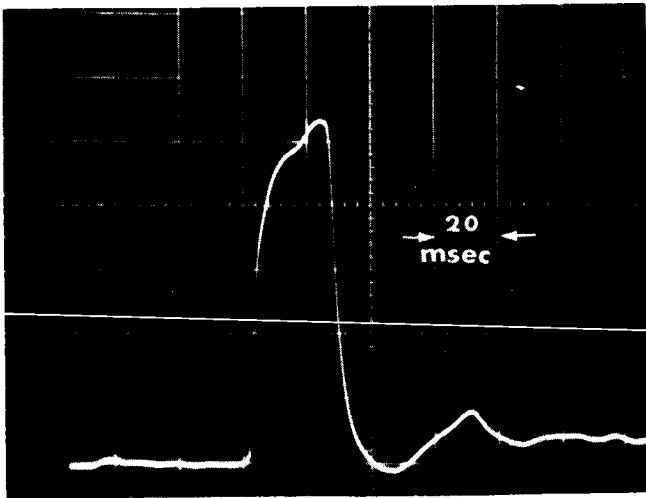
c) Dense-Atmospheric
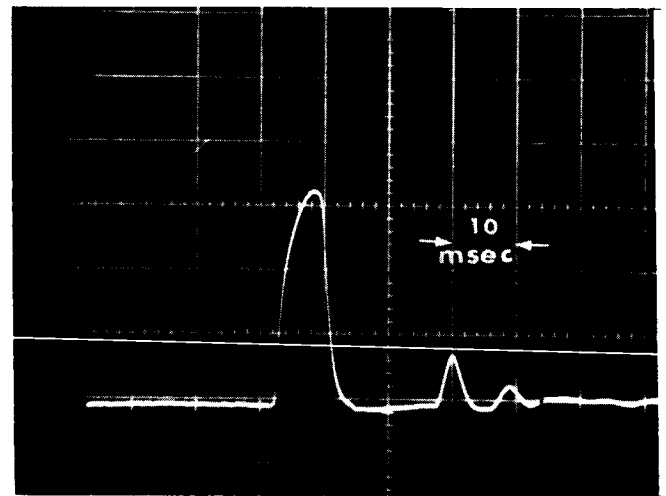
d) Dense-Vac = 1 x 10^{-5} torr

Fig. 41   TYPICAL SIGNATURES FOR FLAT END PENETROMETER
IN OLIVINE POWDER
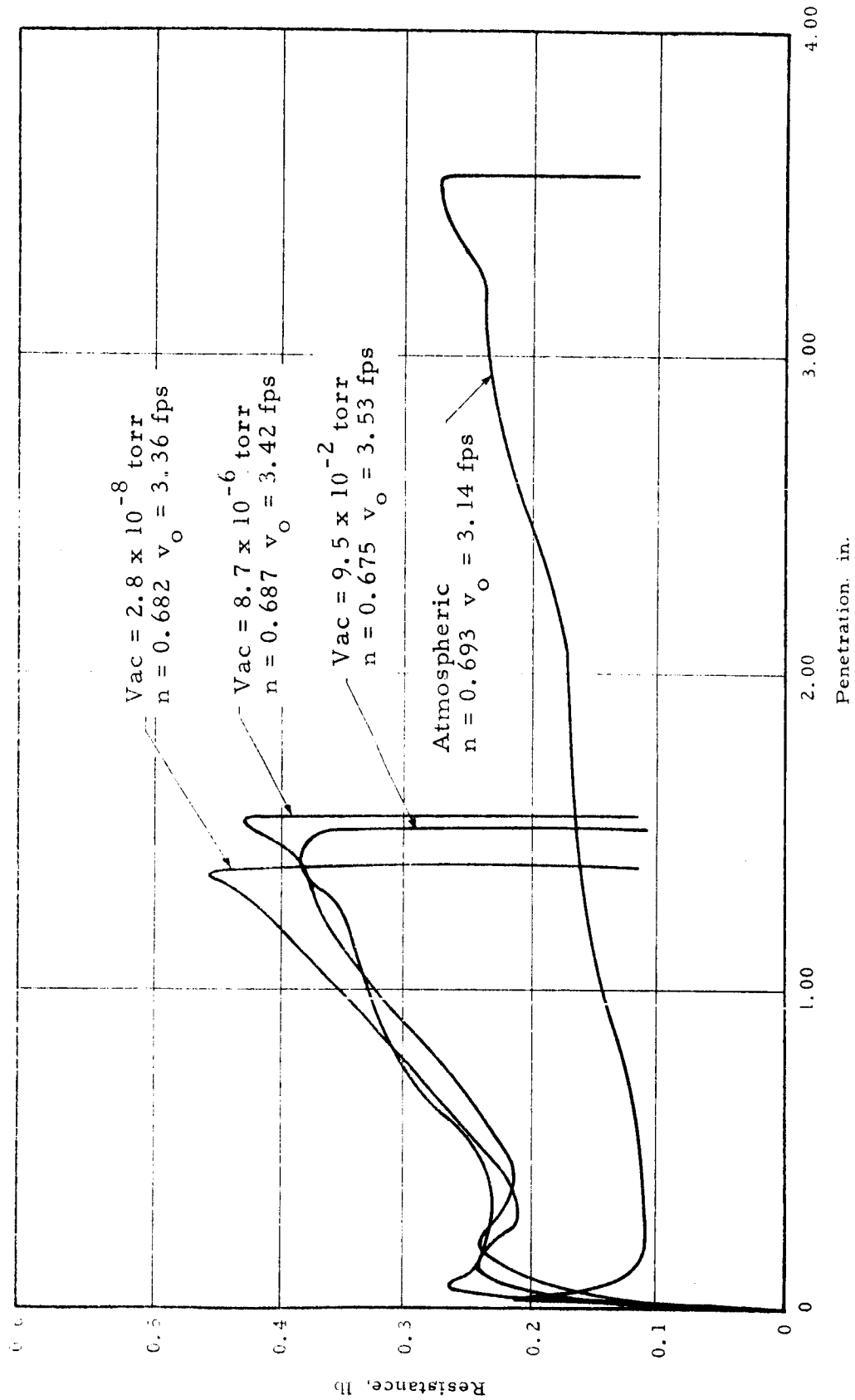
Penetration. in.

Fig. 42 RESISTANCE AS A FUNCTION OF PENETRATION IN OLIVINE POWDER

Vac = 2.8 x 10^{-8} torr
n = 0.682 v$_o$ = 3.36 fps

Vac = 8.7 x 10^{-6} torr
n = 0.687 v$_o$ = 3.42 fps

Vac = 9.5 x 10^{-2} torr
n = 0.675 v$_o$ = 3.53 fps

Atmospheric
n = 0.693 v$_o$ = 3.14 fps

Resistance, lb.

-74-

Fig. 43   EFFECT OF IMPACT VELOCITY ON PENETRATION AT 0.3 IN. - LB WORK
IN OLIVINE POWDER
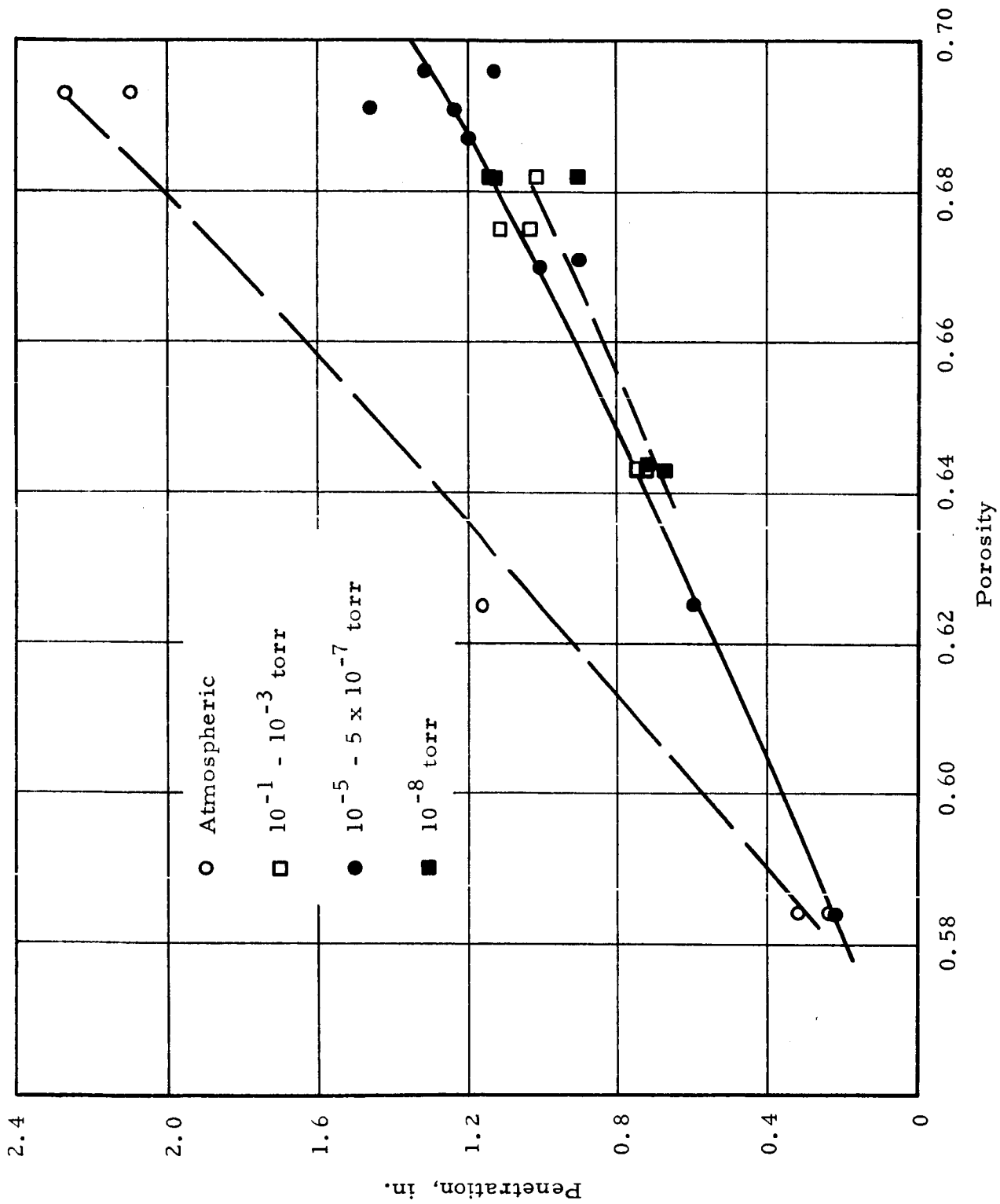
Fig. 44   EFFECT OF POROSITY ON PENETRATION AT 0.3 IN. -LB
WORK IN OLIVINE POWDER

Fig. 45 EFFECT OF VACUUM ON PENETRATION AT 0.3 IN.-LB WORK IN OLIVINE POWDER

Porosity = 0.682 - 0.696
Impact Velocity = 2.94 - 3.42 fps

Absolute Pressure, torr

Penetration, in.

C.   Experiments in Fine Sand

Typical signatures in the fine sand for a flat end penetrometer are shown in Fig. 46. It is evident that in the loose material, shear took place in the soil whereas in the dense material no shear occurred. As was observed in the finer grained materials, an initial spike occurred due to the inertia of the soil. Also, the signature is nearly the same in both vacuum and atmosphere.

Figure 47 shows signatures obtained using a 60 deg cone tip penetrometer. In the loose material the vacuum caused a slight increase in the maximum deceleration and a small decrease in total pulse time.   In the dense soil, however, the effect of vacuum appears to be just the opposite. This would indicate that in the loose material positive pore air pressures were developed in atmosphere due to a decrease in the void ratio whereas in the dense material the void ratio was below the critical value and the soil expanded during shear. Consequently, the pore air pressures were negative and caused an increase in the effective stress. However, the pore air effects are small relative to those in the quartz and olivine powder.

The resistance-penetration curves for the flat-end penetrometer are shown in Fig. 48 for various vacuum levels. In this case, the curves are nearly the same under all conditions. However, in atmosphere and rough vacuum, the resistance decreased rapidly after the initial peak to some minimum value. After this it increased slightly until the end of the penetration.   Under ultra-high vacuum the deceleration decreased less rapidly before the minimum point was reached indicating an increase in shear strength.

The penetration caused by 0.3 in.-lb of work is shown as a function of vacuum level in Fig. 49. While considerably more data are necessary before any definite conclusions can be drawn, it appears that rough vacuum levels had little, if any, effect on the penetration resistance because of the relatively large grain size. Ultra-high vacuum, however, caused an increase in the resistance as the result of an increase in shear strength.
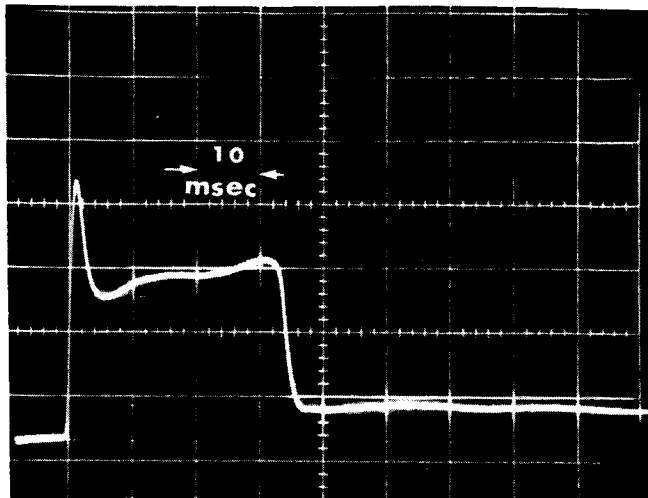
a) Loose-Atmosphere
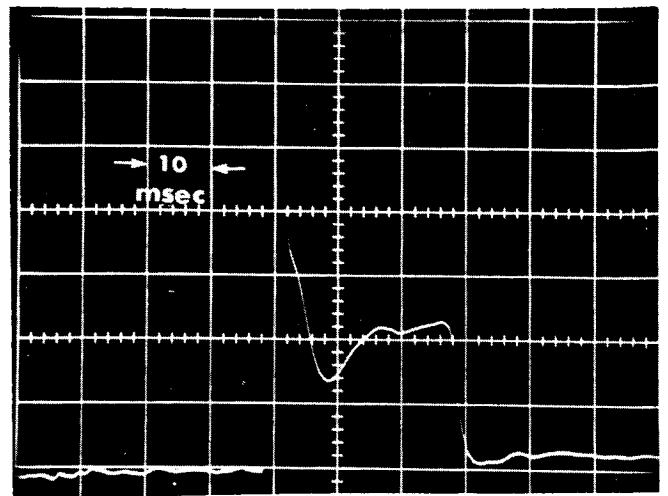
b) Loose - Vac = 2.2×10^{-9} torr
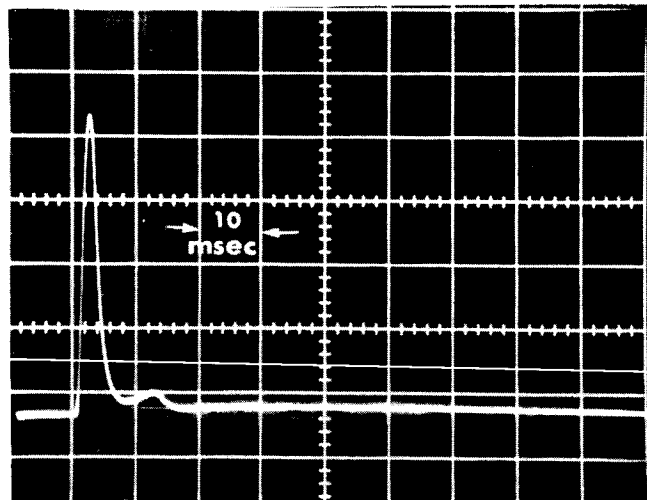
c) Dense-Atmosphere

Fig. 46   TYPICAL SIGNATURES FOR FLAT END
PENETROMETER IN FINE SAND
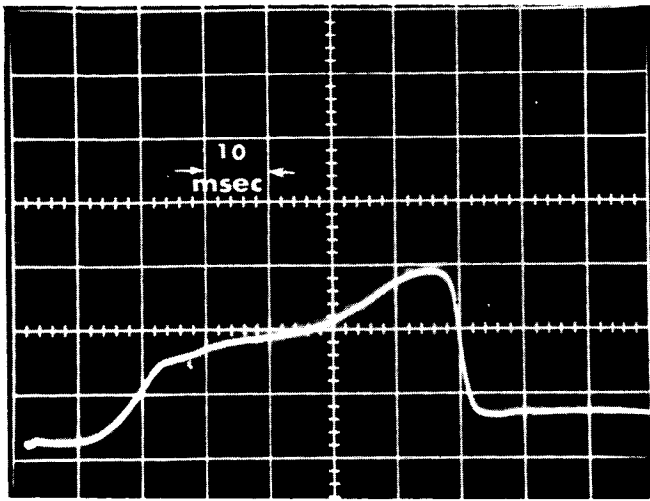
a) Loose-Atmospheric
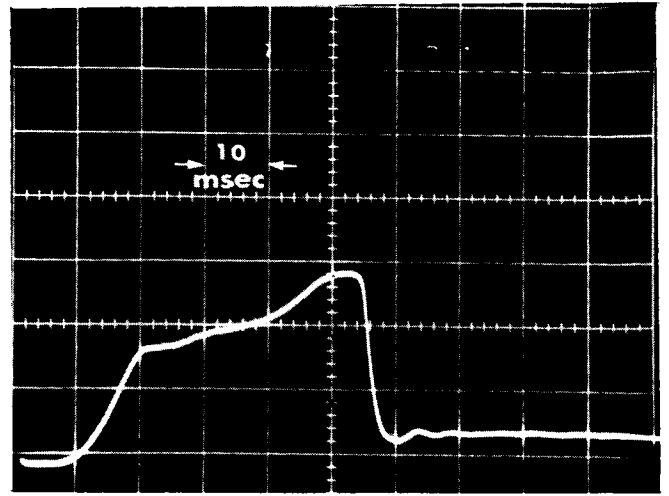
b) Loose-Rough Vacuum
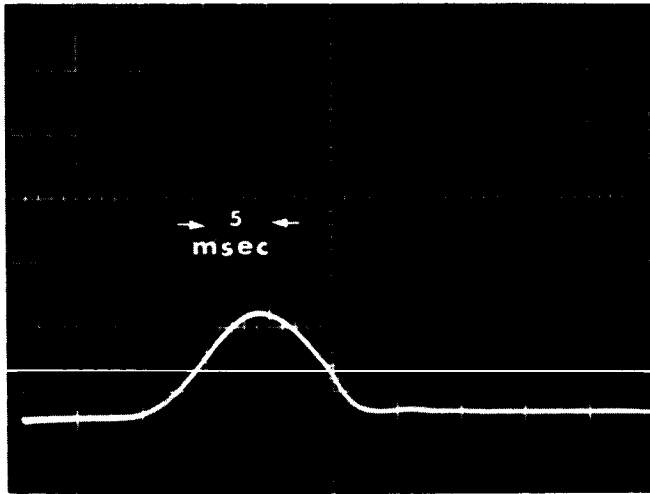
c) Dense-Atmospheric
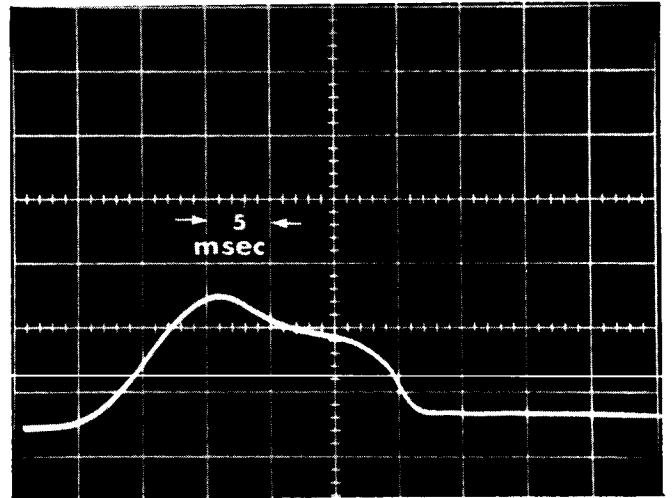
d) Dense-Rough Vacuum
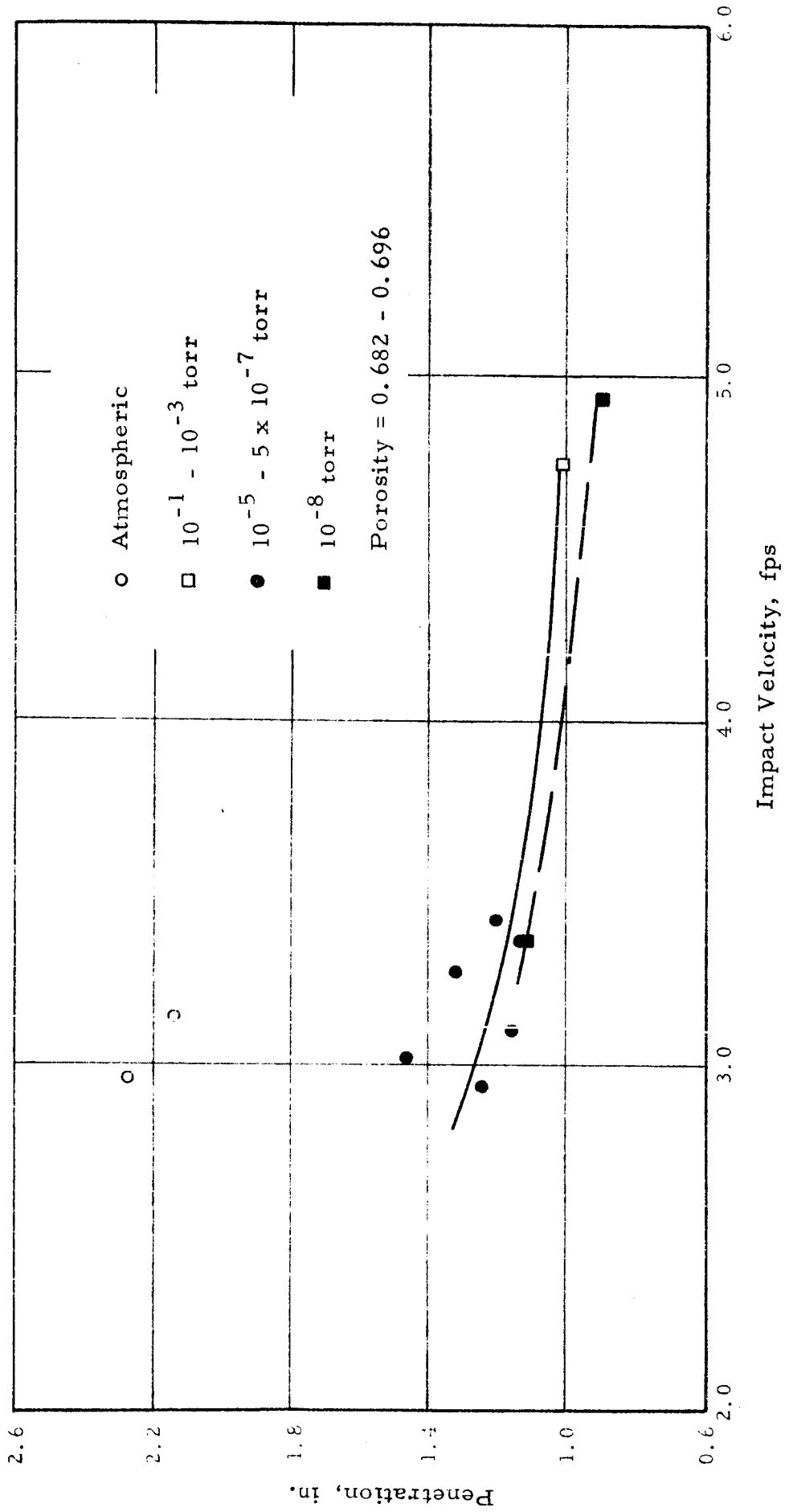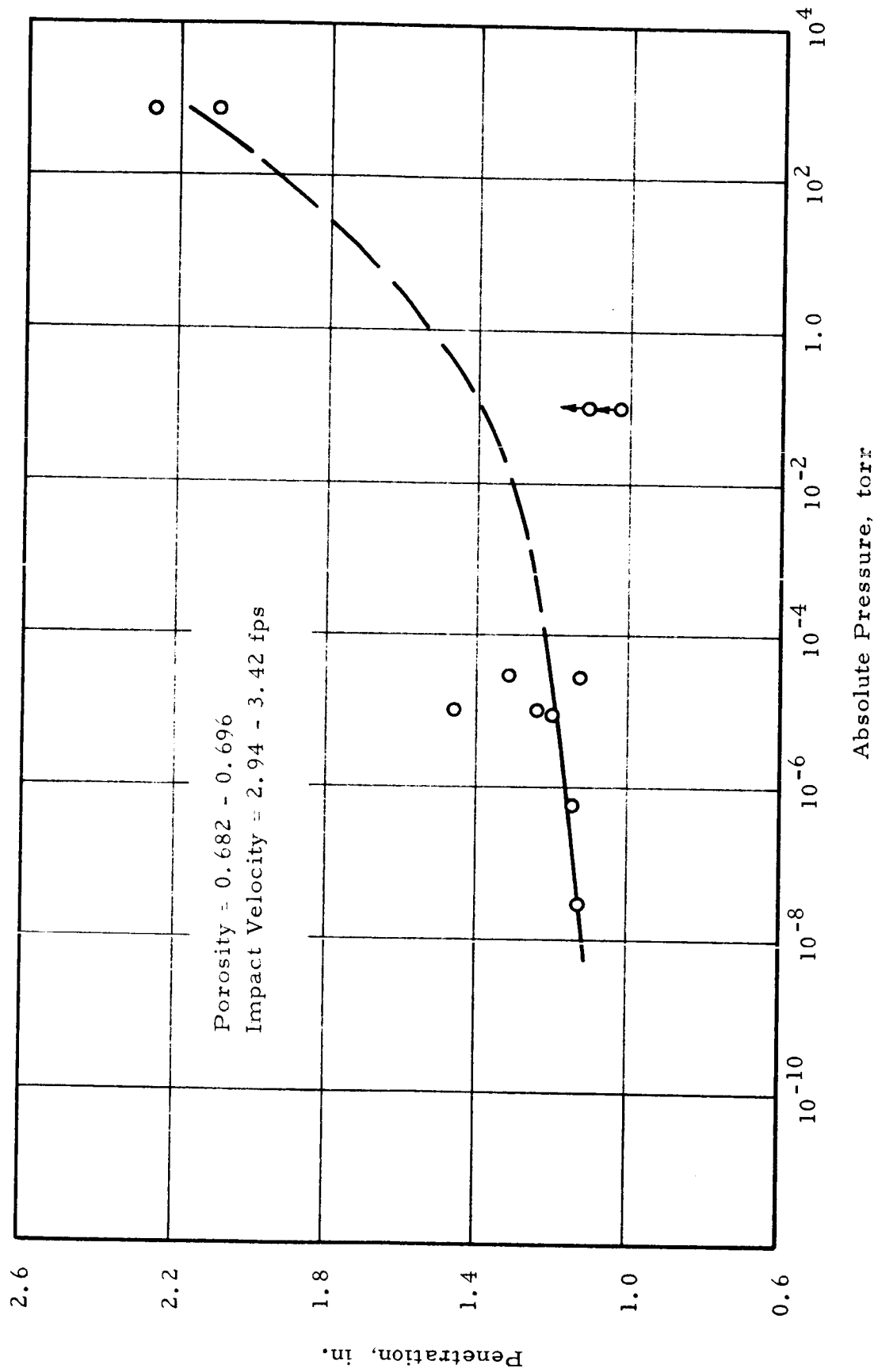
Fig. 47   TYPICAL SIGNATURES FOR 60° CONE IN FINE SAND
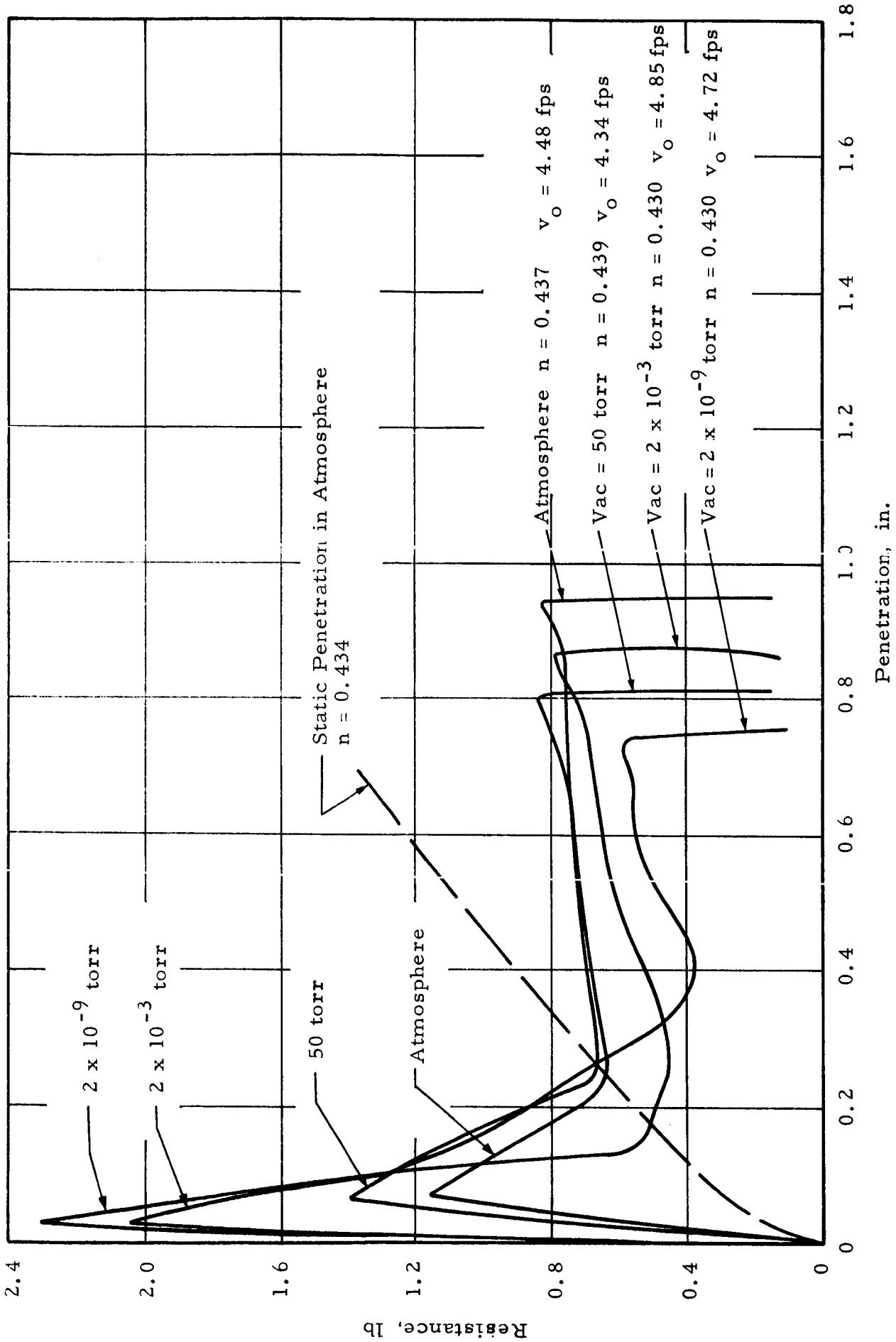
Fig. 48   RESISTANCE AS A FUNCTION OF PENETRATION IN FINE SAND
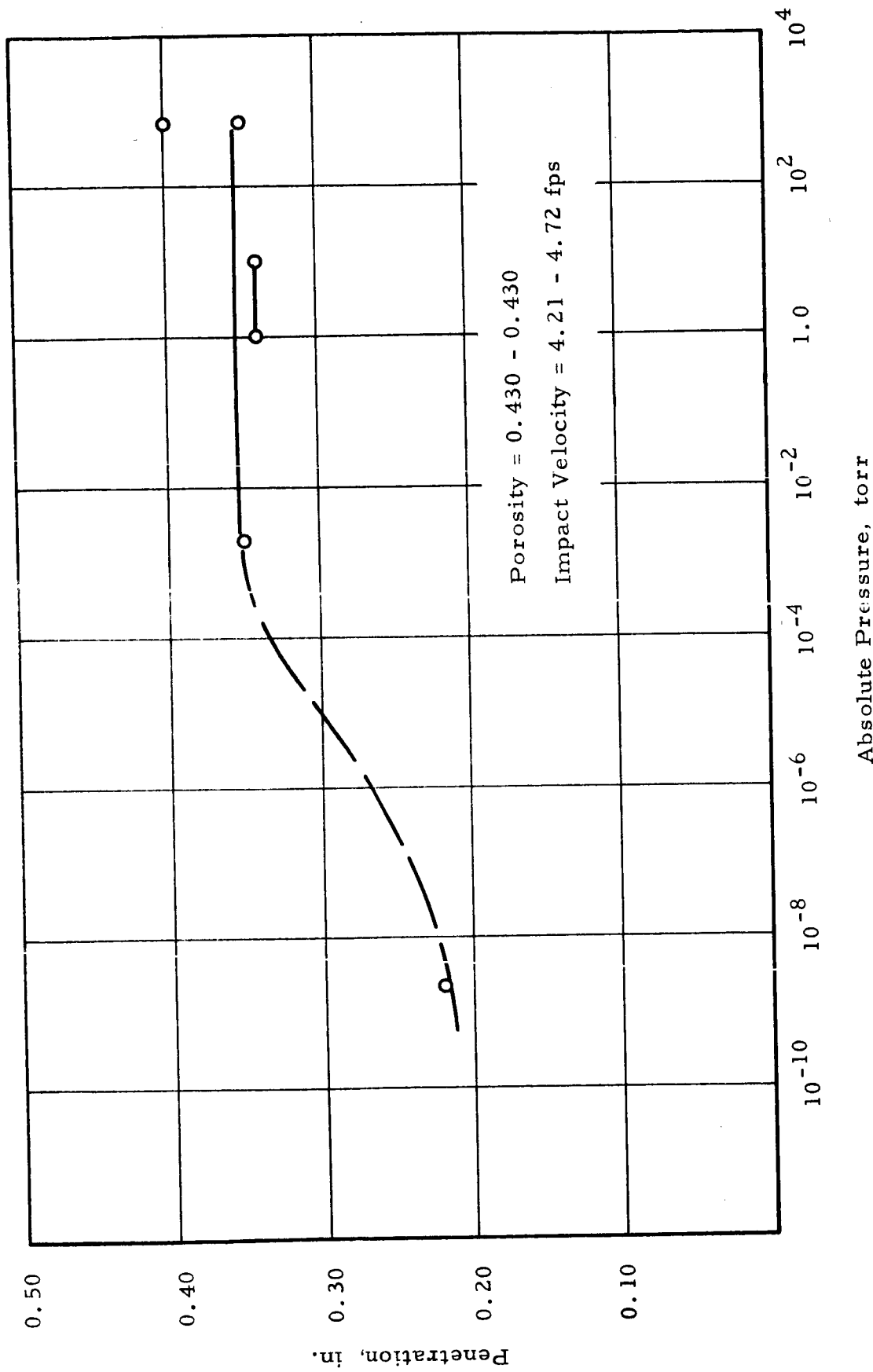
Fig. 49   EFFECT OF VACUUM ON PENETRATION AT 0.3 IN.-LB WORK IN
            FINE SAND

D.   Experiments in Coarse Sand

A limited number of experiments were also conducted in samples of coarse grained Ottawa sand. These consisted only of experiments under atmospheric and rough vacuum conditions using a 60 deg cone penetrometer.

Typical signatures obtained in these experiments are shown in Fig. 50. As would be expected rough vacuum levels had no effect on the penetration resistance because of the large grain size.

Many factors influence the penetration resistance of soil under dynamic loading. In general, when the effects of porosity and impact velocity were eliminated, the penetration resistance was observed to increase under vacuum. The increase in resistance was due to the absence of pore pressures and/or an increase in shear strength depending upon the grain size and mineralogical composition of the soil.
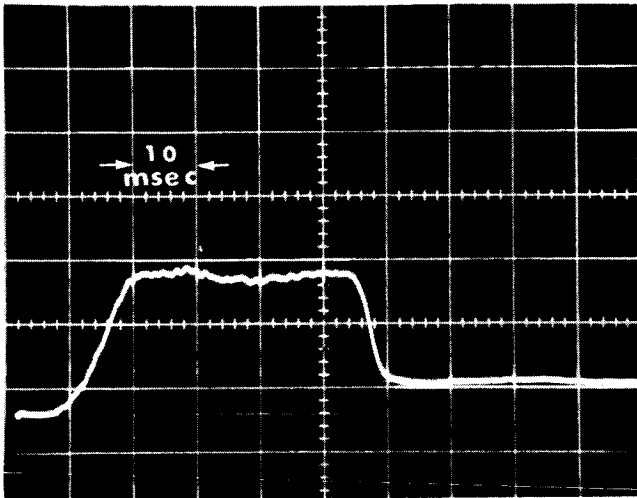
a) Loose-Atmospheric
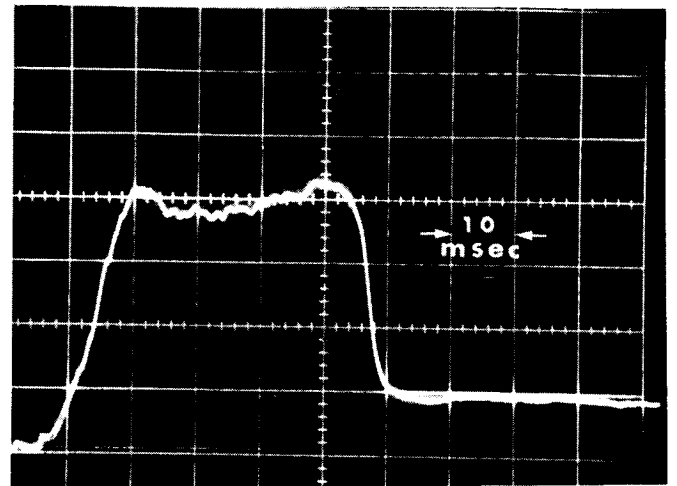
b) Loose-Rough Vacuum
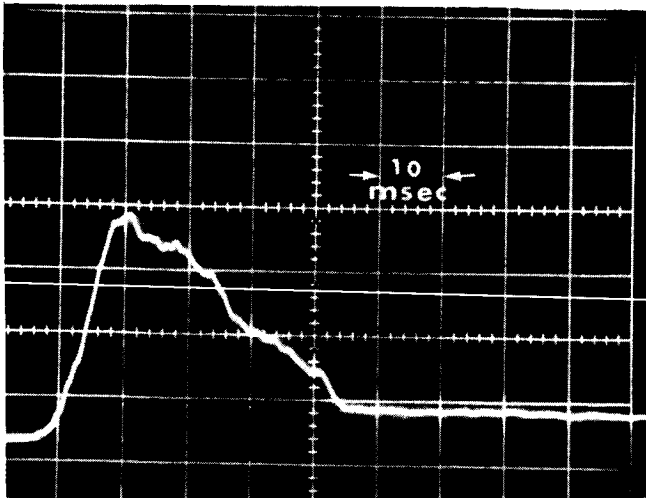
c) Dense-Atmospheric
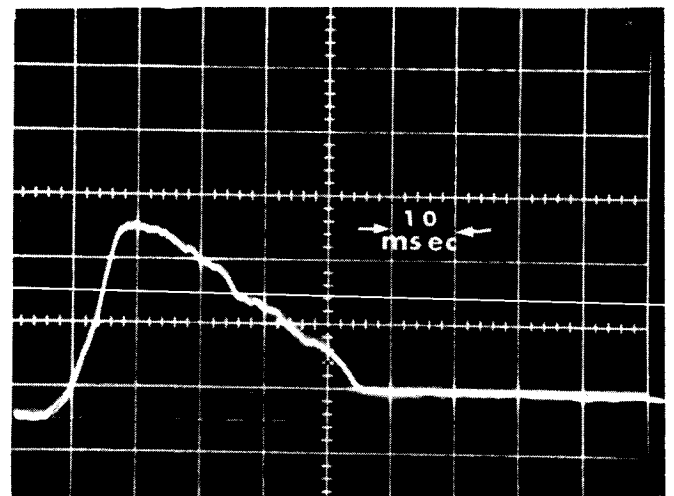
d) Dense-Rough Vacuum

Fig. 50   TYPICAL SIGNATURES FOR 60° CONE IN COARSE SAND

VIII. CONSOLIDATION CHARACTERISTICS

Experiments were performed to investigate one-dimensional consolidation characteristics of the quartz powder in atmosphere and vacuum levels up to the 10^{-9} torr range.

While consolidation tests are conventionally performed using a controlled stress method of load application, the apparatus used in these experiments was of the controlled strain type because of restrictions imposed by the bellows of the vacuum chamber. Results of controlled strain tests using rates of 0.01 and 0.02 inch per minute were compared with results obtained by controlled stress tests under atmospheric conditions. All results were observed to agree closely and, hence, it was concluded that for these rates of loading the rate and/or method of load application had a small effect on the results.

The apparatus consisted of a stainless steel ring 2.50 inches in diameter and 0.74 inches high having a perforated bottom to aid in outgassing the soil. A stainless steel 200 mesh screen was placed in the bottom of the ring to prevent the soil from being forced out through the perforations during load application.

Prior to pumpdown of the vacuum chamber the loading cap was brought in contact with the sample surface being careful not to apply any load to the soil. The sample was, therefore, quite confined during pumpdown and effective outgassing could take place only through the bottom of the sample. Drawdown times consisted of approximately one week during which the sample was first baked and then cooled to room temperature. Consequently, although vacuum levels in the 10^{-9} torr range were achieved in the chamber the actual vacuum in the soil pores was probably two to three orders of magnitude less than this. However, at the lower vacuum levels (10^{-2} and 10^{-5} torr) the difference between chamber vacuum and that in the soil was probably less.

The results of the experiments in the form of the void ratio (e) as a function of the bearing pressure (p) is shown in Fig. 51. Experiments were performed on samples having different initial void ratios (e_o). For the higher initial void ratios, however, the void ratio decreased quite rapidly

IIT RESEARCH INSTITUTE

Vacuum	e_o
○ Atm	1.62
□ Atm	2.05
▽ Atm	2.33
◐ 2×10^{-2} torr	2.20
◧ 2.5×10^5	2.20
● 4×10^{-9}	2.20
■ 4×10^{-9}	2.13
▶ 5×10^{-9}	1.77

Pressure, tons/ft^2
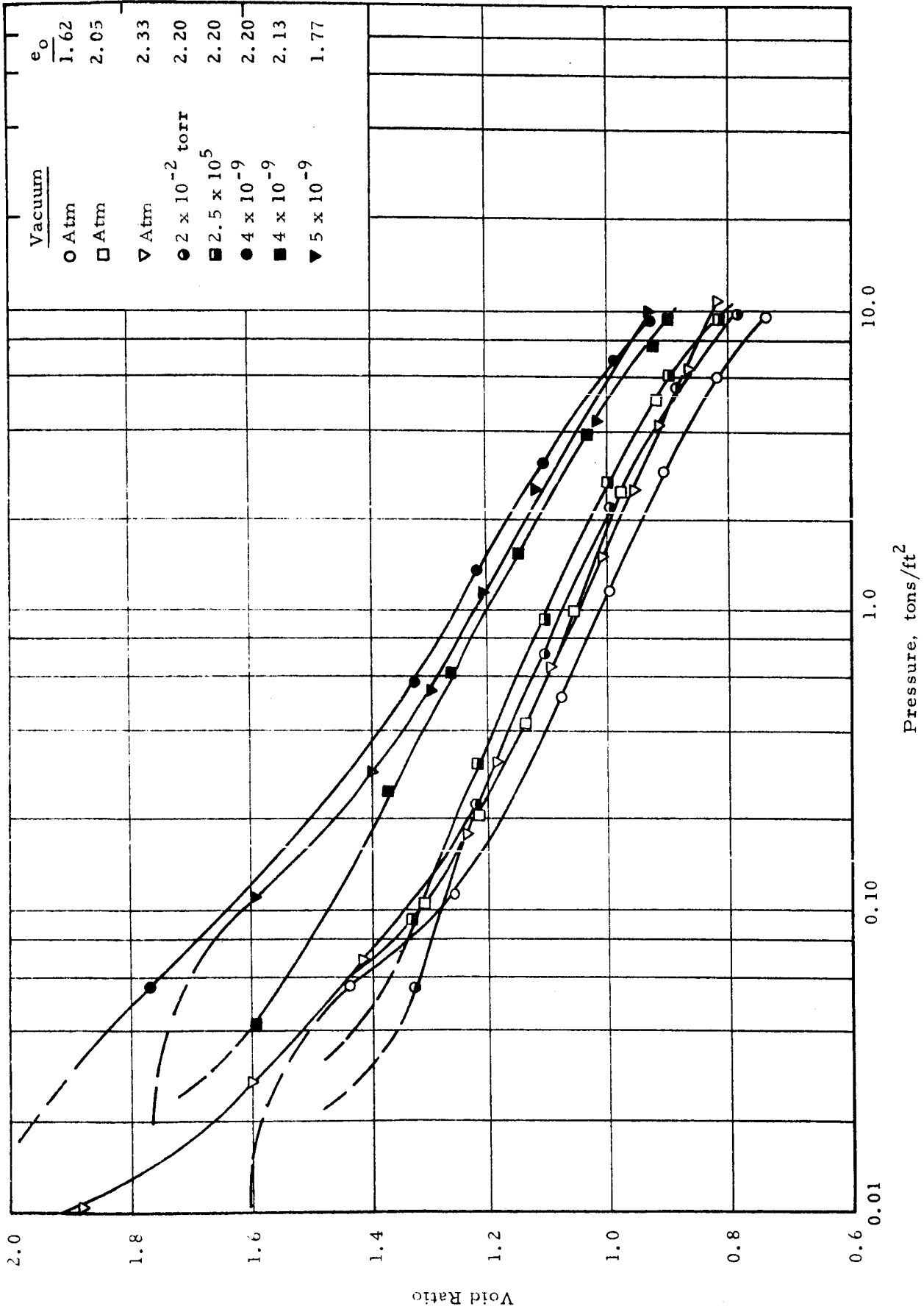
Void Ratio

Fig. 51   e-LOG P CURVES FOR QUARTZ POWDER

-86-

at the low pressures after which the curves leveled off and at bearing pressures greater than approximately 0.10 tons per ft^2 the curves for the different initial void ratios converged and followed the same path. It should be noted, also, that for p > 0.10 the curves are very close to straight lines.

Under the low vacuum levels the curves are almost the same as for atmospheric conditions indicating that the effects of pore air at these low rates of strain are negligible. However, under ultra-high vacuum the shear strength was somewhat greater and consequently the e-log p curves are above those for the lower vacuum levels and atmospheric conditions. Also the curves appear to be slightly steeper under ultra-high vacuum and tend to converge towards those obtained in atmosphere at the higher pressures. At pressures greater than approximately 6 tons per ft^2, the curves in rough vacuum and in atmosphere appear to become steeper than those in ultra-high vacuum indicating further collapse of the grain structure. Additional data are necessary at higher pressures, however, to verify this.

In Section IV of this report note that the grain structure may be different when the soil is deposited in vacuum and, hence, it would be expected that the conditions under which the soil was deposited would affect the consolidation characteristics. Additional data are necessary before more definite conclusions can be drawn regarding consolidation, but it appears that under ultra-high vacuum less settlement may be expected than would occur in the atmosphere.

IX. REVERSIBILITY OF VACUUM EFFECTS

The shear strength of fine grained soil may increase under ultra-high vacuum due to the development of interparticle forces as the result of the removal of adsorbed gas from the soil grains. If these forces were of sufficient magnitude to prevent or retard the formation of the original adsorbed gas layers upon re-exposure to the atmosphere or in the extreme case, if cold welding between the particles had occurred, the effects of the vacuum would then be irreversible.

In order to investigate the reversibility of the vacuum effects, experiments were performed in which soil samples were placed in a vacuum chamber at vacuum levels up to 3.5×10^{-11} torr for time periods ranging from 170 to 935 hours (Fig. 52) after which they were removed and their shear strength measured under atmospheric conditions.

To provide efficient outgassing of the soil, it was desirable to perform these experiments on small unconfined samples having high porosities. Since standard techniques of measurement require considerable confinement of the sample and/or thick samples and since it was not necessary to accurately determine the individual shear strength parameters, a special method was devised which required only very thin samples.

The apparatus used is shown in Fig. 53 and consisted of a thin circular plate resting in a shallow container into which the soil was placed. The shear strength was determined by measuring the force required to cause movement of the plate in the upward direction producing shear in the soil over a cylindrical surface as shown in Fig. 54. Resistance to movement was offered by the weight of the soil on the plate and by shear stresses on the failure surface. Since the normal stress on the failure surface was negligible (i.e., $\sigma \approx 0$), the difference between the maximum force required to lift the plate and the weight of the soil was due primarily to the apparent cohesion of the soil. Also, in a soil having a high porosity the void ratio of the soil would be expected to decrease during shear, and consequently, the amount of interlocking between the particles would be small. For this reason interparticle forces were considered to contribute the major portion of the shear strength at the higher porosities.

IIT RESEARCH INSTITUTE
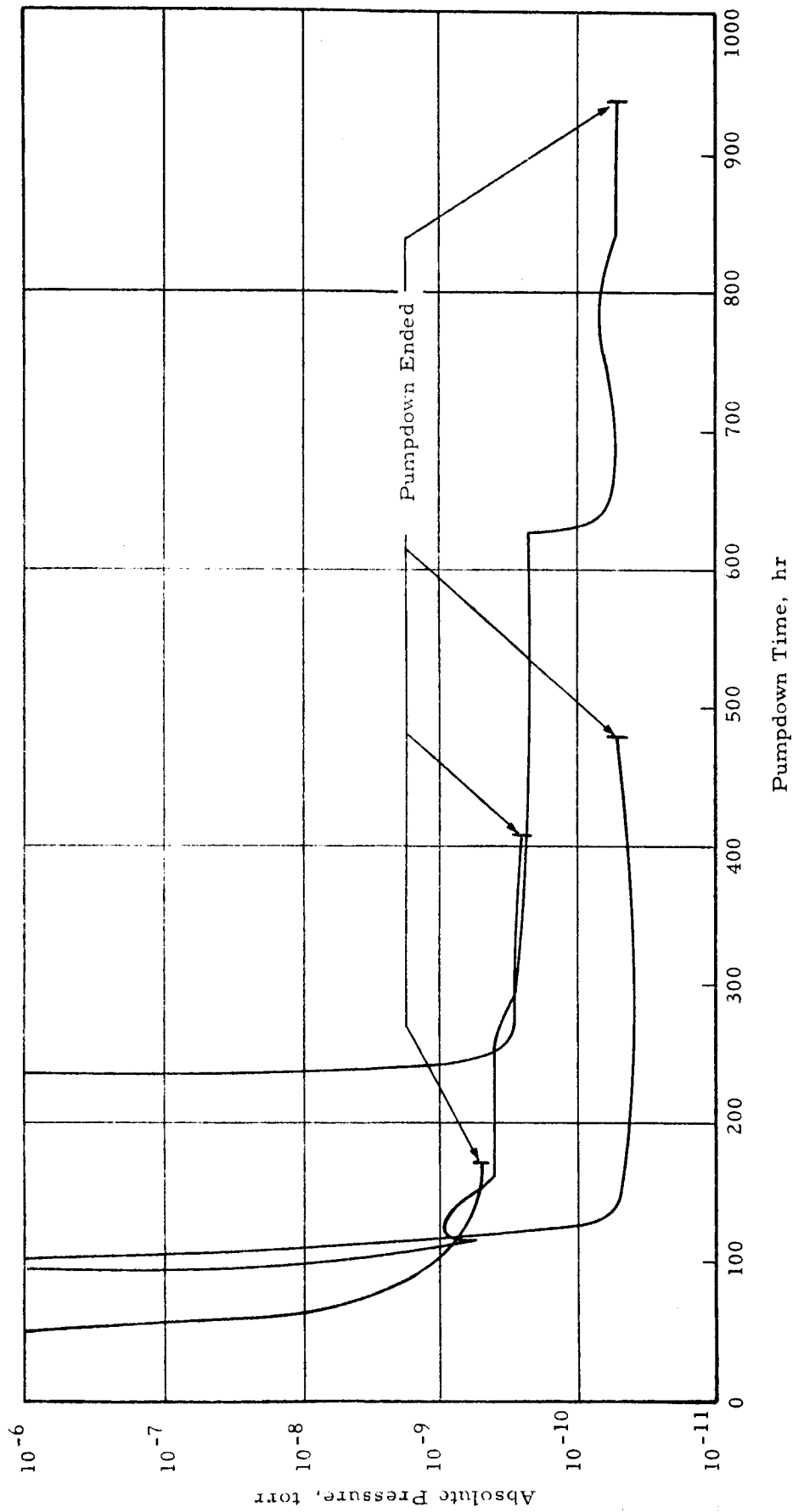
Fig. 52   PUMPDOWN CURVES FOR PLATE SHEAR TESTS

To Gear Box and Motor

Load Cell

Linear Vertical Displacement
Transformer (LVDT)

Soil

Aluminum Plate
and Dish
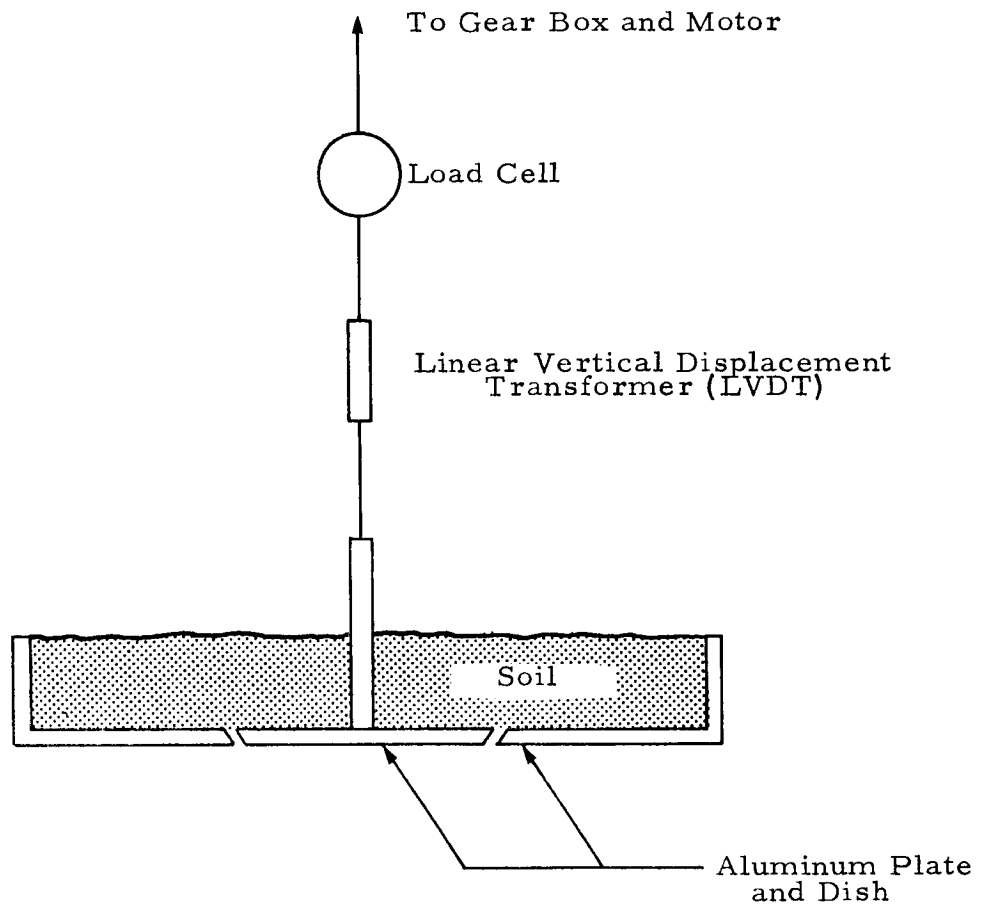
Fig. 53   PLATE SHEAR APPARATUS

a) Quartz Powder
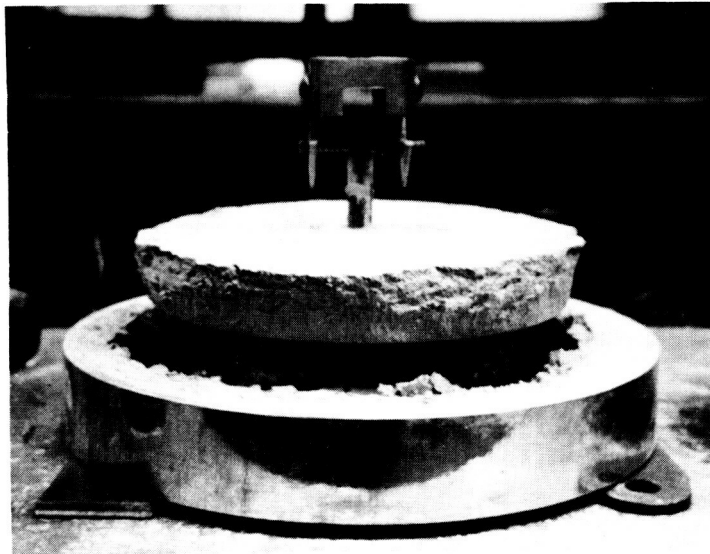
b) Olivine Powder

Fig. 54 SOIL SAMPLES AFTER PLATE SHEAR TESTS

Representative curves showing the force on the plate as a function of displacement for samples stored under atmospheric and vacuum conditions are shown in Fig. 55. The maximum force was developed at quite low values of displacement after which the interparticle forces were overcome and the grain structure collapsed causing a rapid decrease in shear strength. Exposure to vacuum appears to have had a negligible effect on the shape of the curve.

In Fig. 56 and 57 are shown the shear strength of the quartz and olivine powders as determined by the plate shear tests for samples stored under atmospheric and vacuum conditions. For the olivine powder it is evident that the range of scatter is the same for the soil exposed to vacuum as for the soil that was not. While the same is true for the quartz powder at the lower porosities it should be noted that at the higher porosities the shear strength of the soil exposed to vacuum was consistently higher than that of the soil which was not.

In one experiment the soil was deposited in a vacuum ranging from 3×10^{-9} to 1.5×10^{-8} torr after which it remained in the vacuum chamber for four days at approximately 2.5×10^{-9} torr. In a second experiment the soil was deposited through a glow discharge in an attempt to facilitate "cleaning" of the particle surfaces. The glow was sustained by venting the system to dry nitrogen to a pressure of approximately 35μ Hg and applying a potential of 1 kilovolt to a stainless steel ring inside the chamber. Nitrogen was chosen as the sputtering medium because it is pumped readily by ion pumps and its low energy of adsorption makes it easily removed from the particle surfaces.

Portions of the soil were deposited at intervals of approximately 12 hours between which the system was pumped down to the 10^{-8} torr range. The shear strengths of these samples were measured under atmospheric conditions and the results plotted on Fig. 57. The strength of the soil deposited in the vacuum was approximately the same as that of the soil stored in atmosphere while the soil deposited in the glow discharge had a shear strength closer to that of the soil stored in vacuum.
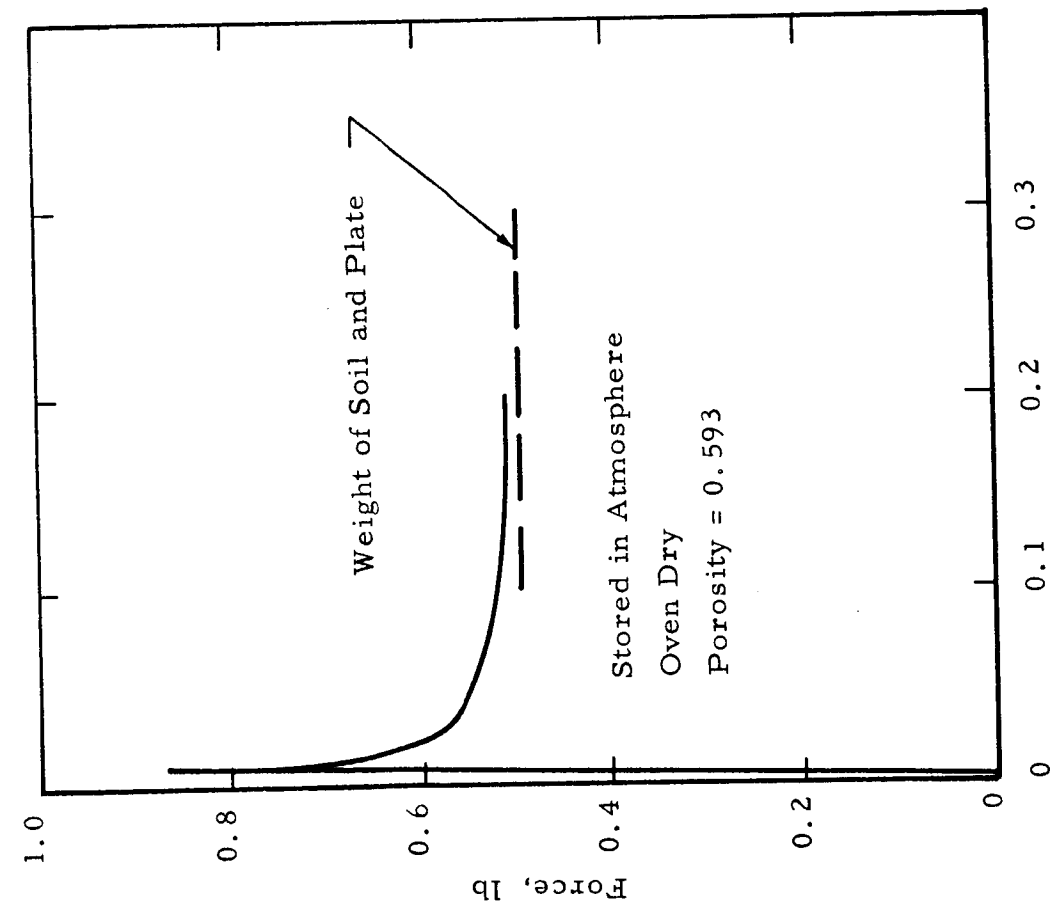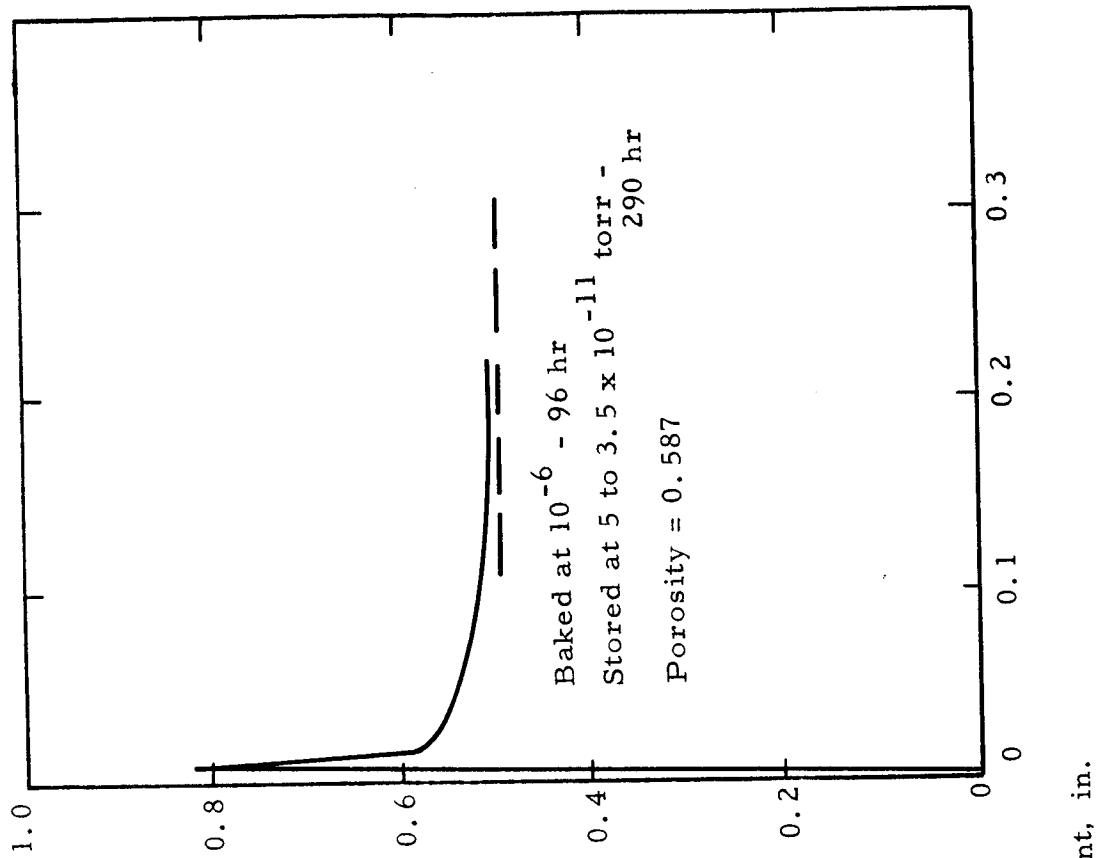
Fig. 55   FORCE REQUIRED TO CAUSE DISPLACEMENT IN PLATE SHEAR TESTS
ON QUARTZ POWDER

- 93 -
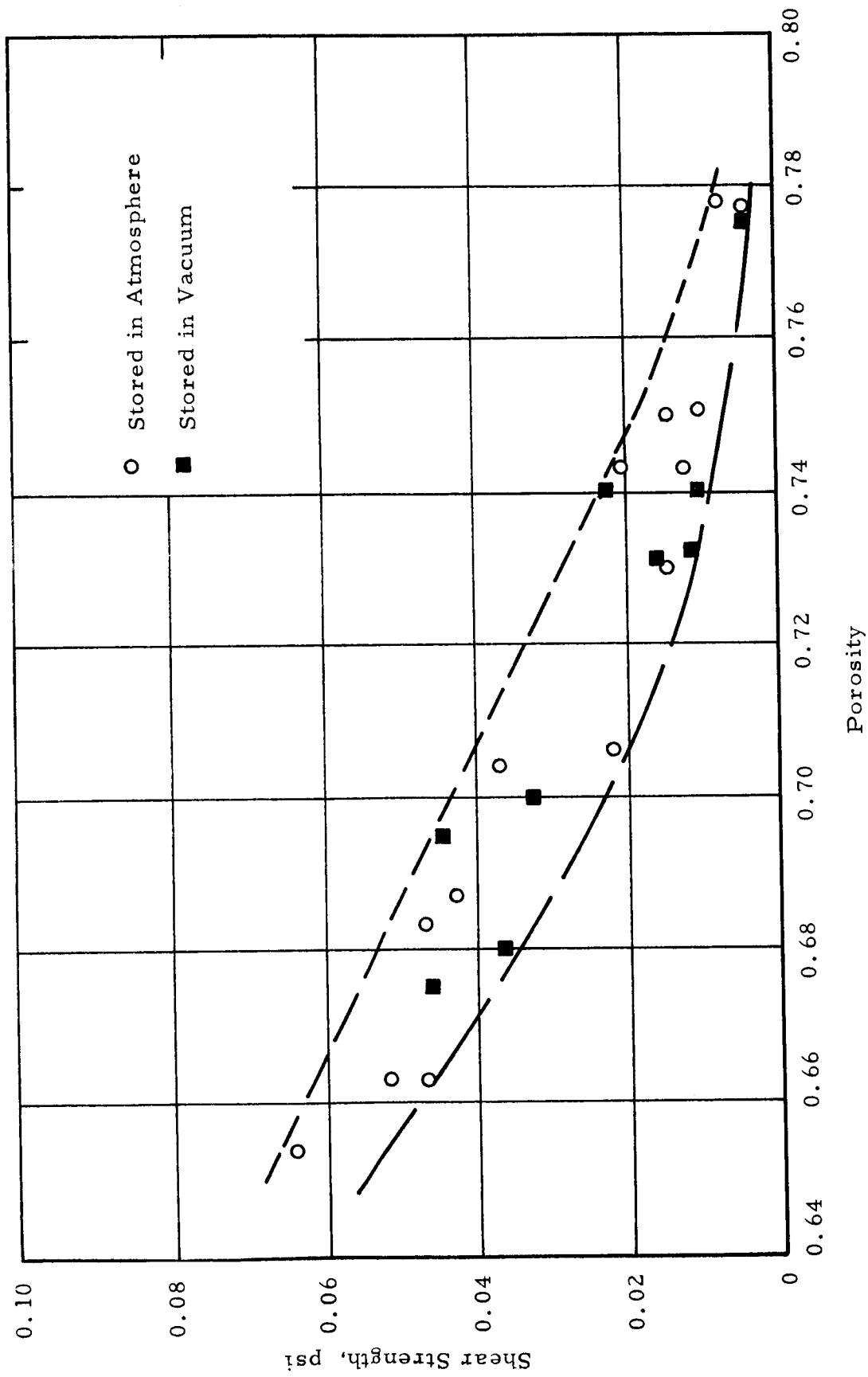
Fig. 56   EFFECT OF POROSITY ON SHEAR STRENGTH OF OLIVINE POWDER
FROM PLATE SHEAR TESTS
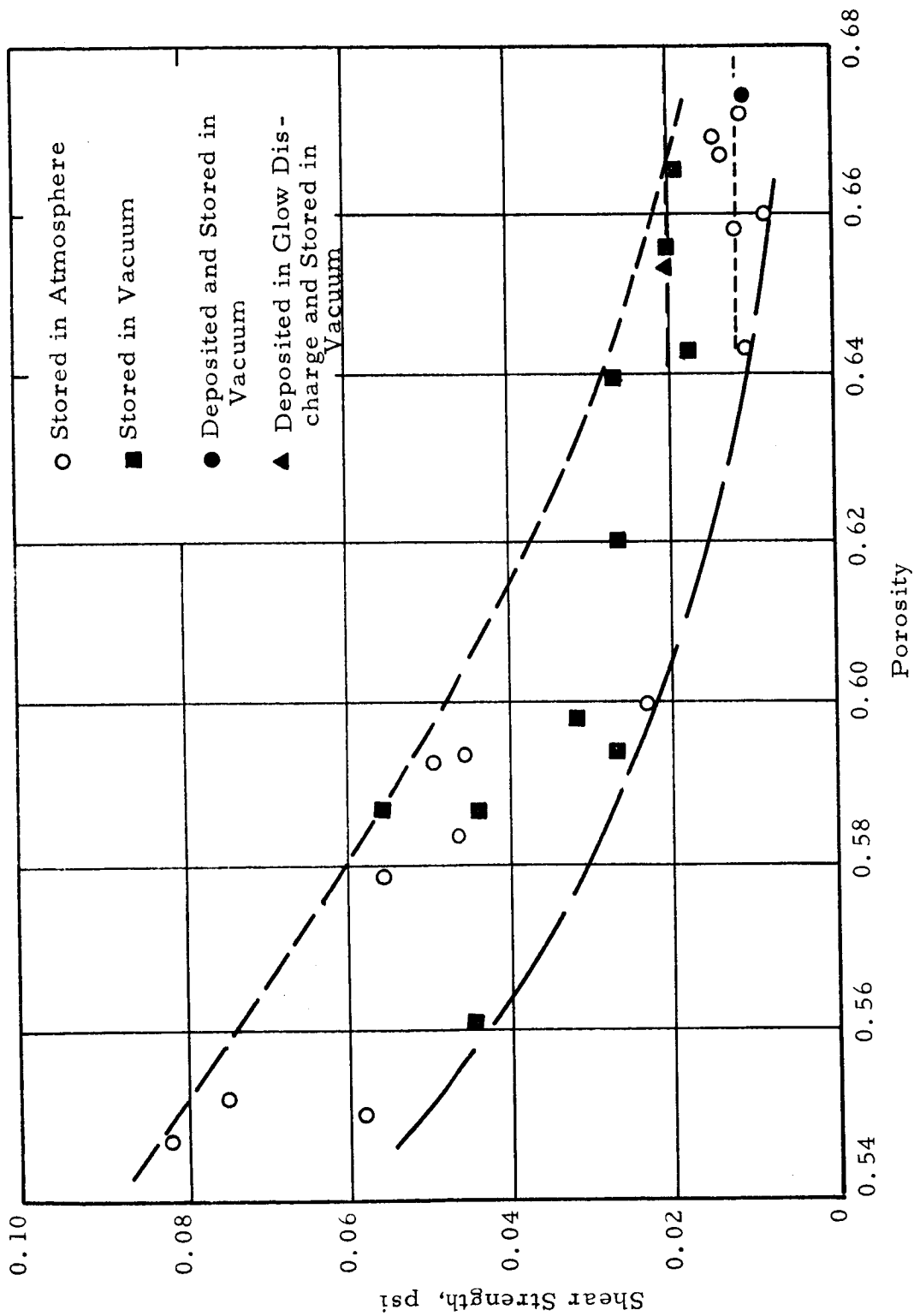
Fig. 57 SHEAR STRENGTH OF QUARTZ POWDER FROM PLATE SHEAR TESTS
AS A FUNCTION OF POROSITY

It is evident, however, that the effects of vacuum on the shear strength of olivine, if any, were reversible as were the vacuum effects on the quartz at the lower porosities. At the higher porosities there appears to have been an increase in the shear strength of quartz due to vacuum storage which is, to some extent, irreversible.

X.   ADHESION CHARACTERISTICS OF SOIL

One problem which may be anticipated in insuring the proper function-
ing of vehicles and instruments on the lunar surface is the adhesion which
may develop between soil and other materials. In order to investigate this
adhesion experiments were performed in which quartz powder was deposited
on small plates of aluminum, stainless steel, teflon and glass under
(1) ultra-high vacuum (2×10^{-9} torr) and elevated temperature (300 deg F)
and (2) a glow discharge in a dry nitrogen atmosphere at a vacuum level of
35μ Hg as described in the previous section. Subsequent to deposition the
plates remained under vacuum in the low 10^{-9} torr range for approximately
5 days after which they were removed and observed under atmospheric
conditions.

A considerable amount of soil was observed to adhere on the metal
surfaces with lesser amounts adhering to the teflon and glass. Figure 58
shows the samples after removal from the vacuum chamber. The general
appearance of the plates was the same for both conditions of deposition
and hence Fig. 58 shows the plates from only one experiment. Before the
photograph was taken, the plates were held upside down to remove as much
of the soil as possible from the surface.

A considerable deposit of soil remained on all plates, the major
portion of which could be removed by wiping the surface and was probably
held in place principally by electrostatic forces. On the metal surfaces,
however, a thin layer of soil was observed to have formed which could be
removed only by scraping the surface. This thin layer was more predominant
on the aluminum and covered a larger area than on the stainless steel.

Photographs of the surfaces as they appeared under a microscope after
removing as much of the soil as possible by wiping are shown in Fig. 59
through 62. The thin layer of soil which adhered to the material shows up
as the darker areas on the photographs of the aluminum and stainless steel.

On the aluminum (Fig. 59) it is seen that the major portion of the
surface was covered by this thin layer. In the photograph showing the soil
deposited under ultra-high vacuum (Fig. 59a) the small round spots as

IIT RESEARCH INSTITUTE

identified by an arrow were determined to be particles bound to the material rather tightly and projected approximately 6 to 10μ above the surface. For the soil deposited in a glow discharge a much lesser amount of these particles was observed.

A much smaller area is seen to be covered by the layer of soil on the stainless steel (Fig. 60). In Fig. 60a showing the soil deposited under ultra-high vacuum, a spot similar to those shown in Fig. 59a can be seen near the center of the photograph. In this case, however, the spot was not raised from the surface but instead formed a small crater approximately 5μ deep. The dark area on the left hand side of Fig. 60b shows the layer of soil adhering to the surface, and as indicated previously can be seen to cover much less of the surface than it did on the aluminum. Individual soil grains can also be seen in this photograph near the top. These grains, however, could be moved about quite easily and were bonded to the surface only by electrostatic forces.

From Fig. 61 it can be seen that the soil exhibited very little adhesion to the teflon. Individual soil grains can be seen on Fig. 61b but it is evident that no tightly bound layer such as formed on the metallic surfaces appeared on the teflon.

On the glass almost the entire surface remained unchanged by the soil except for a very few spots (Fig. 62). However, these spots were probably caused by abrasion during the impact of soil grains with little or no adhesion occurring between the glass and the soil.

Therefore, it is evident that considerable deposits of soil may be built up on the surfaces of other materials due to (1) electrostatic forces, and (2) adhesion between the soil and the surface which could result in "cold welding" between the soil and the material. This "cold welding", however, was greater on the aluminum than on the stainless steel and did not exist on the nonmetallic surfaces of teflon and glass.

Stainless Steel   Aluminum

Glass   Teflon

Fig. 58   QUARTZ POWDER DEPOSITED ON VARIOUS
MATERIALS UNDER GLOW DISCHARGE
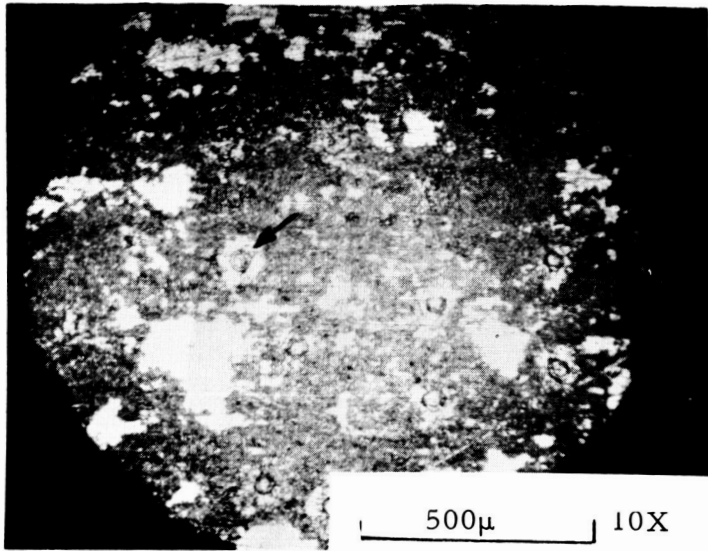
a) Vacuum = 2×10^{-9} torr
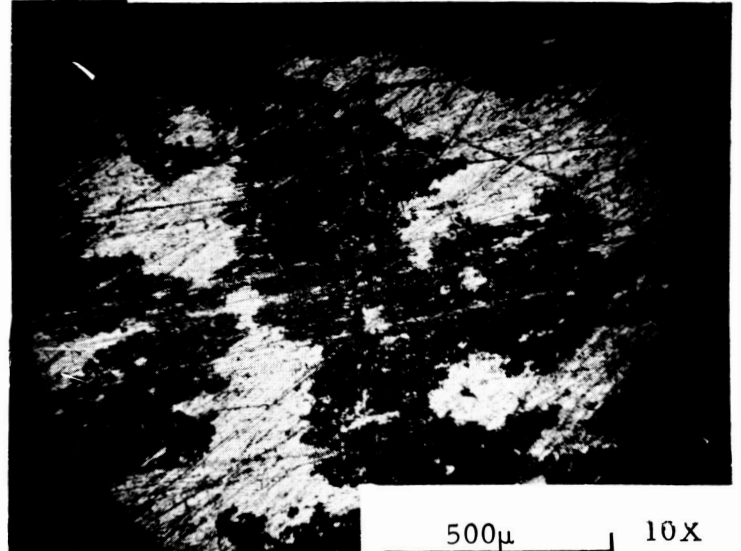
b) Vacuum = 35μ - Glow Discharge
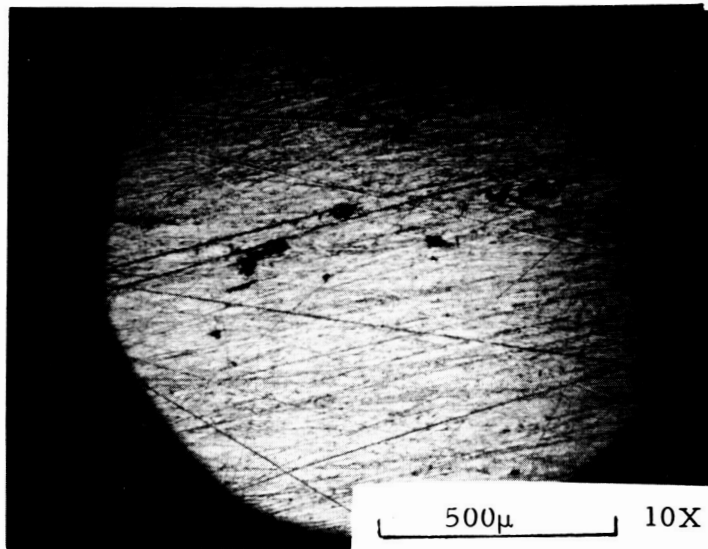
c) Before Deposition

Fig. 59   POLISHED ALUMINUM BEFORE AND AFTER
DEPOSITION OF QUARTZ POWDER
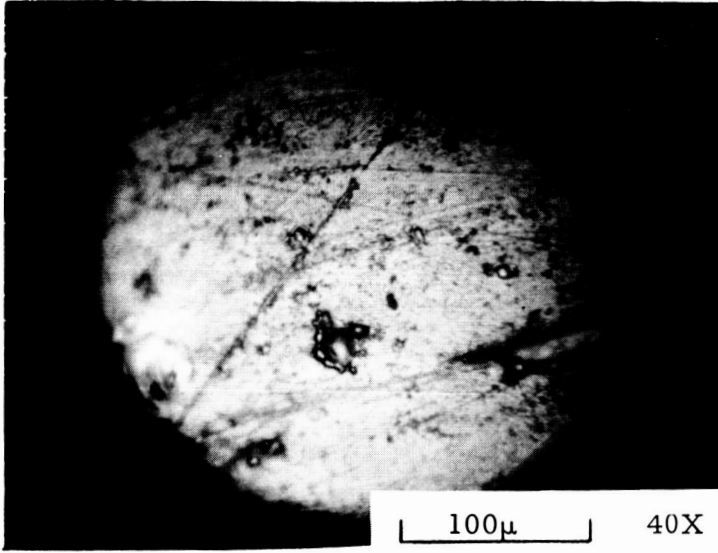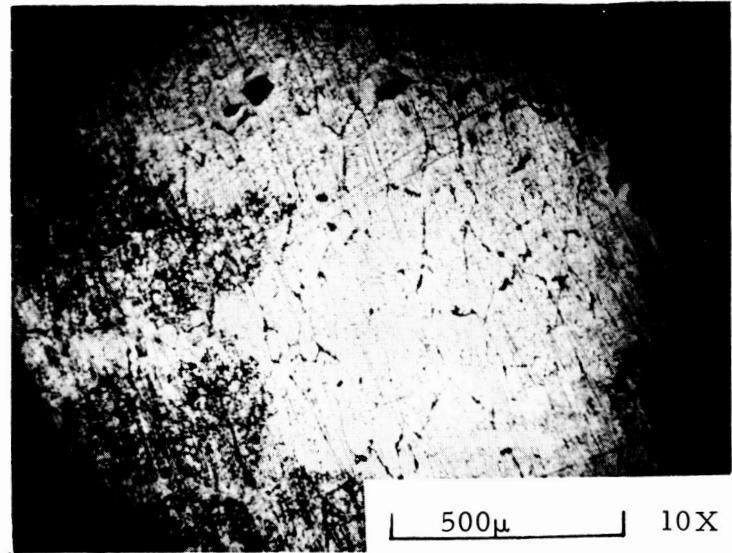
a) Vacuum = 2×10^{-9} torr

b) Vacuum = 35μ - Glow Discharge
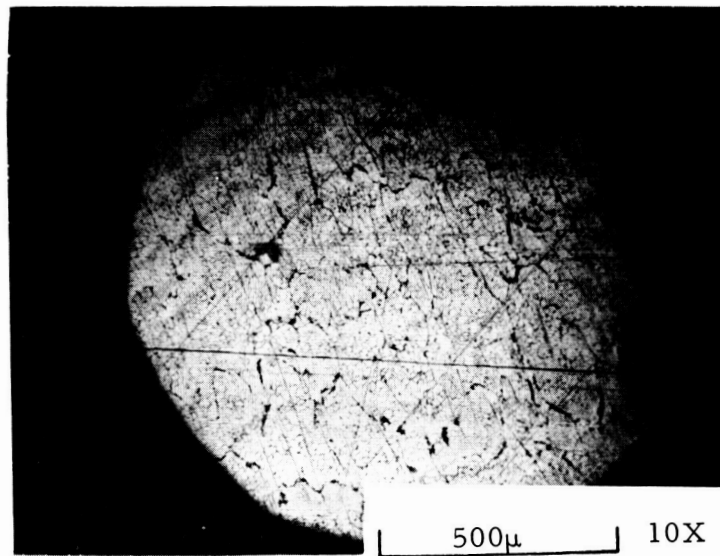
c) Before Deposition

Fig. 60   POLISHED STAINLESS STEEL BEFORE AND
AFTER DEPOSITION OF QUARTZ POWDER
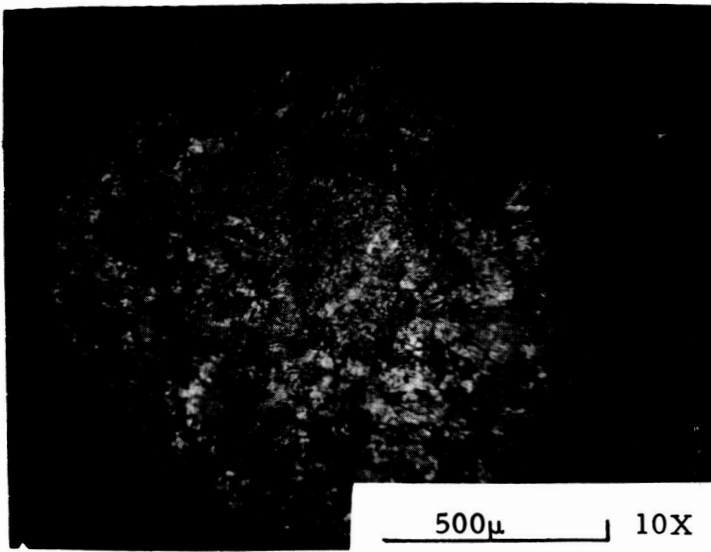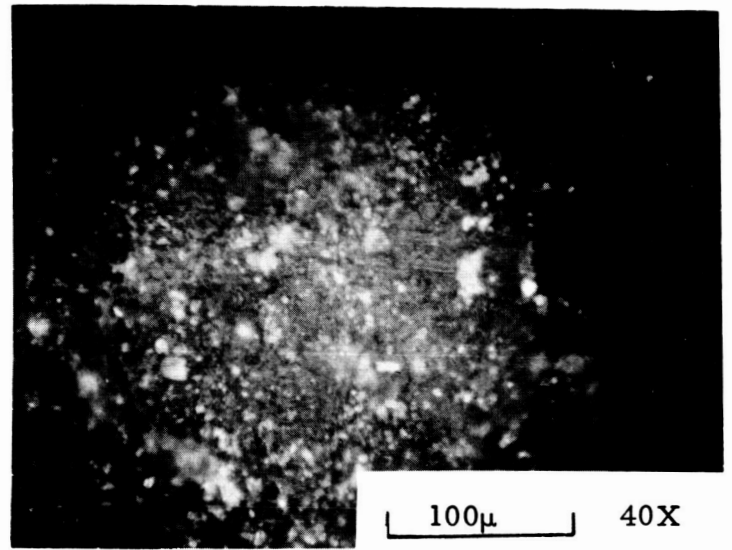
a) Vacuum = 2×10^{-9} torr

b) Vacuum = 35μ - Glow Discharge
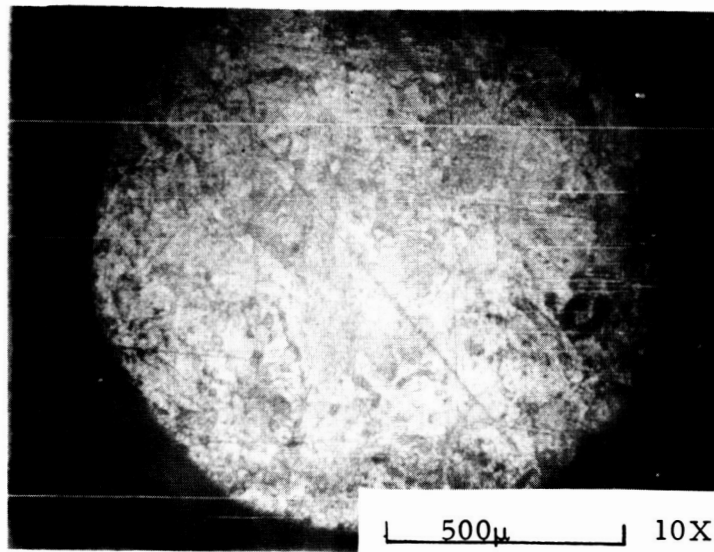
c) Before Deposition

Fig. 61   TEFLON BEFORE AND AFTER DEPOSITION
OF QUARTZ POWDER
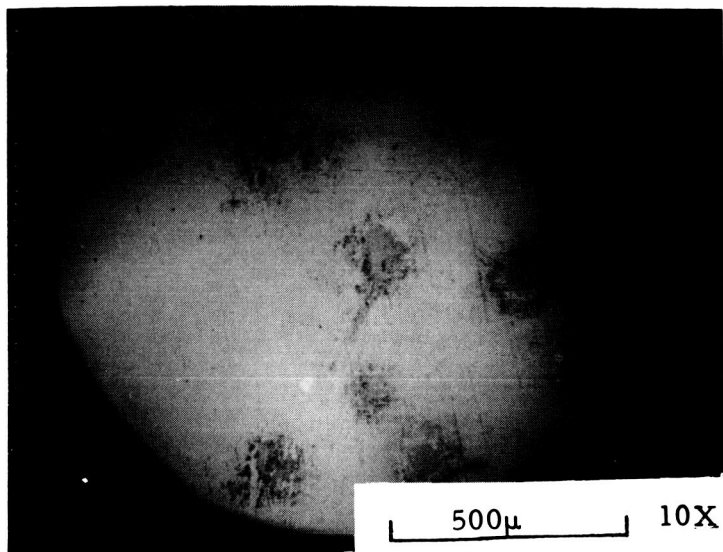
a) Vacuum = 2×10^{-9} torr
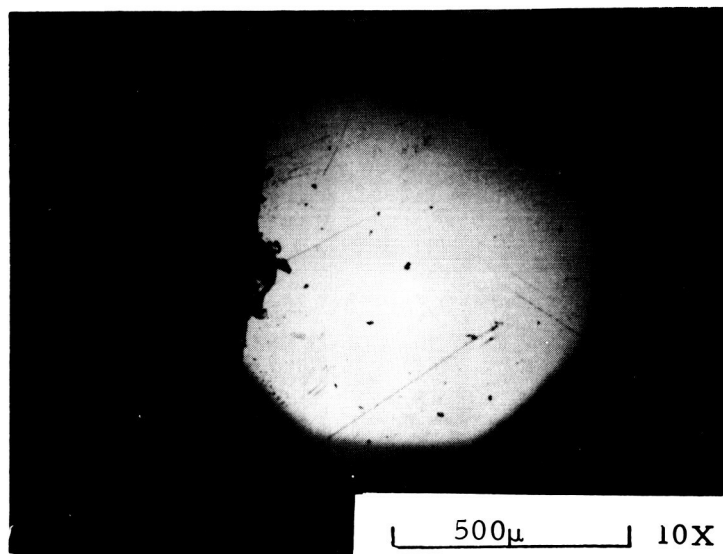
b) Vacuum = 35μ - Glow Discharge

Fig. 62   GLASS AFTER DEPOSITION OF QUARTZ POWDER

XI. CRATERING OF SOIL UNDER LOW VELOCITY IMPACT

On the basis of the recent Ranger photographs various hypotheses have been put forth regarding the soil type on the lunar surface as deduced from the observed shape of the craters. In order to investigate the crater forms, e.g., steepness of walls, height and steepness of lip which various soil types are able to support, a limited number of experiments were performed in atmosphere and rough vacuum in which projectiles were dropped into a few soil types and the crater formation observed. It should be emphasized that this does not actually simulate crater formation on the moon because of the low vacuum levels (2×10^{-2} torr) and the low impact velocities (maximum of approximately 30 ft per sec) that were used. Rather it serves only to demonstrate the types of crater formations that these soils are capable of supporting and to indicate some effects of vacuum on the crater shape and size.

Figure 63 shows craters formed in loose, fine grained Ottawa sand in atmosphere. An interesting feature is the peak formed in the center of the crater. While the crater was only approximately one inch deep the ball penetrated 3 to 4 inches and the central peak was formed by soil forced out by escaping pore air. The soil forming this peak was observed to be thrown upward to distances of approximately six inches during crater formation. In Fig. 63 thru 67 the ball was removed and in those cases where it cannot be seen, it was below the soil surface.

Figure 63 shows four craters formed under rough vacuum with the center crater being formed in atmosphere. It should be noted that the central peak which formed under atmospheric conditions was absent in the vacuum and that the craters formed in vacuum had considerably more of an upraised rim than those formed in atmosphere. The rims were considerably greater than is shown in the photograph because the sample was inadvertently jarred prior to taking the photographs. The conical shape of the craters formed in vacuum should also be noted.

Figure 64 shows the craters formed in atmosphere and vacuum in loose coarse sand. It can be seen that in both cases the craters were conical

and very similar in shape. Also, the central peak which was observed in the fine sand was absent.

Figure 65 shows the craters formed in well graded river bed sand. Under both atmospheric and vacuum conditions it can be seen that the craters were conical but in the vacuum it appears that the crater rim was more prominent than in atmosphere.

Figure 66a shows a typical crater formed in loose quartz powder in atmosphere. It can be seen that there was a considerable amount of ejecta thrown outward by escaping pore air. With a drop height of 20 ft it was observed that some of this ejecta was thrown to a height of two feet or more. It should also be noted that the soil supported a nearly vertical slope on the walls of the crater. The walls closed in slightly after the ball had penetrated and formed a deep hole with an almost conical shape.

Figure 66b shows the crater formed in the same material under rough vacuum. There appears to be little similarity between the one formed in atmosphere and that formed in vacuum. The upraised rim and the ejecta seen in Fig. 66a is absent in Fig. 66b. Also under rough vacuum the soil was not capable of supporting a very steep wall, due probably to the removal of hygroscopic moisture destroying any bonding that may have existed between soil grains.

Figure 67 shows the craters formed in dense quartz powder under atmospheric and vacuum conditions. It can be seen that in the atmosphere there was little disturbance of the surrounding soil except to produce a "smooth" mound around the impact area. However, in the vacuum it appears that shear took place in the soil causing it to move outward along the shear planes from the impact area. It appears that the void ratio of the dense quartz powder was below the critical void ratio and consequently negative pore air pressures could have been developed in the atmosphere, which increased the total effective stress on the shear planes and resulted in an increase in shear strength. Under vacuum, there was no pore air and consequently the shear strength of the soil may have been insufficient to prevent failure. An alternative explanation for the difference in crater forms would be that the stress wave propagation in the soil under vacuum was different than that in the atmosphere and, hence, the reflected waves

IIT RESEARCH INSTITUTE

at the impact area may have been of sufficient magnitude to distort the crater formed under vacuum.

Therefore, while the vacuum had little effect on the crater shape in the coarser material, even rough vacuum levels may have a distinct effect on craters on fine grained sand and powder. Under ultra-high vacuum it would be expected that these effects would be even more pronounced resulting in steeper walls and more prominent crater rims than would be formed in the same material under atmospheric conditions.
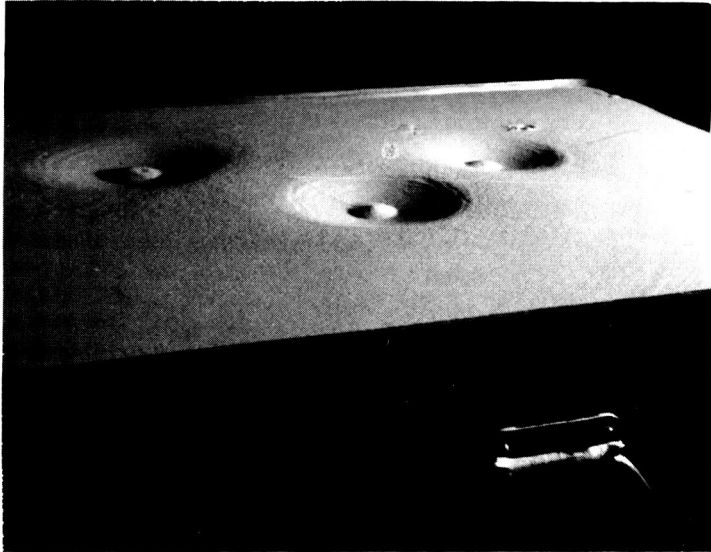
a) Atmosphere

    1-1/4 in. Ball   1-1/4 in. Ball
    20 ft Drop Height   8 ft Drop Height

           1-1/2 in. Ball
           8 ft Drop Height
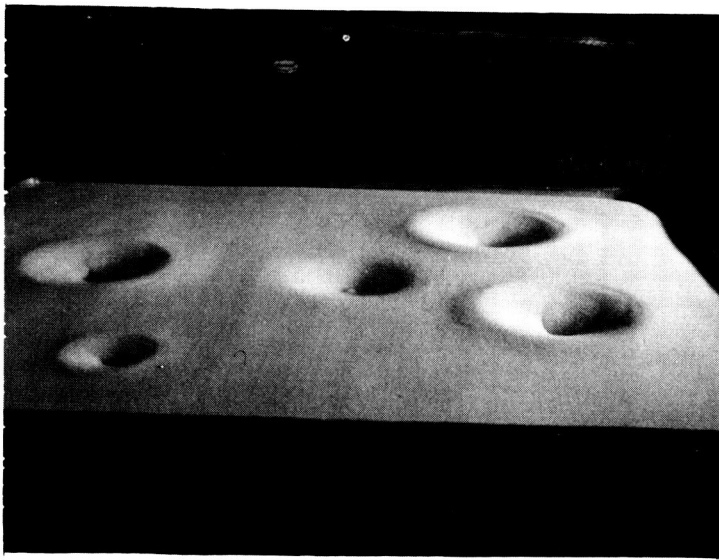
b) Rough Vacuum

    1-1/4 in. Ball   1-1/2 in. Ball
        1-1/2 in. Ball Atmosphere
    1/2 in. Ball   1-1/4 in. Ball

    All-3 ft Drop Height

Fig. 63   CRATERS FORMED IN LOOSE FINE GRAINED
OTTAWA SAND

a) Atmosphere

1-1/4 in. Ball	1-1/2 in. Ball
26 ft Drop Height	26 ft Drop Height
1/2 in. Ball	1-1/4 in. Ball
26 ft Drop Height	8 ft Drop Height

b) Rough Vacuum

1-1/4 in. Ball   1/2 in. Ball

   1-1/4 in. Ball Atmosphere

1-1/2 in. Ball   1-1/4 in. Ball

3 ft Drop Height

Fig. 64   CRATERS FORMED IN LOOSE COARSE GRAINED
OTTAWA SAND

a) Atmosphere

1-1/4 in. Ball	1-1/2 in. Ball
20 ft Drop Height	3 ft Drop Height
1-1/2 in. Ball	1-1/4 in Ball
8 ft Drop Height	8 ft Drop Height

b) Rough Vacuum

1-1/4 in. Ball	1/2 in. Ball
1-1/4 in. Ball Atmosphere	
1-1/2 in. Ball	1-1/4 in. Ball

3 ft Drop Height

Fig. 65   CRATERS FORMED IN WELL GRADED RIVER SAND

a) Atmosphere

1-1/4 in. Ball
3 ft Drop Height

b) Rough Vacuum

1-1/4 in. Ball
2-1/2 ft Drop Height

Fig. 66   CRATERS FORMED IN LOOSE QUARTZ POWDER

a) Atmosphere

1-1/4 in. Ball
2 ft Drop Height
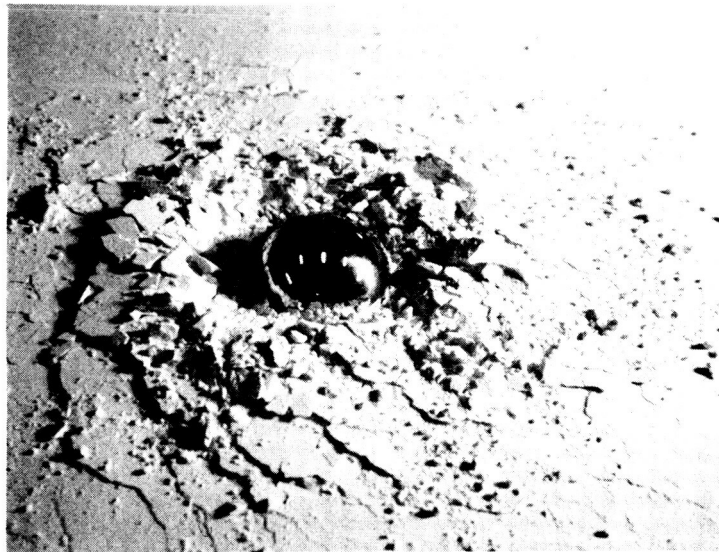
b) Rough Vacuum

1-1/4 in. Ball
2 ft Drop Height

Fig. 67   CRATERS FORMED IN DENSE QUARTZ POWDER

XII. DISCUSSION OF RESULTS

A.   Interparticle Forces

On the basis of the observed increase in porosity and shear strength of the quartz powder under ultra-high vacuum, it was concluded that attractive interparticle forces were developed in this soil under these conditions. However, regardless of the grain size, the increase in porosity of the olivine powder under ultra-high vacuum was much less than that of the quartz and while ultra-high vacuum had little, if any, effect on the shear strength of the olivine at room temperature, a small increase in apparent cohesion was observed to occur at elevated temperatures. This would indicate that attractive interparticle forces were also developed in the olivine powder but were much smaller in magnitude than those which developed in the quartz.

The development of interparticle forces in the quartz was attributed previously to the removal of adsorbed gas from the surfaces of the particles. In a very fine grained material the specific surface to volume ratio is very large and as a result, surface forces on the particles may have a pronounced effect on the shear strength. When the soil was placed in an ultra-high vacuum environment, adsorbed gas layers were removed permitting a closer proximity of the surfaces resulting in an increase in the surface forces which for the soil types used are believed to be primarily of the London-van der Waals type.

The following factors are believed to account for the difference in vacuum effects on the two materials.

(a) The outgassing of a soil mass is primarily a process of removing the adsorbed gas from the individual grains and is influenced greatly by temperature. Thus, it would be expected that the degree to which a soil mass is outgassed, and hence, the effective environmental vacuum would depend upon the original amount of adsorbed gas and the energy required to remove this gas from the particle surfaces.

In all experiments it was observed that the amount of time required to reach the ultimate vacuum level in the chamber was greater for olivine than for quartz. In addition, the ultimate attainable vacuum level was

generally less for olivine. Thus, it would seem that for the same pumpdown and bakeout period a considerably greater amount of adsorbed gas was removed from the quartz than from the olivine. Consequently, for the same conditions under which interparticle forces may be developed in the quartz it is quite probable that the olivine was not outgassed sufficiently for interparticle forces to develop.

The environmental factor of primary concern, therefore is not necessarily the vacuum level in the soil pores but rather the amount of adsorbed gas remaining on the surfaces of the grains. Although the vacuum level in the pores decreased when the soil was heated but increased when the soil cooled, some gas was readsorbed on the particle surfaces during the cooling. This would then account for the fact that while the shear strength of the olivine was apparently unaffected by ultra-high vacuum at room temperature it appeared to increase at these vacuum levels under elevated temperatures.

In the porosity experiments the soil was much less confined than in the direct shear tests, and therefore was undoubtedly outgassed more easily. Consequently, at ultra-high vacuum levels, the porosity of the olivine increased somewhat over that attained at lower vacuum levels, due to the development of interparticle forces which did not appear in the direct shear experiments because of insufficient outgassing.

(b) It was observed that when the quartz was deposited on various materials, "cold welding" occurred between the soil and the metals, but did not occur on teflon or glass. Thus, it is evident that the interparticle forces may depend on the composition of the material. It is possible, therefore, that the magnitude of the interparticle forces was less in the olivine than in the quartz and in order to be of a sufficient magnitude to affect the shear strength, a greater amount of gas may have to be removed from the olivine.

(c) It was observed that in direct shear tests on both the quartz and olivine powders a peak shear stress was developed at low values of displacement for the lower normal stresses. This peak stress may be due to the development of bonds at the asperity contacts of the soil grains due to

adsorbed gas being squeezed out from these points.[7] From Fig. 20 and
27 it can be seen that for both materials, the initial peak increased by
approximately the same amount under vacuum and appears to be independent
of mineralogical composition. These bonds, however, were active only
at the asperity contacts and did not contribute to the shear strength at large
values of displacement.

It is evident that for both materials used in this investigation the
ultra-high vacuum resulted in the development of attractive interparticle
forces, the magnitude of which depended on the mineralogical composition
of the material.

B.   Intergranular Friction

While interparticle forces had a large effect on the shear strength of
the very fine grained soils (powder) the specific surface to volume ratio of
the sand was smaller, and hence, the gravitational forces on the soil grains
were large relative to the surface forces. Consequently, the apparent
cohesion of the fine sand was probably due largely to interlocking of the
particles. As would be expected, the ultra-high vacuum caused an increase
in the intergranular friction as the result of the removal of the adsorbed
gas which acted as a lubricant, with interparticle forces having a small
effect on the apparent cohesion.

As would be expected, the angle of internal friction of the powders
increased also under vacuum. However, it was observed that while elevated
temperatures caused little if any increase in the apparent cohesion over
that at room temperature, the angle of internal friction was affected con-
siderably by the temperature.

This may be explained by the fact that as the normal stress increased,
the area of contact at the asperities also increased and forced out some
adsorbed gas at these points. As heat was applied to the soil the amount of
gas which was forced out increased also and the resulting decrease in
distance between the surfaces caused an increase in interparticle forces.

---

[7] Bradley, R.S., "The Cohesive Force Between Solid Surfaces and the
Surface Energy of Solids", Phil. Mag. and Journal of Science, Vol. XIII,
No. LXXXVI, April 1932.

The interparticle forces, and hence, the shear strength would then depend on the normal stress which would in effect cause a change in the angle of internal friction under vacuum.

C.   Temperature Effects

It was shown that an increase in temperature resulted in the removal of a greater amount of adsorbed gas under vacuum causing an increase in shear strength. Low temperatures resulted in an increase in the shear strength under ultra-high vacuum also although it would be expected that a decrease in temperature would result in readsorbtion of gas onto the particle surfaces. However, if the adsorbed gas is mostly H_2O, temperatures near the freezing point of water would cause it to become bound more tightly to the surfaces and interaction between the adsorbed layers on different particles may take place. This would result in a greater resistance to relative movement of the grains producing an increase in the shear strength. The data at low temperatures were somewhat limited, however, and consequently the above statements cannot be regarded as conclusive.

D.   Bearing Capacity

1. Static

In a loose material such as the quartz powder, failure below a loaded area takes place due to a combination of consolidation and shear. In the consolidation experiments it was observed that less settlement occurred in vacuum than in atmosphere for a particular value of applied bearing pressure. This was due to the fact that in order to cause a change in the grain structure of the soil the particles must move relative to each other and under vacuum conditions, such movement was resisted by the increased friction between grains and interparticle forces.

Therefore, the decrease in consolidation and the increase in shear strength under high vacuum conditions resulted in an increase in bearing capacity.

2. Dynamic

In addition to those factors which increase the static bearing capacity as discussed above one other factor which was seen to affect the penetration resistance of soil under dynamic loading was the absence of pore fluid under vacuum. As discussed in Section VII, pore air pressures were developed in atmosphere which were positive or negative depending on the void ratio of the soil and increased or decreased the penetration resistance accordingly. In Fig. 39 and 44 (penetration at 0.3 in.-lb work versus porosity) the curves for atmospheric and rough vacuum conditions converge at the lower porosities. This was because a soil having a void ratio equal to the critical value does not change in porosity during shear and therefore no pore pressures can be developed even in atmosphere. Consequently, at the critical void ratio the penetration resistance in atmosphere is the same as in a rough vacuum. The fact that the curves for rough vacuum and higher vacuum levels tend to converge is due probably to less efficient outgassing of the denser soil at the high vacuum levels. Also a portion of the shear strength at the low porosity is due to interlocking of the soil grains, a condition which is relatively unaffected by vacuum.

An initial peak resistance was also observed under dynamic loading and was attributed to the inertia of the soil. In the olivine this peak had approximately the same magnitude for all vacuum levels as for atmospheric conditions. In the quartz, however, it was observed that the peak was greater at high and ultra-high vacuum than at rough vacuum or atmospheric conditions. This would indicate that in the quartz bonding occurred between the particles, and the peak resistance was due not only to the inertia of the soil but also to the force required to break these bonds. Also, these bonds probably caused a greater amount of soil to be affected by the penetrometer thereby increasing the mass of the soil being accelerated initially.

In the loose material, the penetration resistance increased under vacuum due to (1) the removal of pore air, (2) a greater inertial resistance of the soil, and (3) an increase in the shear strength and the pressure required to produce consolidation. In the olivine an increase in vacuum level from rough vacuum to ultra-high vacuum did not cause a significant change in penetration resistance indicating that the soil was probably not outgassed sufficiently even at these

vacuum levels to develop interparticle forces. Also, in the sand the rough vacuum did not change the penetration resistance appreciably indicating a negligible effect of pore air pressure, while the penetration resistance increased at ultra-high vacuum due to an increase in shear strength. The manner in which the vacuum affected the dynamic penetration of the soil depended upon its grain size and mineralogical composition.

E.   Adhesion of Soil to Other Materials

It was observed that a layer of soil appeared to "cold weld" on the surfaces of the metallic materials but not on the nonmetallic materials. Thus, it would appear that strong bonds between soil and materials other than soil may develop and depend in some way on the free electrons in the crystal lattice.

The size of small "pits" or craters observed on the stainless steel and the relatively large particles bonded to the aluminum indicates that the major portion of the layer of "cold welded" material consisted primarily of the very fine particles in the soil (smaller than 1 or 2μ). It would also indicate that while relatively strong bonds were developed on the aluminum, these bonds were weak and insufficient to hold the particles in place after impact.

XIII. CONCLUSIONS

On the basis of the foregoing results the following conclusions were drawn.

1. The actual vacuum in the soil pores will generally be less than that recorded in the chamber. However, the dominant factor affecting the soil properties is not the vacuum in the soil pores but rather the amount of adsorbed gas removed from the particle surfaces. For this reason, it would be desirable to select materials for laboratory simulation which can be outgassed in a reasonable period of time in order to more closely duplicate the degree of "cleanliness" expected to exist on the lunar surface.

2. Ultra-high vacuum causes an increase in "stiffness" of soil.

3. Relatively strong bonds may be developed under ultra-high vacuum at the asperity contacts in the soil which do not contribute to the shear strength at large displacements once the bonds are broken.

4. The removal of adsorbed gas from the surfaces of particles results in the development of attractive interparticle forces. The amount of gas removed and the magnitude of the interparticle forces depends largely on the mineralogical composition of the soil. In the case of quartz powder, it also depends on the magnitude of the normal stress. This removal of adsorbed gas and development of interparticle forces affects the soil properties in the following manner:

   (a) As the result of flocculation of the particles, the soil is able to maintain a higher porosity under ultra-high vacuum than at lower vacuum levels. However, the porosity attained at lower vacuum levels is less than that attained in atmosphere. This is due to the removal of frictional air resistance which results in higher impact velocities during deposition. In any given case, the porosity attained under ultra-high vacuum may or may not be greater than that attained in atmosphere since this also depends on the mineralogical composition of the soil.

(b) The apparent cohesion of fine grained materials increases under ultra-high vacuum regardless of mineralogical composition provided the soil is outgassed sufficiently. However, elevated temperatures are necessary to sufficiently outgas fine grained olivine, whereas the apparent cohesion of fine grained quartz increases even at room temperature.

(c) The angle of internal friction of quartz increases under vacuum for both fine grained (powder) and coarse grained (sand) material at elevated temperatures. In the sand, the increase is attributable to the removal of the lubricating effect of the adsorbed gas whereas in the powder it is due both to the removal of the lubricant and an increase in interparticle forces as a function of normal stress.

(d) As the result of the increased resistance to relative movement of the soil grains, the amount of consolidation of quartz powder is less in ultra-high vacuum than in atmosphere.

5. The increase in shear strength and decrease in consolidation under vacuum results in a substantial increase in the static bearing capacity.

6. The dynamic penetration resistance of loose soil increases with vacuum even under low vacuum levels. This appears to be due to one or more of the following factors depending upon grain size and mineralogical composition.

(a) The removal of pore air causes all stresses to appear immediately as effective stresses and hence, eliminates any effects of positive pore air pressures which may occur under atmospheric conditions.

(b) The inertial resistance of fine grained soil is greater in vacuum than in atmosphere due to the development of interparticle bonds which must be overcome as the soil is penetrated. This causes a greater mass of soil to be influenced by the penetrometer.

IIT RESEARCH INSTITUTE

-119-

(c) Once the inertial resistance of the soil has been over-
come the penetration resistance is greater in vacuum
due to the same factors that produce an increase in
the static bearing capacity.

7. For samples of quartz powder at high temperatures the effects
of vacuum on shear strength appear to be irreversible. At lower porosities,
the shear strength appears to be the same for samples stored under ultra-
high vacuum as for samples stored in atmosphere. The latter is also true
for olivine powder at all porosities.

8. A considerable amount of adhesion occurs between soil and certain
other materials. This results in "cold welding" of a thin layer of soil on
the surfaces of aluminum and stainless steel.

9. Rough vacuum has a distinct effect on the size and shape of impact
craters in fine grained soil. This is due to the pore air effects and/or
differences in stress wave propagation under atmospheric and vacuum
conditions.

APPENDIX A

VACUUM AND TEMPERATURE EFFECTS ON STRAIN GAGES

APPENDIX A

VACUUM AND TEMPERATURE EFFECTS ON STRAIN GAGES

The force transducers which were used in this investigation consisted, in most cases, of small aluminum rings on which were mounted four active strain gages and which were calibrated for the force on the ring as a function of the strain.

In order to assure that the results were not influenced by possible creep in the adhesive or change in the gage factor under vacuum and/or elevated temperatures, a small aluminum cantilever was mounted on the same frame as the load cells. An active gage and a dummy gage of the same type as was used on the transducers were mounted on the cantilever using the same adhesive and epoxy coating as for the load cells. Consequently, the gages on the cantilever were exposed to the same temperatures and vacuum as those on the load cells.

At the end of each direct shear test a displacement was applied to the cantilever and strain readings taken as a function of the displacement. Three different cantilevers were constructed and a number of tests performed on each one. Typical results are shown in Fig. 68 both prior to vacuum exposure and after a number of tests.

It is evident from Fig. 68 that vacuum and temperatures had a negligible, if any, effect on the gages.
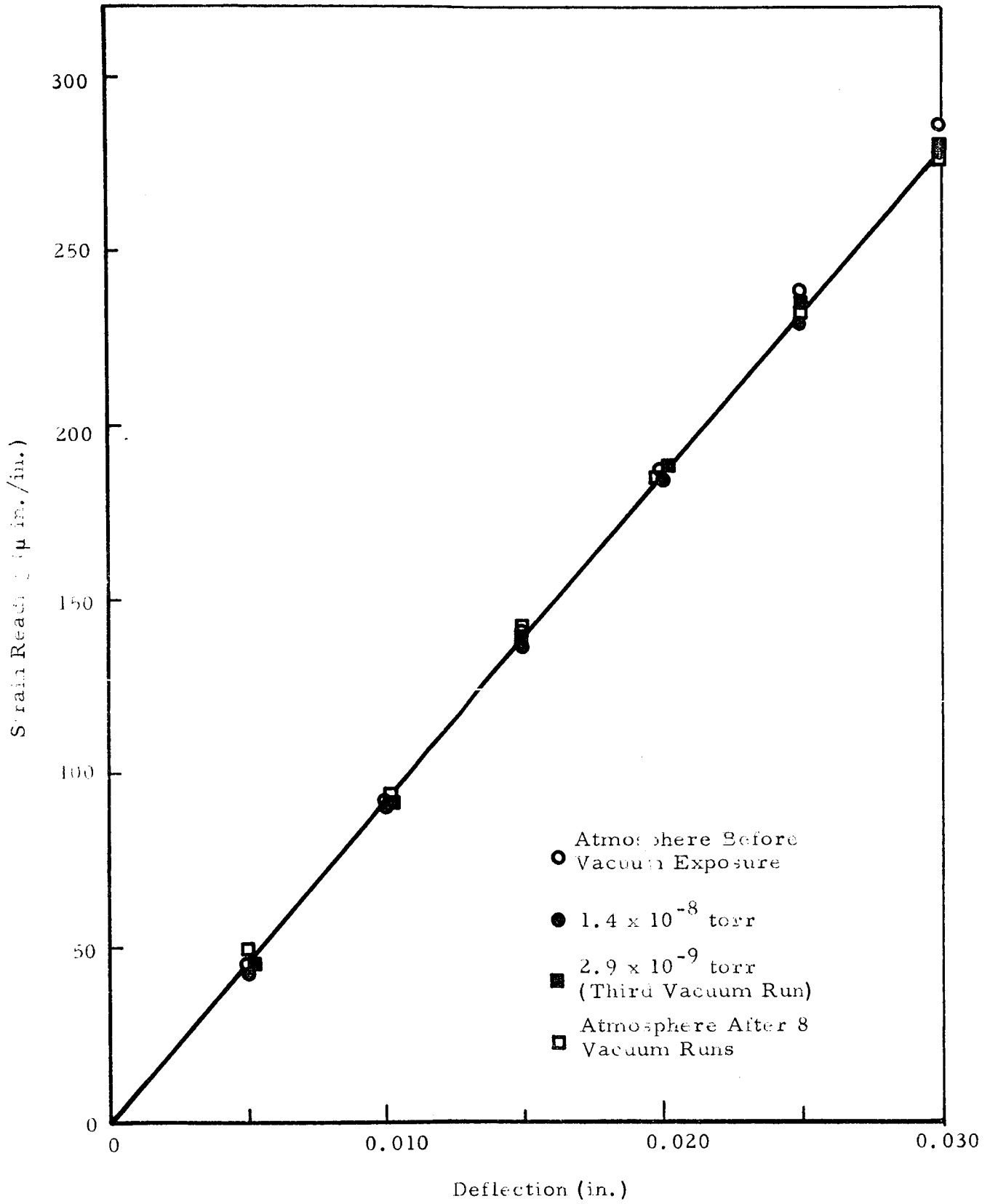
Fig. 63 STRAIN READINGS AS A FUNCTION OF BAR DEFLECTION

- 123 -

APPENDIX B

DEGASSING OF SOIL UNDER VACUUM

APPENDIX B

DEGASSING OF SOIL UNDER VACUUM

1. Material Balance

The material balance for one dimensional flow of gas through a porous medium with desorption of gas where the porous medium is a cylinder with impermeable walls may be written as:

Rate of Accumulation = rate of inflow - rate of outflow
+ rate of material being desorbed

or,

$$\int_{z}^{z+\Delta z} \phi A \frac{\partial \rho}{\partial t} dz = (\rho v)\Big|_{z} A - (\rho v)\Big|_{z+\Delta z} A + \int_{z}^{z+\Delta z} \frac{\partial m}{\partial t} S\, A dz \quad (15)$$

where

ρ = density

ϕ = porosity

v = seepage velocity

A = area of cylinder

S = specific internal area whose value is assumed independent of size of bulk volume used for its measurement.

m = amount of material desorbing per unit internal surface area.

Expanding $\rho v\Big|_{z+\Delta z}$ about $\rho v\Big|_{z}$, using the mean value theorem for integrals and taking the limit as $\Delta z \rightarrow 0$, yields

$$\phi \frac{\partial \rho}{\partial t} = - \frac{\partial (\rho v)}{z} + \frac{\partial m}{\partial t} S \quad (16)$$

2. Equilibrium Physical Adsorption

The simplified derivation[8] of Langmuir assuming monolayer adsorption assumes that the equilibrium adsorption state is made up to two steps, evaporation and condensation. The rate of evaporation is

[8] Adamson, Author W., "Physical Chemistry of Surfaces", Interscience, New York, 1960.

-125-

$$k \ S_1 \ \exp(-Q/RT) \equiv k_1 \ S_1 \qquad (17)$$

where

S_1 = area of occupied surface, and

k_1 = rate constant.

The rate of condensation is $k_2 P S_0$ where k_2 is the rate constant, P is pressure, and S_0 is the unoccupied area.

At equilibrium, the rates are equal and

$$k_1 \ S_1 = k_2 \ P \ (S - S_1) \text{ where}$$

$S = S_0 + S_1$.

If v_m is the amount adsorbed in one monolayer, and $S_1 = \dfrac{v}{v_m} \ S$ where v is the amount adsorbed with S_1 area occupied. Then

$$k_1 \ \frac{v}{v_m} = k_2 \ P \ (1 - \frac{v}{v_m})$$

and $\qquad\qquad\qquad\qquad\qquad\qquad\qquad\qquad\qquad (18)$

$$v = \frac{v_m \ \dfrac{k_2}{k_1} \ P}{(1 + \dfrac{k_2}{k_1} \ P)} \ .$$

At low pressure, $1 >> \dfrac{k_2}{k_1} \ P$, and Eq. (18) reduces to

$$v = v_m \ \frac{k_2}{k_1} \ P \ . \qquad (19)$$

The mass of gas adsorbed per unit area may therefore be expressed as

$$m = CP \ . \qquad (20)$$

Figure 69 illustrates equilibrium adsorption isotherms for ammonia on charcoal.
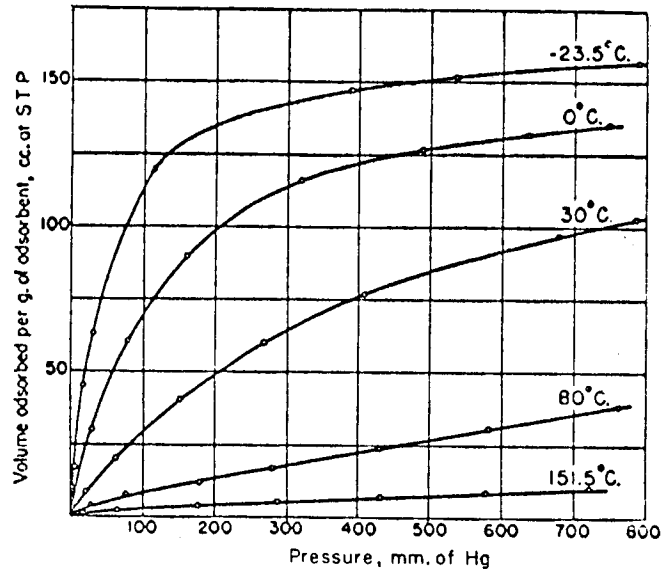
Fig. 69   ADSORPTION ISOTHERMS FOR AMMONIA ON CHARCOAL[8]

Note that at high temperatures, the curves are almost straight lines as Eq. (19) predicts.   At high pressures,

$$1 << \frac{k_2}{k_1} \quad P$$

and Eq. (18) predicts a constant value which agrees well with Fig. 69. Since the outgassing of soil takes place at low pressures and reasonably high temperatures, Eq. (20) will be sufficient for this problem.

3.   Statement of the Physical Adsorption Problem

The following laws will be substituted into Eq. (16).

(a)   Darcy's Law for one-dimensional seepage velocity[9]

[9] Scheidegger, Adrian E., "The Physics of Glow through Porous Media", University of Toronto Press, 1960.

$$\nu = -\frac{k}{\mu}\frac{\partial P}{\partial z} \qquad (21)$$

where

k is the permeability

μ is the viscosity

P is the pressure

and gravity effects have been neglected.

(b) The perfect gas law gives

$$\rho = \frac{P}{RT_o} \qquad (22)$$

where R is the universal gas constant and T_o is the temperature.

Substitution of Eq. (20), (21) and (22) into Eq. (16) yields

$$\frac{Q}{Rt}\frac{\partial P}{\partial t} = CS\frac{\partial P}{\partial t} - \frac{1}{RT}\left(-\frac{k}{u}\right)\frac{\partial^2 P^2}{\partial z^2} \qquad (23)$$

with the boundary conditions

$$P(0,z) = P_o$$
$$\qquad (24)$$
$$P(t, \pm L) = P_1$$

The solution of this equation must be done numerically.

4. Approximate Solution of the Physical Adsorption Problem

An approximate solution may be obtained, however, which is more readily solved. If the equation

$$\rho\nu = -D\frac{\partial P}{\partial z} \qquad (25)$$

is used in Eq. (16) instead of the Darcy law the resulting equation is

$$\left(\frac{\phi}{RT} - CS\right)\frac{\partial P}{\partial t} = \frac{D}{RT}\frac{\partial^2 P}{\partial z^2} \qquad (26)$$

IIT RESEARCH INSTITUTE

which may be written as

$$\frac{\partial P}{\partial t} = K \frac{\partial^2 P}{\partial z^2} \tag{27}$$

Equation (27) is easily solved by separation of variables and was used to provide an approximate representation of the degassing of a soil mass.

5. Discussion

It should be noted while all heat of desorption effects have been neglected, the amount of heat involved in the liberation of water is not negligible and should be included. This however will lead to simultaneous heat and mass transfer equations. Guidelines to the solution of this much more complex set of equations are provided in the area of research of fiber drying.

APPENDIX C

VACUUM SYSTEMS

APPENDIX C

VACUUM SYSTEMS

The vacuum systems used in this program were pumped by either oil diffusion pumps or ion pumps with titanium sublimation. The systems used are presented in Table 3. The experiments for which each system was used is shown by the number of that section of the report in which the results of the experiment are presented.

Table 3

VACUUM SYSTEMS

Section	Chamber	Pump	Ultimate Vacuum
III, VI	36 x 48 in. bell	35 in. diffusion	5×10^{-8} torr
IV, V, VIII	24 x 24 in. horizontal cylinder	4 in. UHV diffusion	8×10^{-10}
VII, XI	36 x 48 in. bell	10 in. UHV diffusion	1×10^{-10}
IX	18 x 30 in. bell	400ℓ/sec ion with titanium sublimation	2×10^{-11}
IX, X	12 x 18 in. bell	140ℓ/sec ion with titanium sublimation	2×10^{-11}